Regulators of Centromeric Nucleosomes in *Saccharomyces cerevisiae*

Thesis

UNRESTRICTED

Regulators of Centromeric Nucleosomes in *Saccharomyces cerevisiae*

A Thesis Submitted for the Degree of

Doctor of Philosophy

By

Manjunatha Shivaraju

To

The Stowers Institute for Medical Research

The Open University

May 2011

Date of Submission: 12 April 2011

Date of Award: 8 July 2011

ProQuest LLC.
789 East Eisenhower Parkway
P.O. Box 1346
Ann Arbor, MI 48106 – 1346

Acknowledgement

It is immense pleasure that I express my deep sense of gratitude and heartfelt respect to my mentor Dr. Jennifer Gerton, for bringing me here to Stowers Institute and for her constant support, endless encouragement, valuable and constructive suggestions and keeping me ever alert throughout the period of investigation. It was a great pleasure and privilege for me to be associated with her.

I am thankful to my advisory committee members: Sue Jaspersen, Jerry Workman, Rong Li and Leanne Wiedemann for their advice and suggestions throughout my investigation.

I want to thank all the past and present members of the Gerton lab and special thanks to Ray Camahort and Mark Mattingly for the good time we had out side of the lab.

I owe big thanks to Bing Li, Swaminathan Venkatesh, Kenneth Lee, Samantha-Pattenden and Jeong-Hoon Kim for reagents and helpful discussions.

I would like to thank Kimberly Carter and Shelly Hornbuckle for administrative assistance and Ron Conaway for being my third party monitor.

Finally, I would like to thank my final examination committee membres Robb Krumlauf, Joan Conaway and Robin Allshire for their advice and suggestions.

Abstract

The centromere is a specialized chromosomal structure that regulates faithful chromosome segregation during cell division, as it dictates the site of assembly of the kinetochore. In all organisms, the centromeric nucleosomes are specified by a H3 variant, known as Cse4 in budding yeast. How these centromeric nucleosomes are assembled and perpetuated is only beginning to be understood. Scm3 is an evolutionarily conserved essential inner kinetochore protein that has been shown to be important for centromere specification. Plasmid supercoiling assays performed *in vitro* with recombinant proteins demonstrate that Scm3 can act as a Cse4-specific nucleosome assembly factor. Assembly activity depends on an evolutionarily conserved domain of Scm3 and the centromere targeting domain (CATD) of Cse4, but is sequence independent. Interestingly, micrococcal nuclease digestion of Scm3 assembled Cse4 nucleosomes reveals that less DNA is protected compared to Nap1 assembled Cse4 nucleosomes, suggesting structural differences. Fluorescence correlation spectroscopy in combination with brightness measurements and confocal imaging experiments in live cells revealed that centromeres at G1 phase have one copy of Cse4 per centromeric nucleosome whereas two copies are detected at anaphase. The apparent structural change occurs at the "metaphase to anaphase" transition. We propose a model in which the structure and composition of centromeric nucleosomes is cell cycle regulated. Our model reconciles experimental evidence for the existence of both the hemisome and the octasome.

Table of contents

List of Figures

List of Tables

Abbreviations

°C	degrees centigrade
DNA	deoxyribonucleic acid
DTT	dithiothreitol
EDTA	diaminoethanetetra-acetic acid
g	gram
h	hour
kb	kilobase
M	molar
mg	milligram
min	minute
ml	milliliter
mM	millimolar
NP-40	Nonidet P-40
OD	optical density
PAGE	polyacrylamide gel electrophoresis
PBS	phosphate buffered saline
PCR	polymerase chain reaction
pmol	picomole
rpm	revolutions per minute
Tris	2-amino-2-(hydroxymethyl)-1,3-propanediol
UV	ultraviolet
V	volts
GFP	green fluorescent protein
YPD	yeast peptone-yeast extract-dextrose medium

Chapter 1.

Introduction

I Chromatin Organization and Function

Eukaryotic cells are faced with the daunting task of compacting a huge amount of DNA into the limited dimensions of the nucleus while keeping the DNA template accessible to factors involved in different cellular processes. The cell packages the genome into a complex nucleoprotein structure; the fundamental unit of this packaging is the nucleosome [1]. The nucleosome, which forms the first level of organization, consists of 147 base pairs of DNA wound 1.65 times in a left-handed configuration around a proteinaceous central core consisting of two copies each of four histones. Adjacent nucleosomes are separated by short stretches of linker DNA varying between 20-60 base pairs, thereby establishing a regular spacing of the nucleosomes. Arrays of nucleosome core particles are further compacted into higher-order chromatin structures involving binding of linker histones and a plethora of nonhistone chromatin proteins.

1. The histones

Histones are the group of basic proteins that help compact the structure of all eukaryotic DNA in the form of chromatin. They are of great importance in the organization of chromatin structure and control of gene activity. Based upon their genetic and structural functions, histones are classified into two categories, core or nucleosomal histones and the linker histones. Core histones, including histone H2A, H2B, H3 and H4, are small highly basic proteins with molecular weights between 11 and 16 kDa. The linker histone H1, which is not well-conserved between species, functions in spacing adjoining nucleosomes. H1 helps to modulate higher order chromatin packing by providing an interaction region between adjacent nucleosomes. The core histones are evolutionarily conserved proteins, and have 3 distinct domains: 1) the histone fold domain, formed by three α-helices connected by two loops, is involved in histone/histone and histone/DNA interactions, 2) the relatively unstructured and highly charged N-terminal tail domain, which

projects out from the nucleosome into the surrounding environment, is the place for extensive covalent post-translational modifications and 3) a short C-terminal domain. In most eukaryotes synthesis of core histones is highly regulated and balanced in the cell cycle. Indeed, in *S. cerevisiae* over-expression of either H2A/H2B or H3/H4 pairs, leads to frequent chromosome loss. Synthesis of the so-called replication-dependent core histones is coincident with S phase. A less abundant form of histones is synthesized outside of S phase. These are the replication independent or replacement histones such as H3.3, H2A.X, and H2A.Z [2]. These variants are deposited onto DNA independent of DNA replication and are known to contribute to distinct nucleosomeal architectures and to play critical roles in the regulation of nuclear functions.

2. The histone octamer and the nucleosome

The histone octamer consists of two copies of each of the four core histone proteins, H2A, H2B, H3 and H4. The histone fold domain (HFD) of histones is involved in the formation of the heterodimers, H3-H4 and H2A-H2B. At physiological ionic strength, H3-H4 stably oligomerizes into a tetrameric structure, while H2A-H2B remains as a dimer. In 2M sodium salt, two copies of each histone can form an octamer. Intramolecular interactions occur mainly through hydrogen bonding between charged groups buried in the helix bundle. Hydrophobic interactions within the dimers also contribute to the stability of the structure (Figure 1).

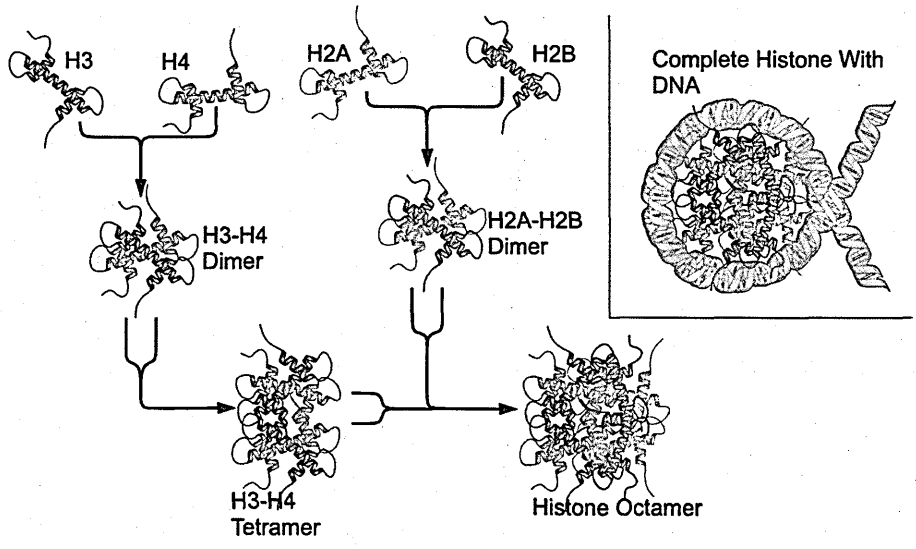

Figure 1. Organization of the nucleosome: the nucleosome consists of two copies of each core histone, (H3-H4-H2A-H2B) forming a proteinacious scaffold around which the DNA wraps itself. (Adapted from Albert *et al* [3])

Nucleosomes are the basic unit of DNA packaging in eukaryotes, consisting of a segment of DNA wound around a histone octamer. Extensive work *in vitro* has demonstrated that the assembly of nucleosomes belived to be occurs in two steps. First, a tetramer of $(H3/H4)_2$ binds to the central 60bp of the nucleosomal DNA to form a subnucleosomal particle. Secondly, addition of two H2A/H2B dimers helps to form a DNA protein complex called nucleosome. Each dimer organizes an additional 30 bp towards the ends of the DNA. Each histone fold pair leaves a 4 bp linker between the units. The distortion of the DNA helix is brought about by the interaction between the structured regions of the histone protein and the minor groove of the DNA over 14 different locations. The interactions include hydrogen bonds between the main chain amides and the phosphate oxygen of the DNA, along with the electrostatic interactions with the basic side chains [4]. The histone tails are unstructured and protrude out of the core particle through the gyres of the DNA superhelix. These flexible histone tails do not contribute to the stability of the core particle structure as they extend beyond the region involved in the DNA binding, and hence may contribute to the higher order chromatin structure.

3. Chromatin assembly

Chromatin assembly is the process by which the DNA is packaged in the nucleosomes. The basic process is mediated by histone chaperones and ATP-dependent chromatin spacing and organizing factors to result in a regularly spaced array of nucleosomes [5, 6]. Cell cycle progression involves the duplication not only of the DNA, but also the chromatin organization. Chromatin assembly results in the formation of a diverse and dynamic structure, with spatial-temporal variation in the compaction, resulting in different degrees of compaction. The organization and the accessibility of the genome is determined by the assembly of DNA into the chromatin. There are two fundamental types of chromatin assembly. The first is known as replication-dependent chromatin assembly which happens immediately after DNA replication or DNA repair during the cell cycle. The assembly of nucleosomes during DNA replication is achieved by two different pathways. The first pathway is known as parental nucleosome transfer, where histones from parental DNA are recycled by direct transfer and deposition onto the replicated daughter DNA strands. This recycling of parental histones only contributes to the assembly of half of the replicated DNA into chromatin. The other half is assembled by the second pathway known as de novo nucleosome assembly, which is mediated by chromatin assembly factors that can act as histone chaperones targeting soluble histones to the sites of assembly at DNA replication forks [7, 8].

Another type of chromatin assembly occurs outside of S phase or in non-dividing cells and is known as replication-independent chromatin assembly [9, 10]. A few histone variants, which are thought to be involved in this event, appear to be concentrated in regions of active transcription by incorporating in to these regions. For instance, the assembly of histone variant H3.3 is mediated by the HIR family of histone chaperones in a manner that is analogous to the role of CAF-1 in replication–dependent assembly [11].

4. Histone chaperones

Histone proteins are positively charged proteins that have a very high affinity for the negatively charged phosphate groups in DNA. Though nucleosomes can be assembled by salt dialysis, the direct mixing of the histones and DNA under physiological salt conditions, results in aggregation. Histone chaperones are cellular anionic components that neutralize the positive charge on the histones, resulting in ordered association with DNA, without aggregation.

The term molecular chaperones was originally used by Ron Laskey to describe the function of the nuclear protein nucleoplasmin, which plays several important roles in macromolecular assembly of nucleosomes during early development of the amphibian, *Xenopus* [12]. Until recently, the histone chaperones were defined as factors that associate with histones and stimulate a reaction involving histone transfer to DNA without being part of the final product [13]. A new definition has recently been proposed which states that histone chaperones are those factors prevent promiscuous association of histones with DNA [14]. However, a fundamental biochemical property shared by all histone chaperones, is the ability to histone transfer onto DNA *in vitro*. This can be revealed using a 'nucleosome-reconstitution' assay with purified DNA and histones. Notably, not all histone chaperones are involved in histone deposition onto DNA *in vivo,* and they can also use their transfer capacity to fulfill other important roles in histone dynamics, such as histone transport, transfer or storage and thus they can play other important roles in histone dynamics [13, 15].

Many histone chaperones are conserved throughout eukaryotic evolution. In budding yeast a number of chaperone proteins have been identified and characterized biochemically *in vitro* and functionally *in vivo*. The histone H3-H4 chaperones function in either one of two pathways, replication-dependent or replication-independent. The chaperone complex CAF-1 facilitates loading of $(H3\text{-}H4)_2$ onto DNA in a replication-dependent manner. CAF-1 physically associates with the DNA polymerase processivity

clamp PCNA (proliferating cell nuclear antigen) and $(H3\text{-}H4)_2$, allowing nucleosomes to be deposited immediately after DNA replication or DNA repair [16, 17]. The HIR complex is another evolutionarily conserved H3-H4 chaperone. HIR has been shown to function outside of DNA replication, helping to deposit or reassemble $H3_2\text{-}H4_2$ onto DNA during transcription [18] [19].

The histone H2A-H2B chaperones assist in addition of the H2A-H2B dimer onto the pre-formed $H3_2\text{-}H4_2$ tetrasome. The H2A-H2B dimer is not maintained in the nucleosome with as high affinity as $H3_2\text{-}H4_2$, therefore H2A-H2B dimers are more dynamic and removed more readily from the nucleosome during transcription [20, 21]. The histone chaperone Nap1 is a major regulator of H2A-H2B dynamics, facilitating both the shuttling of H2A-H2B into the nucleus and its deposition into nucleosomes during S phase [22]. The FACT complex is a key histone chaperone that functions during transcription [23]. It has been observed both *in vivo* and *in vitro* that RNA Pol II-mediated transcription removes H2A-H2B dimers from nucleosomes [24]. It is hypothesized that the FACT complex removes H2A-H2B dimers ahead of the replicating polymerase, facilitating transcription through nucleosome-dense regions. Additionally, FACT has been shown to possess chaperone activity *in vitro*, leading to the hypothesis that FACT is necessary to re-deposit H2A-H2B dimers after Pol II has passed through a region [25]. In additionto their interaction with histone, histones chaperones can associate with other key proteins thereby providing an interface between histone assembly/removal and other processes. These interactions allow histones to be provided at the right time and the right place when and where they are needed. For example during replication or repair, the chaperone CAF-1 is targeted to sites of DNA synthesis through its interaction with PCNA [26].

5. Histone variants

A large number of histone variants have been identified for H1, H2A, H3 and H2B, whereas H4 appears to lack a sequence variant [27]. These histone variants are a group of proteins which closely resemble the core histones but have distinct biochemical properties which are thought to alter the charateristics of the nucleosomes. Histone variants are often coded by a single gene which is expressed throughout the cell cycle, and are thought to replace their core histone counterpart to form a specialized nucleosome. Histone variants can be species specific, or found ubiquitously in all eukaryotes, and have been implicated in regulation of multiple cellular processes including transcriptional activation and repression, formation of heterochromatic barriers, gametogenesis, and maintenance of genome stability [28-31] (Table 1). It is also important to note that in some species the predominant core histone may actually be a histone variant in another species. For example, the budding yeast core histone H3 is actually the H3 variant H3.3 in higher eukaryotes [27].

Histone	Variants	Species	Chromatin effect	Function
H1	H1°	Mouse	Chromatin condensation	Transcription repression
	H5	Chicken	Chromatin condensation	Transcription repression
	SpHt	Sea urchin	Chromatin condensation	Chromatin packaging
	H1t	Mouse	Open chromatin	Histone exchange, recombination ?
H2A	MacroH2A	Vertebrate	Condensed chromatin	X-chromosome inactivation
	H2ABbd	Vertebrate	Open chromatin	Transcription activation
	H2A.X	Ubiquitous	Condensed chromatin	DNA repair/recombination/transcription repression
	H2A.Z	Ubiquitous	Open/closed chromatin	Transcription activation/repression, chromosome segregation
H2B	SpH2B	Sea urchin	Chromatin condensation	Chromatin packaging
H3	CenH3	Ubiquitous	CEN nucleosome positive DNA wrap	Kinetochore formation/function
	H3.3	Ubiquitous	Open chromatin	Transcription

Table 1. List of known histone variants and their function
Adapted from Kamakaka *et al.* [27].

The centromeric histone variant

A specialized histone H3 variant is found at centromeres, known generically CenH3, or, more specifically, Cse4 in *S. cerevisiae*, CENP-A in humans, and CID in flies. The CenH3 variant is more divergent among all the H3 variants (Figure 2) and is thought to physically replace histone H3 at centromeric nucleosome(s). CenH3 containing nucleosomes are the fundamental structural unit of centromeric chromatin in all eukaryotes and are required for proper chromosome segregation and mitotic division [32]. Structurally, CenH3 orthologs have two major domains: an evolutionarily conserved histone fold domain (HFD) and a divergent amino-terminal domain. The most striking feature of CenH3 resides in the presence of a highly variable N-terminal domain, ranging from 20 to 200 amino acids, that shows essentially no sequence homology to the N-terminal tail of histone H3 or across different eukaryotic lineages [33]. This tail can also vary greatly between species (Figure 3). The N-terminal tail of yeast Cse4 is much longer than any of its eukaryotic counterparts. It is essential for Cse4 function when Cse4 is expressed at normal physiological levels [34]. Its exact molecular function is unknown [35]. On the other hand, the HFD of CenH3 orthologs has a high degree of amino acid identity to histone H3 (Figure 2). The function of the CenH3 nucleosome is highly conserved, as demonstrated by the functional complementation of RNAi-depleted CENP-A in human cells by yeast Cse4 [36].

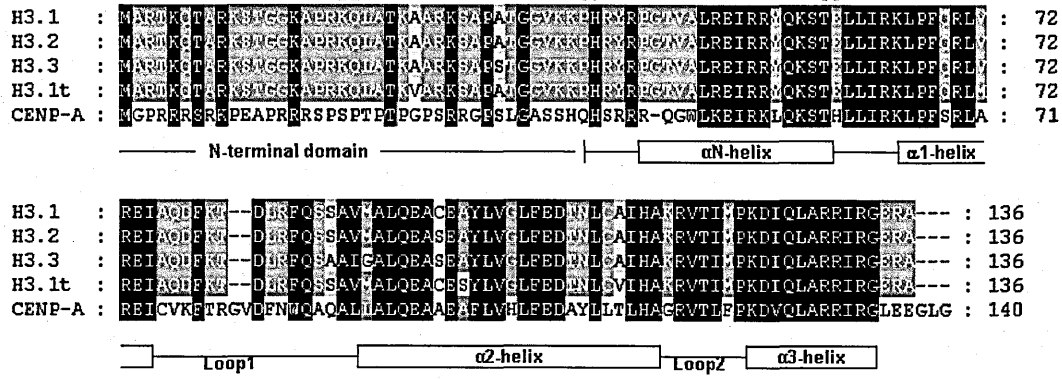

Figure 2. Sequence alnalysis of human H3 variants
ClustalW was used for sequence comparision of human H3 variants. CENP-A is more divergent among all the H3 varinats.

One interesting question regarding centromeric chromatin is the timing of Cse4/CENP-A deposition at centromeres during the cell cycle. Although all centromeres are universally marked by the presence of a histone H3 variant, the timing of deposition varies throughout eukaryotes. In budding yeast Cse4 has been shown to be incorporated into the centromere during S-phase [37]. Cse4 bound to DNA after S-phase remains very stable throughout the remainder of the cell cycle, with new Cse4 replacing the old Cse4 during the subsequent S-phase [37]. In humans CENP-A is expressed during G2, after S-phase is completed, but deposition occurs in late telophase to early G1 phase [39]. In Drosophila embryos, CID deposition takes place at anaphase [40]. In fission yeast *Schizosaccharomyces pombe,* CENP-A (Cnp1) loads in two distinct pathways. The S-phase coupled Cnp1 loading pathway requires the proteins Mis6 and Ams2 for proper localization of the CenH3 variant [41]. In additionto the S-phase loading pathway, fission yeast can also load Cnp1 in a replication-independent pathway during late G2 [42]. In the case of *Arabidopsis*, it is reported that loading of CENP-A occurs mainly in G2 phase [43]. All these reports suggest that there is a vast difference in timing of CENP-A deposition during the cell cycle in different organisms; it even varies between yeast species, i. e., *S. cerevisiae* and *S. pombe*.

Given that CENP-A defines centromeres, another fundamental question is how CENP-A is targeted to and assembled only at centromeres and excluded from other non-centromeric regions. In humans CENP-A is targeted to centromeres by a protein that sorts the (CENP-A: H4) heterotetramer/heterodimers away from core histones, known as HJURP [44, 45]. An evolutionarily conserved HJURP domain forms a complex with newly synthesized CENP-A protein by recognizing the CENP-A Targeting Domain (CATD) on the CENP-A: H4 tetramer [44, 46]. This CATD consists of 22 amino acid substitutions within the classic histone fold domain (loop 1 and helix 2) [47, 48]. When the CATD is substituted into histone H3, it is not only sufficient to confer centromere targeting capabilities to H3 [48], but it also enables the hybrid H3-CATD to maintain centromere function when CENP-A is reduced [48]. In budding yeast the HJURP ortholog is Scm3 [49]. Scm3 interacts with Cse4 and Ndc10 and is required to recruit both proteins efficiently to centromeres [50-52].

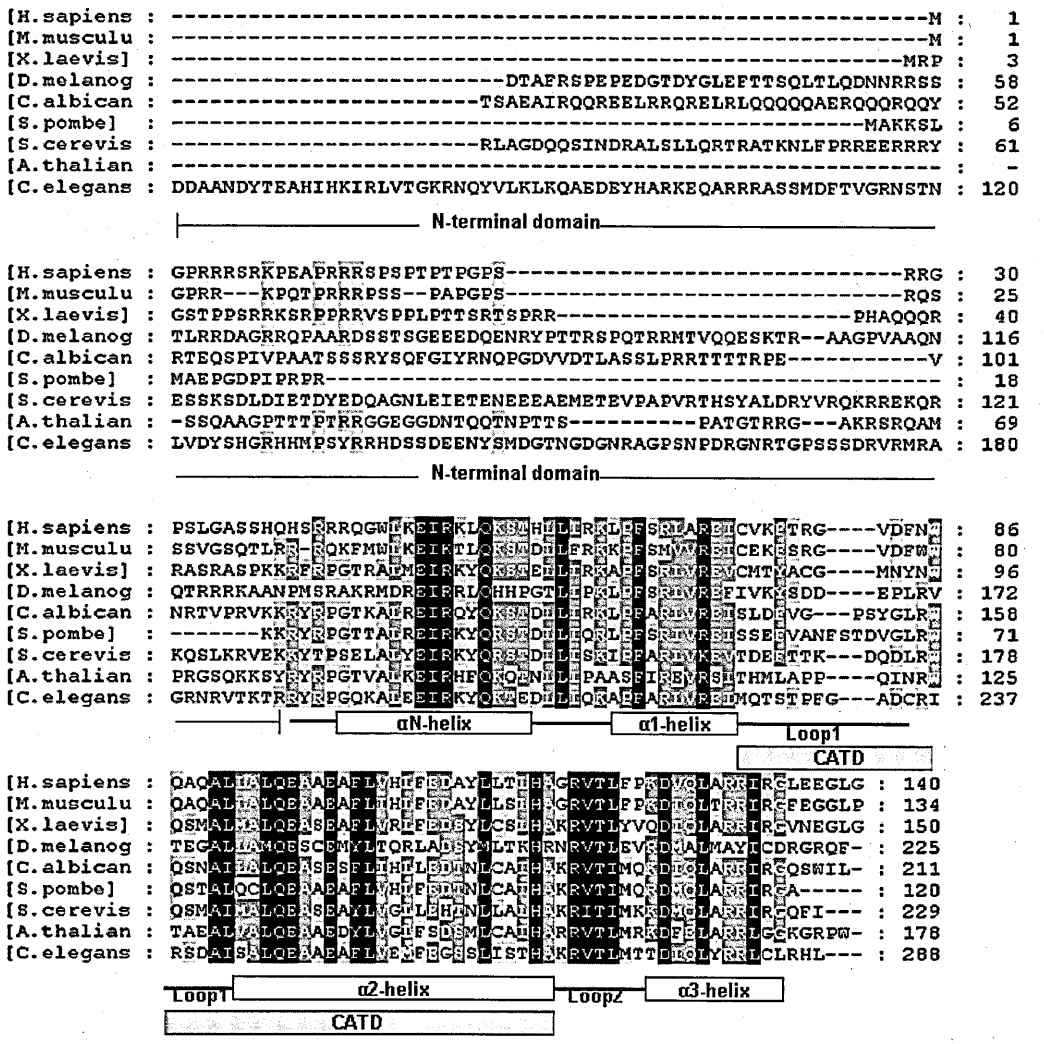

Figure. 3 Multiple sequence alignment of Cse4 orthologs
ClustalW was used for sequence comparision of Cse4 orthologs from different species. The location of the N-terminal tail and the secondary structure of conserved histone fold domain (HFD) are indicated. The position of the CATD, which mediates centromeric targeting of Cse4 and confers distinct structural properties to CenH3-nucleosomes is also indicated.

II. Cell cycle and its phases

Cell division is a very important process in all living organisms. During a cell cycle, a cell grows and divides into two daughter cells containing the same genetic information [3]. Before each division, all the components of the cell need to be duplicated. Of these processes, DNA replication (S phase) and chromosome segregation (M phase) are of special importance. It is crucial that the genetic information is passed onto the next generation by a careful duplication of DNA and a proper distribution of sister chromatids

to each daughter cell. In most eukaryotes, S and M phases are separated in time by the gap phases G1 and G2. If S phase occurs repeatedly without an accompanying M phase, the cell remains viable with several copies of DNA.

The cell cycle is a step-wise process and can be divided into two main phases: Interphase and M phase. Interphase is relatively long when compared to M phase, and it is during this time that the cell prepares itself for the cell division. Interphase is divided into three sub-phases: first gap (G_1), synthesis (S phase), and second gap (G_2) [3]. During G_1 the cell grows and prepares for S phase, producing the proteins necessary to duplicate its genome. DNA replication occurs only once per cycle during S phase, resulting in the formation of a duplicate chromosome known as a sister chromatid. G2 phase is the temporal gap between the end of replication and the beginning of mitosis. The physical separation of the sister chromatids occurs in M phase, in five different stages: prophase, prometaphase, metaphase, anaphase and telophase. In prophase, the chromosomes condense and mitotic spindles form. At this time, each chromosome consists of two sister chromatids. The chromatids are each carefully folded up into very compact structures (condensed chromosomes), which are held together in pairs at kinetochores situated at the centromere. In early prophase, thin fibers (microtubules), are assembling a bipolar spindle. The microtubules attach to the chromosomes and pull them into alignment on the metaphase plate between the two poles of the spindle. When aligned, one chromatid of each chromosome is attached by a microtubule to one pole of the spindle, and the other sister chromatid is attached by another microtubule to the other pole of the spindle. This brief cell state is called metaphase. Triggered by a signal, the glue that holds the sister chromatids together is dissolved allowing each chromatid, separated from its sister, to be pulled by the microtubules to one of the poles of the spindle. The cell is now in anaphase. During telophase, a nucleus reforms around each of the separated bundles of chromatids, and the cell divides at the final step, cytokinesis, in two daughter cells. The daughter cells are then back in G1 phase each having one copy of the genetic information

of the mother cell. The end product of mitosis will be a newly formed cell that is genetically identical to it progenitor [3].

2. Chromosome segregation

Chromosome segregation refers to the coordinated movement of chromosomes to opposite poles of the cell during either cellular reproduction (mitosis) or the production of sex cells (meiosis). Chromosome segregation is an extremely accurate process: for example, chromosome loss in mitosis in yeast occurs once in every 10^5 divisions [53]. In eukaryotes chromosome segregation mechanisums are evolutionarily well conserved. There are a number of components essential to properly segregate chromosomes. The DNA component of the segregation machinery is a specialized, non-conserved sequence called the centromere. Directly over the centromere a large proteinaceous structure called the kinetochore will form. Microtubules emanating from oppositely oriented spindle poles (centrosomes) physically attach to the kinetochore. Using the energy generated by de-polymerization of the microtubules, the sister chromatids are physically separated and pulled in opposite directions. In budding yeast a single microtubule will bind at each kinetochore, while in higher eukaryotes, multiple microtubules can attach to a single chromosome. Once chromosome segregation is complete, one copy of the genome will remain in the original cell and the other copy will have been transferred into what will become the daughter cell.

3. Cell cycle Checkpoints

The cell cycle proceeds by a defined sequence of events where late events depend upon the completion of early events. During division, many kinds of mistakes can be fatal to the cell. In order to avoid catastrophic mistakes/failures, cells are always equipped with "checkpoints" that are set at various stages of the cell cycle. At a "checkpoint" the cell verifies that proper conditions are satisfied at critical steps in cell division. As it progresses through the division cycle, cellular events are monitored by three checkpoints: in G1, G2 and M phases. Before entering S phase, the cell must be large enough and have

undamaged DNA. If these conditions are not met, the cell arrests in G1. When the conditions are satisfied, cells can enter S phase. Before entering mitosis, at the G2 checkpoint, the cell verifies that DNA synthesis is complete. In M phase, two criteria must be achieved. First of all, the chromosomes need to be properly paired and DNA replication needs to be complete. Secondly, the chromosomes must achieve biorientation on the spindle. When these conditions are verified, the metaphase checkpoint is lifted and the cell can divide.

Spindle assembly checkpoint

The spindle assembly checkpoint is very important to ensure equal distribution of chromosomes. Its function is conserved from yeast to humans. This checkpoint basically makes sure the cell met all the criteria to enter the segregation/anaphase stage. This checkpoint detects defects in the spindle structure or in the alignment of chromosomes on the spindle, and delays the onset of chromosome segregation until these defects are corrected. It can also detect more subtle defects, such as the presence of a single kinetochore that is not attached to spindle microtubules [54].

In budding yeast components of the spindle checkpoint have been identified [55, 56], making it possible to determine which defects arrest cells in mitosis by activating the checkpoint, and which induce arrest by other means. Some of the potential defects that activate the spindle checkpoint are spindle depolymerization [55, 56] or microtubule defects [57], presence of multiple minichromosomes and dicentric chromosomes [58, 59], defects in spindle pole body duplication [60, 61], and the inability to form a kinetochore [62].

4. Centromere function and organization in eukaryotes

The centromere is the DNA region where the kinetochore is formed, a structure with the ability to interact with spindle microtubules to ensure separation of chromosomes in mitosis and meiosis. The centromere is of vital importance for genetic stability. Eukaryotic centromeres have evolved over several millions of years. Different organ-

isims have different sizes of DNA sequences at centromeric loci. Although the function of the centromere is conserved across the species, the centromeric DNA is extremely variable in sequences among different species. As discussed above, however, despite this diversity, all centromeres display a unique feature where the canonical histone H3 is replaced by a H3 variant [38,63-66]. The main function of the centromere is to provide a place for kinetochore assembly on each chromosome. Any defects in centromere function or mis-localization of the kinetochore proteins can lead to chromosome mis-segregation, which is associated with human diseases such as cancer [67].

Centromeres can be classified into two types: point centromeres and regional centromeres. The simplest centromere is the 'point' centromere and is found in fungi, including *S cerevisiae*. The budding yeast point centromere is a sequence of only ~125bp and is comprised of three centromeric DNA elements (CDE I-II-III) that are present on each chromosome and are required for full mitotic function [68] (Figure 4A). CDEI and CDEIII are short (10-20bp) sequences conserved on each chromosome, while CDEII is an A+T rich (>90% A+T) non-conserved sequence [68, 69]. Mutational analysis reveals that the majority of nucleotides of the CDE III sequence are essential for proper chromosome segregation [70]. CDE I and CDE II have less stringent sequence requirements to maintain centromere function. Single base pair deletions or insertion in CDE II are well-tolerated, and complete deletion of CDE I does not abolish mitotic segregation [71].

In contrast to the simple centromere of the budding yeast, regional centromeres are considerably more complex. Regional centromeres are found from fungi to humans and can vary greatly in sequence composition. However, all retain some type of repetitive nature. Centromeres in the fission yeast *S. pombe* are the simplest of the regional centromeres. They range from 35-110 kilobases (Kb) in length and are composed of a unique core sequence (cnt) that is flanked by a set of inner (*inr*) and outer (*otr*) repeats (Figure 4) [72, 73]. In Drosophila, centromeres are located in repeated DNA. The only Drosophila centromere characterised at the DNA level corresponds to a 420 kb long re-

gion composed of tandem arrays of short satellite DNA repeats interrupted by transposable elements [74, 75]. There are two adjacent blocks of microsatellites, AATAT and TTCTC satellites, that are interspersed with transposons as well as AT-rich DNA [74]. Similarly, in human cells, centromeres are made up of highly repetitive DNA known as alpha-satellite arrays extending for 0. 1–4Mb. Alpha satellite sequences were first discovered in the human genome. Each repeat is approximately 171 bp [76]. Though all human centromere are composed of alpha satellite DNA, organization of alpha satellite varies from centromere to centromere. Plant centromeres too are 'regional', containing variable amounts of tandem arrays of satellite repeats and transposable elements [77-79].

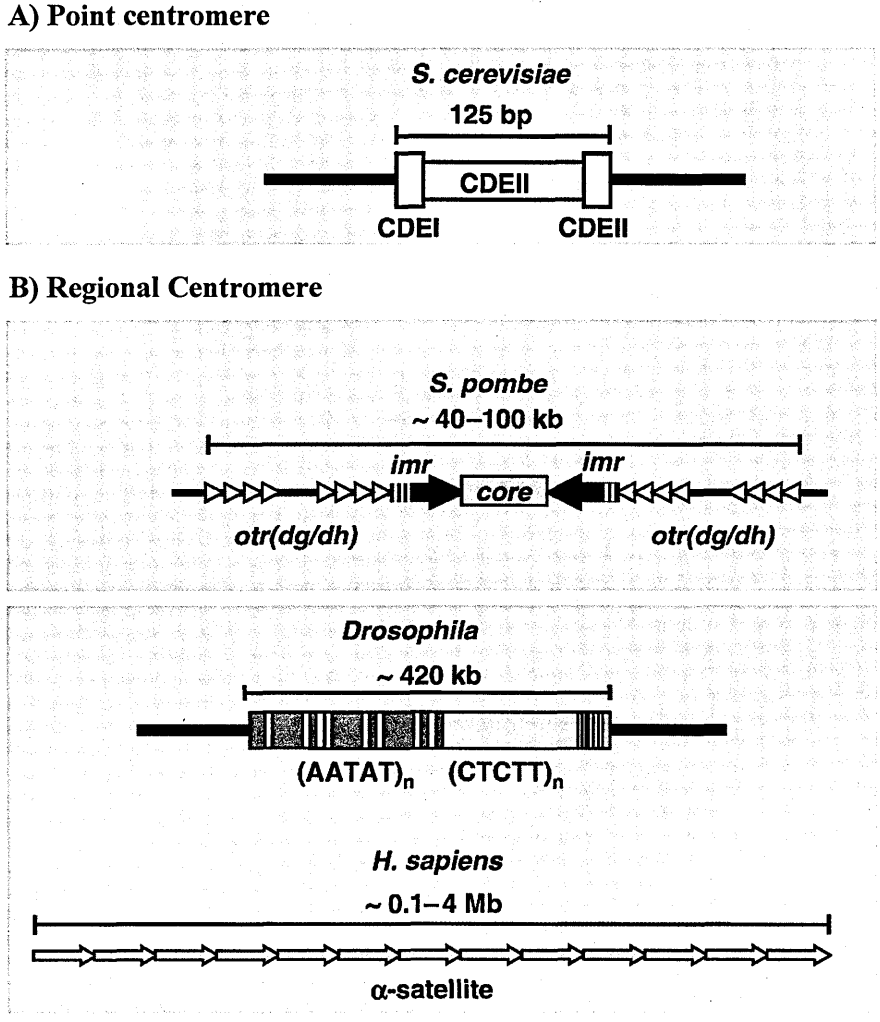

Figure: 4 Structural organization of the eukaryotic centromeres
Schematic depiction of centromeric DNA in A) The budding yeast "point" centromere, is a 125 bp consensus sequence comprised of three centromeric DNA elemetnts: CDE I, CDE II, and CDE III. B) Regional centromeres, in fission yeast possess the simplest of

the "regional" centromeres. In drosophila and humans centromeres are generally large chromosomal regions. Adapted from Torras-Llort [33].

5. Structure and function of kinetochores

The kinetochore is a multiprotein complex that assembles on centromeric DNA and mediates the attachment and movement of chromosomes along the microtubules of the mitotic spindle. Kinetochore proteins functions are evolutionarily conserved. Eukaryotic kinetochores are more complex and a large number of kinetochore proteins have been identified. The simplest known kinetochores are those found in budding yeast. However, even these kinetochores consist of >65 different protein subunits [80, 81] (Table 2). Many of the kinetochore proteins are conserved from yeast to humans [82]. The kinetochore proteins are grouped into three functional groups: 1) inner kinetochore proteins function at the interface with centromeric DNA, 2) central kinetochore proteins function at the interface between the inner and outer kinetochore proteins, and 3) outer kinetochore proteins function at the interface with spindle microtubules. Kinetochore assembly is thought to be hierarchical in nature. The first step of kinetochore assembly occurs shortly after DNA replication. The inner kinetochore protein binds to DNA and facilitates the recruitment of additional kinetochore proteins and protein comlexes. In budding yeast the inner kinetochore CBF3 complex (Ndc10p, Cep3p, Ctf13p, and Skp1p) directly binds to CDE-III [83]. In the absence of CBF3, kinetochore function is abolished *in vivo* and *in vitro*. The yeast inner kinetochore also contains three additional DNA binding proteins, Cbf1, Mif2 and Scm3. Cbf1 binds to CDE I and is not essential for kinetochore function but induces bending of DNA [84]. In higher eukaryotes CENP-B has structural similarity and limited sequence identity to Cbf1, binds to centromeric DNA, and also induces bending [85]. Mif2 protein has sequence similarity to CENP-C and also binds to centromeric DNA near Cbf1 [86]. Scm3 is a recently identified protein which also binds to DNA *in vitro* [52]. After the localization of the inner kinetochore components, the proteins of the central kinetochore are recruited to the centromere. This

central kinetochore protein mediates the linkage between the inner and outer kinetochore [87-90]. The most critical function of outer kinetochore proteins is to connect chromosomes to microtubules. These proteins can include motor proteins such as kinesin and dynein, which play roles in chromosome movements and anaphase A [91]. The outer kinetochore also comprises the proteins which are responsible for the regulation and maintenance of the kinetochore itself.

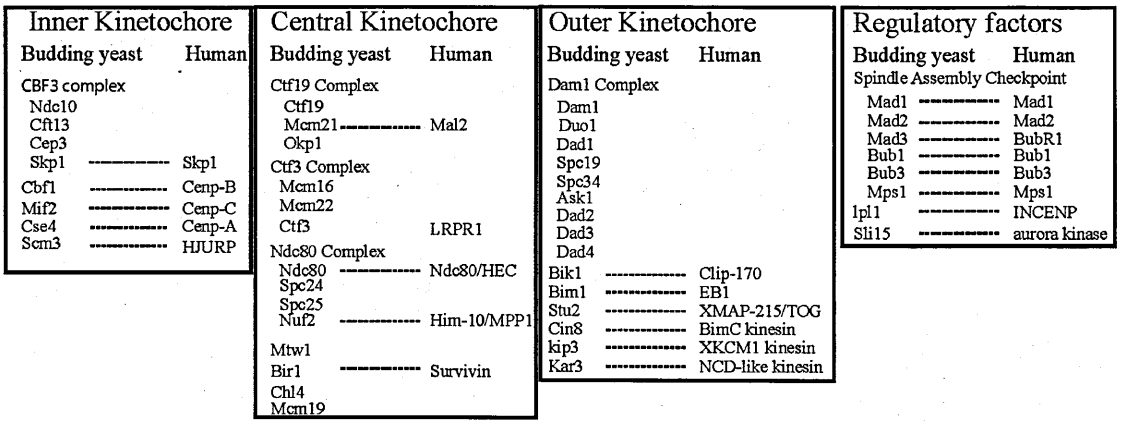

Table. 2 Budding yeast kinetochore and their homologues
Classification of budding yeast kinetochore proteins based on known function and interations within the kinetochore. Proteins essential for viability in yeast are shown in red and those that are non-essential are shown in black. If applicable, the human ortholog for each protein is listed. Adapted from Cheeseman *et al.* [80].

III. Budding yeast as a model system to study regulators, composition and structure of centromeres.

There are a number of organisms being used as a model system to understand biological processes. These include one of the first model systems for molecular biology, the prokaryotic bacterium, *E. Coli,* to single and multiple cell eukaryotic organisms. Model organisms are generally selected based on the wealth of biological data and ease of experimental manipulation that makes them attractive to study as examples for other species including humans that are more difficult to study directly. The *Saccharomyces cerevisiae* system model has a number of special attributes that make it uniquely attrac-

tive as an experimental system for the analysis of many cellular processes. First of all, its genome is fully sequenced and is composed of about approximately 6000 functional genes [92]. It posesses 70,000 positioned nucleosomes occupying 81% of the genome [93]. The human genome, which is estimated to contain approximately 25,000 genes is a more complicated organism [94]. Secondly, budding yeast is a single cell organism with a short generation time (90 min). It can be maintained as a haploid. Therefore, the budding yeast is easy to keep and grow in large volumes and is easier to manipulate genetically. Thirdly, many of the cellular processes in budding yeast, such as DNA replication, recombination, cell division, and metabolism are very comparable to those in higher eukaryotes, such as nematodes, fruit fly, frog, and humans, so the knowledge gained about the control of the budding yeast cell cycle can be used as a basis for our understanding of more sophisticated multicellular organisms. Budding yeast represent a simple eukaryotic model system to study the structure and function of centromeres, since budding yeast centromeres are comprised 125bp of DNA packaged in to a "single" nucleosome. This streamlined centromere combined with the ease of genetic manipulation makes budding yeast an excellent model system for our studies.

IV. Aim and Scope of this study

Faithful segregation of chromosome dependes on several critical factors, among them the assembly of kinetochores and attachment of chromosomes to microtubules. Kinetochore assembly is dependent on the assembly of centromeric nucleosomes, as these nucleosomes specify the site of and form the foundation for kinetochore assembly. Recent evidence shows that while Scm3 is necessary to recruit Cse4 at centromeres, it is also required throughout the cell cycle in budding yeast [52]. In this context we have analysed the functional role of Scm3 in regulating centromeric nucleosome assembly.

Chapter 2.

Materials and Methods

I. Bacteria culturing and strains

The *Escheria coli* strain DH5α was used for all standard cloning and plasmid preparation techniques. One Shot library efficiency chemically competent *E. coli* (Invitrogen) were used for all standard plasmid transformations. All *E. coli* strains were grown in Luria Bertani (LB) growth media supplemented with appropriate antibiotics at 37°C. Ampicillin and Kanamycin were used at 100 μg/ml and 25 μg/ml respectively.

1. Plasmid manipulation

Standard restriction digest cloning was performed using techniques found in Molecular Cloning: A Laboratory Manual [95]. All restriction enzymes, calf intestinal phosphatase (CIP) and T4 DNA ligase were obtained from New England Biolabs (NEB) and used with supplied buffers at recommended concentrations. Constructs for cloning were amplified from genomic or plasmid DNA using standard polymerase chain reaction (PCR). Phusion polymerase (Finnzymes) was used for high fidelity PCR as per supplied protocol. Primers for cloning and sequencing were synthesized by Integrated DNA Technologies (IDT). Plasmid sequencing was performed in the Stowers Institute for Medical Research molecular biology facility using ABI 3730 48-capillary DNA analyzers. The reactions were performed by PCR according to Applied Biosystems protocols (Big Dye Terminator ver. 3. 1). Unincorporated nucleotides were removed by exclusion columns from Edge Biosystems or by SPRI technology from Agencourt. Sequencing results were analyzed using VectorNTI Contig Express (Invitrogen). For constructing the H3/Cse4 hybrid, the region from A76 through I113 of H3 was replaced by the corresponding region containing the loop 1 and α2 helix of Cse4 (T166 through L206) based on previous studies [48].

2. Expression and purification of recombinant protein

The expression vector pET15-HIS-Scm3 encodes a N-terminal 6-Histidine tagged Scm3 protein (6xHIS-Scm3), and was a gift of Carl Wu (NIH, Bethesda, MD). For expression of recombinant 6-HIS Scm3, pET15-HIS-Scm3 was transformed into One Shot BL21 Codon Plus competent *E. coli* (Invitrogen). Recombinant 6xHIS-Scm3 expression was induced by addition of IPTG (0. 3 mM final). Cultures were induced at 25°C for 4-6 hours. Expression of 6xHIS-Scm3 was monitored by polyacrylamide gel electrophoresis and subsequent Coomasie Brilliant Blue staining (Bio-Rad). 5L cultures were used for each round of expression. *E. coli* were lysed by sonication in the presence of high salt lysis buffer (1X PBS, 500 mM NaCl, 10 mM imidazole) supplemented with protease inhibitors (Complete tablets, Roche) and lysozyme (1 mg/ml) and Benzonase (25 U/ml, Novagen). Lysates were cleared via ultracentrufigation, and 6xHIS-Scm3 was isolated using Talon metal affinity resin (BD Biosciences). After several hours of incubation with the lysate, Talon resin was collected in an disposable chromatography column (Bio-Rad), washed with several column volumes (CVs) of wash buffer (1X PBS, 500 mM Nacl, 20 mM imidazole), and protein was eluted from the resin with several CVs of elution buffer (1X PBS, 500 mM NaCl,150 mM imidazole). Lysate, flow-through, wash, elution and bead-bound fractions were all subjected to PAGE (polyacrylamide gel electrophoresis) and Coomasie blue staining. To further polish the 6xHIS-Scm3 prep and to remove any contaminating proteins the eluate, from the talon beads was subjected to fast pressure liquid chromatography (FPLC). The eluate was diluted ten fold with FPLC running buffer (50 mM NaPO4, 10% glycerol) and loaded onto a HiTrap MonoQ anion-exchange column (Amersham) using an AKTA FPLC system (Amersham). Bound 6xHIS-Scm3 was eluted from the column using an increasing gradient of NaCl from 0-500 mM. 6xHIS-Scm3 elutes at ~50 mM NaCl. All collected fraction were subjected to PAGE and Coomasie blue staining. For Scm3 lethal mutants (pET15-HIS-Scm3-Δ25N and pET15-HIS-Scm3-I110H) we used the same protocol.

Yeast recombinant histones (H3, H4, H2A, H2B, and Cse4) were individually expressed in *E. coli* and purified from inclusion bodies as previously described [96].

3. Reconstitution of protein complexes

Both H3-containing and Cse4-containing histone octamers were reconstituted by using established protocols (Luger et al. , 1999). Briefly, equal molar amounts of the four purified recombinant histones (H2A, H2B, H3 and H4, or H2A, H2B, Cse4 and H4) were dissolved in unfolding buffer (7M guanidine-HCl, 20mM Tris-HCl, pH7. 5, 10mM DTT) at 2mg/ml. This histone mixture was dialyzed against four changes of two liters each of refolding buffer (10mM Tris-HCl, pH7. 5, 1mM EDTA, 5mM -mercaptoethanol, 0. 1mM PMSF) containing 2M NaCl for overnight at 4°C. The mixture was transfered to 1. 5ml Eppendorf tubes and centrifuged at 15,000 rpm in a micro-centrifuge to remove any insoluble material. Reconstituted octamers were separated from H2A-H2B dimers and H3-H4 or Cse4-H4 tetramers by size fractionation on a Superdex 200 column (Amersham Biosciences, Inc.) and an AKTA FPLC (GE Healthcare) in refolding buffer containing 2M NaCl.

Reconstitution of Scm3-Cse4-H4 complex from individually purified proteins was performed by using the same reconstitution protocol as for histone octamer reconstitutions except Scm3-Cse4-H4 mixture was dialyzed against six changes of one liter each of refolding buffer (10mM Tris-HCl, pH7. 5, 1mM EDTA, 5mM -mercaptoethanol, 0. 1mM PMSF) containing 2M NaCl for two days at 4°C. The complex was further purified by size fractionation on a Superdex 200 PC 3. 2/30 gel filtration column (Amersham Biosciences) on a SMART system (Pharmacia Biotech). The second method used to purify the Scm3-Cse4-H4 hexamers was addition of 6xHIS-Scm3 to preassembled octamers in hexamer reconstitution buffer (2 M NaCl, 10 mM Tris 7. 5 pH) followed by gel filtration using a Superdex 200 PC 3. 2/30 gel filtration column (Amersham Biosciences) on a SMART system (Pharmacia Biotech).

4. *In vitro* chromatin assembly

The assembly of chromatin was performed as previously described [97, 98]. Briefly, 200ng of plasmid was relaxed with Topoisomerase I. Purified canonical or Cse4 containing octamers (H3 or Cse4/H2A/H2B/H4) or Scm3/Cse4/H4 complex, and 6xHIS-Scm3 or lethal mutants were added and incubated for 2 hr at room temperature in the presence of Topoisomerase I with 8. 3 mM HEPES pH 7. 4, 0. 5 mM EGTA, 0. 65 mM $MgCl_2$, 1. 7% glycerol, 0. 005% NP-40, 33 mM KCl, 0. 33 mM DTT, and 0. 02 mg/ml BSA. Plasmid DNA was deproteinized and purified by standard methods, and then topoisomers were resolved in agarose gels. Recombinant topoisomerase I was a kind gift from S. Venkatesh, Stowers Institute. There are two plasmid used: 1) pG5E4-5S contains five repeats of 5S flanking each side of an E4 core promoter downstream of five Gal4-binding sites (gift from the Workman lab, Stowers Institute) and 2) pCEN1-10X contains 10 tandem repeats of Centromere 1 sequence.

5. Labeling and purification of labeled histones

Histones are labeled with fluorescent dyes using established method [99]. Briefly, H4 was mutated to engineer a single cysteine at site T71 [100]. The modified histone is then individually bacterially expressed, purified and lyophilized. The lyophilized histone is resuspended to 0. 1 mM in Labeling Buffer (20 mM Tris, pH 7. 0, 7 M Guanidinium HCl, 5 mM EDTA) at room temperature. The histone is incubated for 2 hours after addition of 0. 5 M, pH 7. 0 TCEP (tris 2-carboxyethyl phosphine) (Pierce) to a final concentration of 1. 25 mM. Maleimide conjugated Alexa Fluor 488 (Invitrogen) is dissolved to 100 mM in Labeling Buffer and added to the histone at 3 mM final concentration. The reaction is kept in the dark at room temperature for 3 hours, and is subsequently stopped by adding beta-mercapto-ethanol to a final concentration of 80 mM. A small aliquot of the reaction is saved for quantification later. Unreacted dye is removed from the remaining reaction by six successive rounds of concentration and dilution at room temperature using a Microcon unit with a 10 kDa MW cut-off (Millipore). Each

round consists of concentrationto one-third the original volume followed by resuspensionto the original volume with Labeling Buffer. A fresh Microcon unit is used for each round. Labeled H4 was used to make Cse4 containing octamers.

6. Mass Spectroscopy

The percentage of Alexa Fluor 488 labeling on H4T71C was determined by multidimensional protein identification technology (MudPIT). MudPIT mass spectrometry (MS) was performed by the Stowers Institute proteomics facility using the following protocol. TCA-precipitated proteins were resuspended in 30 µl of 100 mM Tris-HCl, pH 8. 5, 8 M urea, reduced with 5 mM TCEP (Tris(2-Carboxylethyl)-Phosphine Hydrochloride, Pierce), and alkylated with 10 mM CAM (chloroacetamide, Sigma). As described in [101], a two-step digestion procedure was used. Endoproteinase Lys-C (Roche) was added to 0. 5 µg for at least 6 hours at 37°C, and then the sample was diluted to 2 M urea with 100 mM Tris-HCl, pH 8. 5. Calcium chloride was added to 2 mM and the digestion with trypsin (0. 5 µg) was incubated overnight at 37°C while shaking. The reaction was quenched by adding formic acid to 5%. The peptide mixtures were then loaded onto 250 µm fused silica microcapillary columns packed first with 3 cm of 5-µm Strong Cation Exchange material (Partisphere SCX, Whatman), followed by 1 cm of 5-µm C_{18} reverse phase (Aqua, Phenomenex). Loaded 250 µm columns were connected using a filtered union (UpChurch) with 100 µm fused-silica columns pulled to a 5 µm tip using a P 2000 CO2 laser puller (Sutter Instruments) and packed with 9 cm of reverse phase material. The split three-phase column was placed in-line with a Quaternary Agilent 1100 series HPLC pump. Overflow tubing was used to decrease the flow rate from 0. 1 ml/min to about 200–300 nl/min. Fully automated 10-step MudPIT runs were carried out on the electrosprayed peptides.

MS/MS spectra were first searched using SEQUEST and without specifying differential modifications against a protein database 54404 non-redundant sequences, consisting of 27026 *E. Coli* proteins and budding yeast H4 mutant T71C sequence, 177

usual contaminants (such as human keratins, IgGs, and proteolytic enzymes), and, to estimate false discovery rates, 27202 randomized amino acid sequences derived from each non-redundant protein entry. To account for alkylation by CAM, +57 Da were added statically to cysteine residues.

As described in [102], differential modification searches were set up to query a protein database containing only the sequences for budding yeast H4-T71C for peptides containing AF488 labeled cysteine (+641 Da, the difference between AF488 molecular weight 698 Da and alkylation 57 Da). After this round of search, an in-house developed script, sqt-merge, was used to combine the SEQUEST output files (sqt files) generated from the normal search (i. e. without modifications) and PTMs searches described above into one set. This merging step allowed only the better matches out of the normal and the differential SEQUEST queries to be ranked first. For the second round of searches, only spectra matching modified peptides were selected (-m 0 –t 0 DTASelect parameters), and their coordinates written out into smaller ms2 files using the "-- copy" utility of DTASelect. These subsetted ms2 files contained at best a few hundred MS/MS spectra and were subjected to the same differential search against the complete database described above (including shuffled sequences). Again sqt-merge was used to bring together the results generated by these different searches. This step allowed us to check that spectra matching modified peptides from budding yeast H4-T71C sequences did not find a better match against the larger protein database. Spectra/peptide matches were only retained if they had a DeltCn of at least 0. 08 and, minimum XCorr of 1. 8 for singly-, 2. 0 for doubly-, and 3. 0 for triply-charged spectra. In addition, peptides had to be fully-tryptic and at least 7 amino acids long. DTASelect (Tabb, McDonald et al. 2002) was used to select and sort peptide/spectrum matches passing this criteria set. U_SPC6 software(in-house by Tim Wen) was used to extract total and modified spectral counts for each amino acid within Sc H4-mutant T71C and calculate modification levels based on local spectral counts.

II. Yeast culturing and strains

Yeast strains used were constructed in the W303 background for biochemical and genetics assays and S288C was used for microscopic studies. For a complete list of yeast strains used see appendix 1. In general, yeast were grown at 30°C for wild type (WT) strains. The various epitope-tagged and knock-out strains were constructed by homologous integration using yeast transformation as previously described [103]. Yeast transformation was carried out using the standard LiOac transformation method. Yeast growth on rich medium was carried out on either yeast-peptone-dextrose (YPD) or YP-Galactose. When nutritional selection was required, yeast were grown on either synthetic dextrose or synthetic galactose (SD or SGal) medium supplemented with the appropriate amino acid drop-out powder (Clontech). The antibiotics Geneticin (G418) and Hygromycin were used at 200 μg/ml and 300 μg/ml respectively. G1, S-phase and G2/M arrests were achieved using final concentrations of 5μM α-factor (Zymo Research), 0. 2M Hydroxyurea (Sigma), or 15 μg/ml nocodazole (Sigma) respectively.

1. Chromatin immunoprecipitation

For chromatin immunoprecipitation (ChIP), 220-500 ml yeast cultures were grown to mid-log phase prior to any cell cycle arrest or harvest for ChIP. Cross-linking of cultures was done with formaldehyde (1% final) for 10 minutes and chromatin was harvested by beatbeating in the presence of lysis buffer (100 mM Tris pH 7. 5, 150 mM NaCl, 0. 1 mM EDTA, 1 mM DTT, 0. 1% NP-40, 10% glycerol) plus protease inhibitors (Complete tablets, Roche). For lower resolution ChIP studies, chromatin was sonicated to obtain fragments ~300-500 base pairs (bps) in size. For high-resolution mononucleosome ChIPs, $CaCl_2$ (3 mM final) and micrococcal nuclease (MNase) were added (~250-500 units, Worthington) to the chromatin after beatbeating and lysates were incubated at 37° for 30 min. in lieu of sonication. The MNase reaction was stopped by addition of EDTA and EGTA to 25 mM each and placing lysates at 4°C. Lysates were then

cleared by sonication (15K rpm, 15 min.) and diluted 1:10 in IP dilution buffer (0. 01% SDS, 1% Triton X-100, 1 mM EDTA, 20 mM Tris pH 7. 5, 150 mM NaCl, protease inhibitors). Input samples and no antibody controls were taken at this time. Primary antibodies were all used at a 1:500 dilution unless otherwise noted. Antibodies used for ChIPs are as follows: αHA (12CA5, Roche), αMyc (Santa Cruz, 9E10), and αFlag M2 (Sigma), αH2B (gift from Carl Wu- NIH 1:1000, Lake Placid AR-0264), αH4 (Abcam 31287, Millipore 05-858). Lysates were incubated with primary antibody overnight (ON) and harvested by incubation with Protein G sepharose (Amersham) for several hours-ON. Protein/DNA bound beads were extensively washed with TSE-150 (0. 01% SDS, 1% Triton X-100, 1 mM EDTA, 20 mM Tris pH 7. 5, 150 mM Nacl), LiCl detergent wash (1% NP-40, 1% DOC, 1 mM EDTA, 10 mM Tris, 250 mM LiCl) and TE (pH 8). In the case where cultures were not crosslinked the beads were washed several times with lysis buffer and TE. After the final TE wash ChIP samples were eluted with SDS lysis buffer (TE pH 8, 1% SDS) at 42°C for 30 min while shaking. After elution, the crosslinks are then reversed by addition of NaCl to 300mM and incubation at 65°C ON. Eluates were treated with RNase and Proteinase K for several hours, phenol-chloroform extracted and EtOH precipitated.

2. Immunoprecipitation, Co-Immunoprecipitation, and Western Blotting

Whole cell extracts for co-immunoprecipitation (Co-IP) were obtained by bead-beating in the presence of lysis buffer (100 mM Tris pH 7. 5, 150 mM NaCl, 0. 1 mM EDTA, 1 mM DTT, 0. 1% NP-40, 10% glycerol, protease inhibitors). Chromatin fractionation was performed as previously described [104]. Co-IPs were performed with αMyc antibody (Santa Cruz, 9E10), αFlag M2 (Sigma) and αH3 (Abcam) and were all used at 1:500 dilution. IPs were harvested on proteinG sepharose beads. Beads were washed several times with lysis buffer and eluted in SDS buffer (1% SDS, TE). Denaturing PAGE was performed on the eluates using the Novex 4-12% bis-tris pre-cast PAGE gel system (Invitrogen) as per the manufacturer's protocol. Electrophoresed IPs

were transferred to a nitrocellulose membrane and Western blots were performed using standard molecular biology protocols [95]. Primary antibodies for Western blots were as follows: αMyc antibody (Santa Cruz, 9E10, 1:5000), αFLAG M2 (Sigma, 1:5000), αH2B (Lake Placid Biologicals, 1:5000), αH4 (Abcam 31827, 1:1000, Millipore 05-858, 1:1000). Polyclonal rabbit antibodies against a c-terminal Scm3 peptide (aa210-223) and Cse4 were generated and affinity purified by YenZym Antibodies, and used at 1:5000 & 1:10000 respectively. For visualization of Western blots, a horseradish-peroxidase (HRP) coupled secondary antibody (αMouse-HRP, αRabbit-HRP, GE Health-care) was used in conjunction with an ECL detection kit (Amersham). Westerns were exposed onto BioMax imaging film (Kodak) and developed using an X-O200A processor (Kodak).

3. Quantitative PCR

All Quantitative PCR (pPCR) was performed on an iCycler real-time PCR machine using IQ Sybr Green Supermix (Bio-Rad). Specific primer sets used were Centromere 1, forward 5'TGACATTGAACTTCAAAACCTTT3' and reverse 5'GGCGCTTGAAATGAAAGCTC3' and cetromere 3, forward 5' GATCAGCGCCAAACAATATGG3' and reverse 5'AACTTCCACCAGTAAACGTTTC3', as previously described [52, 105]. PCR of ChIP DNA was quantified for biological replicates by comparing IP and total input samples against a standard curve established with PCRs of serial 10-fold dilutions of genomic DNA. Dynamic well factors were used and cycling parameters were as follows: 94°C/30 sec., 50°C /30 sec., 72°C /30 sec. repeated 40X. A melt curve analysis was performed starting at 50°C /10 sec. and increasing 0. 5°C /cycle for 80 cycles, with all primers used exhibiting a single melt peak. Occupancy levels were determined by dividing the average of the ChIP DNA by the relative abundance of a control total chromatin sample. This ratio represents the enrichment of ChIP DNA over the input DNA for a specific target. All ratios for biological replicates routinely fell within 10% of each other for a given experiment. · No antibody controls were

performed for all qPCRs.

4. Flow cytometry

FACS - Fluorescence activated cell scanning (FACs) was performed to confirm all cell cycle arrests. For FACs analysis, cells were fixed in 70% EtOH followed by a wash in FACS buffer (50 mM Na Citrate). Fixed cells were then resuspended in FACs buffer, treated with RNase (Sigma), stained with 1 μM final Sytox Green (Molecular Probes), and analyzed using a Cyan cytometer (Dako Cytomation). FACs data was analyzed using FlowJO cytometry software (Treestar Inc.).

III. Microscopic techniques

All microscope images were acquired using a Carl Zeiss LSM-510 Confocal microscope (Jena, Germany), outfitted with a ConfoCor 3 module and two single-photon counting avalanche photodiodes (APD's). A C-Apochromat 40x 1. 2 NA water objective was used. A HFT 488/561 main dichroic allowed excitation of GFP (488 nm laser line) and mCherry (561 nm laser). A secondary NFT 565 beam splitter was used as an emission dichroic. After passage through a 505-550 nm BP or LP 580 filter for GFP and mCherry, respectively, photon counts were collected on APD's in single photon counting mode.

1. Fluorescence Correlation Spectroscopy (FCS) calibrated intensity measurement of number of Cse4-GFP molecules in the centromere.

In order to quantify the number of Cse4-GFP molecules in the yeast centromere, we took advantage of the unique ability of FCS to determine the number of molecules in the focal volume for a mobile, diffuse protein. Once this was determined, calibrated imaging was performed to compare the spot intensity of centromeric Cse4-GFP to the intensity obtained for this diffuse protein using identical imaging parameters. The maximum intensity of a single immobile fluorophore (also defined as the molecular brightness, ε) can be determined from the intensity of a solution of known concentration: $\varepsilon = I/N$ [106]. N here is the number of particles in a predefined volume (e. g. the focal volume) which

can be accurately determined using FCS measurements (see below). Once the intensity of a single particle is determined, it is straightforward to determine the number of particles in a diffraction limited puncta: $N_{puncta} = I_{puncta}/\varepsilon$. Note that all immobile intensities here refer to the maximum intensity of the observed diffraction limited spot. We emphasize that this method calculates Cse4-GFP molecules in the centromere from first principles, without the need to make any assumptions about concentration of any control samples or proteins.

For this method, we used as a control cytosolic eGFP under the control of the endogenous BZZ1 promoter in yeast [107]. As it is driven under an endogenous promoter at one gene copy per cell, concentration on a cell by cell basis is remarkably consistent. Previous analysis has shown that cytosolic GFP in yeast is diffuse, relatively uniform over the yeast cell, and mobile [107]. Using the Zeiss ConfoCor 3, FCS was performed on cytosolic EGFP proteins using the identical imaging set-up described above. A pinhole of 1. 0 airy units was used, with an excitation intensity of approximately 5 μW at the sample. Autocorrelations were calculated from raw data with a bin time of 50 μs. Data processing was performed using custom written plugins for the ImageJ software package. Correlation functions were fit to the following formula using non-linear least squares:

$$G(\tau) = \frac{\gamma}{N\left(1+\frac{\tau}{\tau_D}\right)\sqrt{1+r^2\frac{\tau}{\tau_D}}}.$$

γ is a shape factor reported to be ~ 0. 35 for Gaussian focal volumes [108]. Here, we explicity measured γ using diffraction limited (100 nm) fluorescence beads by collecting three dimensional confocal images of the bead and integrating the signal from the bead as follows:

$$\gamma = \frac{\int PSF^2(\vec{r})dr}{\int PSF(\vec{r})dr}$$

We found γ to be 0. 27 on our microscope with our acquisition conditions. N is the average number of particles in the focal volume, τ_d is the average diffusion time

through the focal volume per particle, and r is the radial to axial size ratio of the focal volume reported to be approximately 5 for systems with a pinhole close to 1 Airy unit [109]. Note the only parameter needed for our calibrated imaging procedure is N, the average number of molecules in the focal volume.

Once N was determined for freely diffusing cytosolic GFP from the FCS measurements, we performed calibrated imaging comparing the yeast strain expressing cytosolic GFP and the yeast strain expressing Cse4-GFP as its sole copy of Cse4 according to the theory presented above. A z-series with 8 total slices was acquired with a 0. 5 μM step size and 6. 4 μs pixel dwell time. Great care was taken to calibrate the system each day and to take images of Cse4-GFP and cytosolic GFP with identical imaging parameters, and only to compare data taken on the same day. For cytosolic GFP, the fluorescent intensity was calculated as the average over approximately 5 square pixels in the most intense region of the cell. As the centromere may be most in focus at any of the z-slices, we took Cse4-GFP intensity in the slice where the centromere was most intense.

To compare the intensity of cytosolic GFP to centromeric Cse4-GFP, we first had to acknowledge that the intensity observed for centromeric Cse4-GFP consisted of two parts. The first part coincided with the intensity from the GFP in the diffraction limited or near-diffraction limited point source of the centromere. The second contribution is due to the nuclear, non-centromeric fraction of Cse4-GFP that resides ontop of, below, and next to the centromere. Due to the size of the focal volume, especially in the z-dimension, it is not feasible to collect fluorescence emission from solely the centromere, and exclude the nuclear pool directly above or below the point centromere, with standard confocal techniques. To separate fluorescence intensity of centromeric Cse4-GFP from non-centromeric, nuclear Cse4, we fit the intensity residing at the centromere to a 3-dimensional Gaussian (Figure 5) with non-zero background outside the peak. The fit was performed using a grid-search algorithm over the x and y coordinates as well as the standard deviation with linear least squares determination of the best fit amplitude and

background at each point in the grid. This algorithm ensured robust convergence to the absolute best fit for even the noisiest peaks. The non-zero background was subtracted from the peak intensity to give a maximum intensity emanating from the Cse4-GFP in the centromere. This intensity was compared to the intensity of cytosolic GFP taken with identical imaging parameters. This comparison, with the knowledge of the number of cytosolic GFP particles per focal volume, gives us number of Cse4-GFP molecules in the yeast centromere. These calculations were done also as a function of spindle pole distance. For spindle pole measurements, Spc42-mCherry was recorded using 561 nm excitation and emission was collected through a LP 580 nm filter. Distance between the spindle poles was measured in 3D using ImageJ.

To ensure that differences in fluorescence intensity of Cse4-GFP and cytosolic free eGFP were due to differences in concentration and not quenching, fluorescent lifetime images were obtained using pulsed two-photon excitation at 920 nm and the same detection setup as used for confocal imaging. A Becker and Hickl (Berlin, Germany) SPC 830 lifetime system attached to the Zeiss ConfoCor 3 was used. No differences in fluorescent lifetime were observed between the yeast strains, suggesting differences in fluorescence intensity were not artifacts of quenching of GFP in different environments.

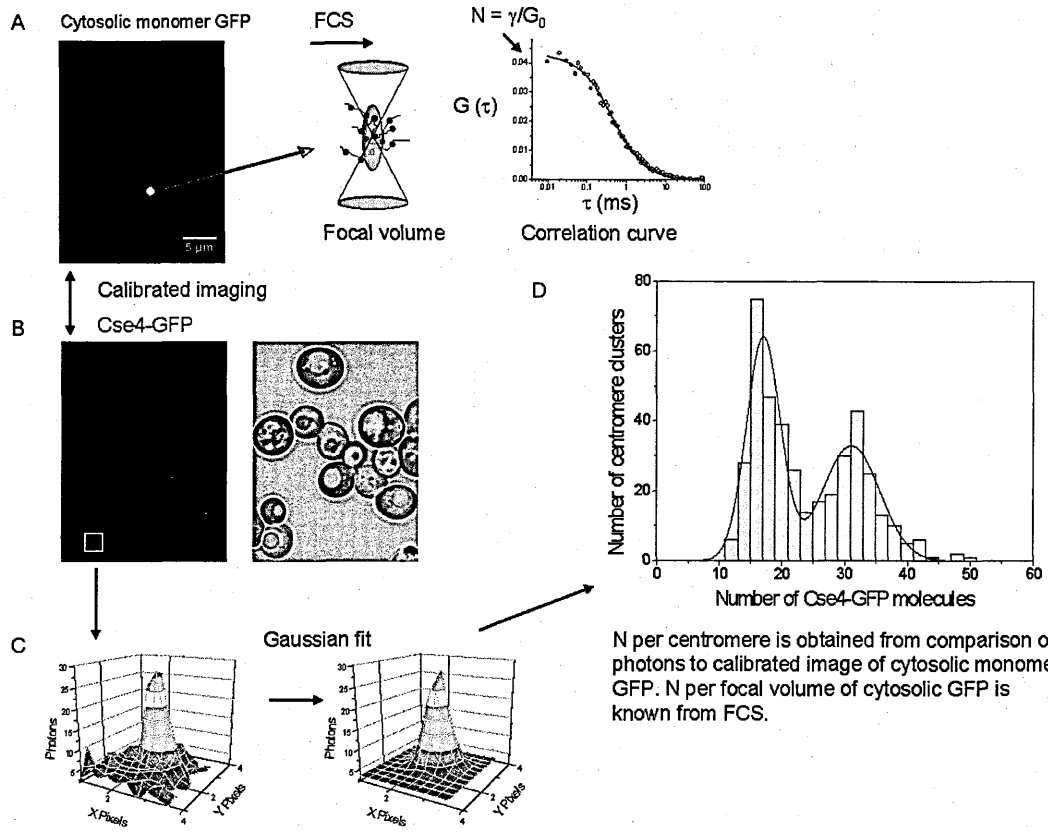

Figure 5. Experimental design to determine the number of Cse4-eGFP per centromere.

A). Yeast strain expressing cytosolic eGFP was analyzed by fluorescence correlation spectroscopy (FCS) to determine the average number of eGFP molecules in the focal volume for this strain. The number of molecules in the focal volume in FCS is determined by γ/G_0, where G_0 is the amplitude of the correlation curve propagated to $\tau = 0$. γ was determined to be 0. 27, consistent with values published for FCS with 1-photon excitation. B. Calibrated images were acquired for cytosolic eGFP(A) and a yeast strain expressing Cse4-eGFP as the only copy of Cse4 from the endogenous loci (B). Identical pixel dwell times of 6. 3 μs were used, and emission photons were collected on single-photon counting avalanche photodiodes. A 3-dimensional z-stack was acquired with 8 total slices, each with 0. 5 μM spacing. A pinhole of 1 airy unit was used to reject out of focus light. Data was spatially binned 2x2 prior to processing. C. To determine number of Cse4-eGFP per each centromere, it was necessary to distinguish the emission emanating from the point centromere from the background nuclear Cse4. Thefore, we selected the z-slice where each centromere was best in focus and fit the centromere profile to a Gaussian, and selected the value of the peak minus the background as the intensity. D. γ from a point source is = 1, therefore we directly compared the intensity of the centromere to the intensity we obtained for cytosolic eGFP using identical imaging parameters. With the known number of molecules of cytosolic eGFP from the FCS measurement, comparison allows for calculation of number of Cse4-eGFP per centromere.

2. Fluorescence Recovery After Photobleaching (FRAP)

FRAP measurements were performed to examine the ability of centromeric Cse4-GFP to exchange with the non-centromeric pool. Yeast cells expressing Cse4-GFP as the only copy of Cse4 were grown to mid-log phase in synthetic complete media, spun down, and sandwiched between a slide and cover slip in a 10% agarose solution made with media. Long time lapse imaging demonstrated yeast cells were alive and divided at a normal rate in the agar pad for up to 4 hours.

Prior to photobleaching, a z-series was taken with 0. 5 μM step size and 6. 4 μs pixel dwell time. Due to the mobility of the centromere in living yeast cells, acquisition of a z-stack was essential to ensure proper quantitation of centromere intensity. After the initial acquisition, either centromeric Cse4-GFP, or Cse4-GFP in the entire cell were irreversibly photobleached by 4 rapid scans with high 488 nm laser power. The ability of the cells to continue to grow and divide was verified to ensure that photobleaching did not damage the cells. After photobleaching, movies were acquired to examine for recovery of the Cse4-GFP at the centromere. In most cases, cells were used that also expressed Spc42-mCherry from a centromeric plasmid to mark the cell cycle. Recovery of centromeric Cse4-GFP was observed as a re-appearance of a punctuate spot centered in the nucleus.

3. Fluorescence resonance energy transfer (FRET) measurements.

FRET between EGFP and mCherry labeled proteins was performed using the acceptor photobleaching method [110]. A diploid yeast strain expressing Cse4-GFP and Cse4-mCHERRY as the only copies from the endogenous locis was used. The fluorescence intensity of the Cse4-GFP was measured at the centromere from the most intense focus of a z-stack with 0. 5 μm spacing, as discussed above. Immediately following the initial z-stack, the Cse4-mCHERRY in the entire cell was irreversibly photobleached using 561 nm excitation. The intensity of Cse4-GFP in the centromere was re-measured after acceptor photobleaching. In the scenario where the donor is undergoing FRET, ir-

reversible photobleaching of the acceptor probe will result in one less pathway for relaxation of the donor, and hence the fluorescence of the donor will increase

Apparent FRET efficiencies for each centromere cluster was calculated as follows: $E = 1 - I_{before} / I_{after}$. Here I_{before} and I_{after} denote the average fluorescence intensity of the donor before and after acceptor photobleaching.

4. *In vitro* FCS measurement of H4 stoichiometry in purified protein complexes

To examine the stoichiometry of H4 in purified complexes *in vitro*, a variation of moment analysis was employed. Once purified complexes were obtained, FCS was used to determine the number of molecules of a sample in the focal volume (see above equation). The overall fluorescence intensity (I) of the measurement was divided by the average number of species in the focal volume (N) to obtain an average molecular brightness of the species (B = I/N). The brightness of these values was compared to the molecular brightness of freely diffusing, non-conjugated Alexa-Fluor 488.

As opposed to the GFP, considerable quenching of Alexa-Fluor 488 in different environments is common. If not corrected for, this quenching will render brightness comparisons meaningless. Therefore, as described above for GFP, fluorescence lifetime measurements of all Alexa-Fluor 488 labeled samples were made and compared to non-conjugated Alexa-Fluor 488. Differences in fluorescence lifetime were used to normalize the molecular brightness comparisons.

Chapter 3.

Functional analysis of Scm3

I. Abstract

The Cse4 nucleosome at each budding yeast centromere must be faithfully assembled during each cell cycle in order to specify the site of kinetochore assembly and microtubule attachment for chromosome segregation. While Scm3 is required for the localization of the centromeric H3 histone variant Cse4 to centromeres, its role in nucleosome assembly has not been tested. We demonstrate that Scm3 is able to mediate the assembly of Cse4 nucleosomes *in vitro*, but not H3 nucleosomes, as measured by a supercoiling assay. Localization of Cse4 to centromeres and the assembly activity depend on an evolutionarily conserved core motif in Scm3, but localization of the CBF3 subunit Ndc10 to centromeres does not depend on this motif. The centromere targeting domain (CATD) of Cse4 is sufficient for Scm3 nucleosome assembly activity. Assembly does not depend on centromeric sequence. We propose that Scm3 plays an active role in centromeric nucleosome assembly.

II. Introduction

The centromere is a cis-acting chromosomal region that provides all living cells with the ability to faithfully transfer their genetic material during mitotic and meiotic cell divisions. The centromere is the location for the assembly of the kinetochore, a multiprotein complex which enables the attachment of chromosomes to the spindle microtubule and ensures the equal segregation of chromosomes to the daughter cells. The budding yeast kinetochore is composed of more than 65 proteins, many of which are evolutionarily conserved from yeast to man [81, 111]. The inner kinetochore or DNA binding layer is comprised of several proteins, including Mif2, the CBF3 complex (Ndc10, Cep3, Skp1, and Ctf13), a centromeric histone H3 variant Cse4, and Scm3, all of which are essential for kinetochore function [50, 52, 66, 112-114]. The CBF3 complex binds specifically to the budding yeast centromere sequence. Budding yeast centromeres con-

sist of ~125 bps divided into three DNA elements: CDE I (14bp), CDE II (87-88bp) and CDE III (11bp) [68, 115]. The Ndc10 subunit of CBF3 is critical to nucleate kinetochores [116, 117]. Cse4, Ndc10 and Scm3 are dependent on each other for efficient localizationto centromeres [52].

While the sequence composition of centromeres is highly variable between organisms, centromeres in all eukaryotes are universally marked by the presence of a centromere specific histone H3 variant, termed CENP-A in humans, Cse4 in budding yeast and CID in *Drosophila melanogaster* [118]. The centromere targeting domain (CATD), consisting of loop 1 and helix 2 of the histone fold domain, is required for centromere loading of centromeric histone variants [47, 48]. Canonical nucleosomes, the basic module of chromatin, consist of 146 base pairs of DNA wrapped around an octamer of four core (H3/H4/H2A/H2B) histones [4]. At the centromeric nucleosome, Cse4 replaces canonical H3 [66]. While the *S. cerevisiae* genome contains approximately 70,000 nucleosomes [93], a single Cse4 nucleosome defines the centromere on each chromosome [97, 119]. The histone fold domain of Cse4 is more than 60% identical to H3 [120], raising the question of how Cse4 is specifically targeted to the centromere sequence.

Histones are often associated with specific chaperones/nucleosome assembly factors that assist their interaction with DNA, both deposition and removal. Nucleosome assembly factors can be defined as factors that associate with histones and stimulate a reaction involving histone transfer. Some histone variants have specific chaperones that play an important function in their deposition [13]. For instance, Chz1 is a histone chaperone that has preference for H2AZ and can deliver H2AZ for SWR1-dependent histone replacement [121]. Nucleosome assembly factors also play an important role in assembly of histone H3. 1 and H3. 3, in a replication dependent and independent manner respectively, thereby differentially marking the active and inactive regions of the genome [10, 11]. It is unknown if there is a specific assembly factor involved in Cse4 deposition at centromeres. One candidate for a Cse4-specific assembly factor is Scm3 (Suppressor

of Chromosome Missegregation 3). Scm3 and its orthologs in *S. pombe* ($Scm3^{sp}$) and humans (HJURP) are required for localization of the centromeric histone variant at centromeres [44, 52, 122]. In additionto its role at the centromere sequence, Scm3 is required to deposit Cse4 at the stable partitioning locus (STB) within the 2μ plasmid [123]. HJURP has been shown to facilitate the association of CENP-A/H4 tetramers with DNA *in vitro* [46].

In budding yeast, Scm3 has been shown to bind to both Cse4 and Ndc10, and is required for their efficient localizationto centromeres, leading to the hypothesis that Scm3 serves as a molecular link between a centromere specific DNA binding complex (CBF3) and the centromeric histone variant [52]. Herein we provide evidence that Scm3 is more than a simple adapter and possesses unique nucleosome assembly activity. The assembly activity depends on an evolutionarily conserved core motif shared with $Scm3^{sp}$ and HJURP. The assembly activity is specific for Cse4, but independent of DNA sequence. Furthermore, assembly activity depends on the CATD of Cse4. We conclude Scm3 plays an active role in the assembly of centromeric nucleosomes.

III. Results

1. Scm3 contains two essential motifs

Scm3 is a relatively small protein (~25 kDa) containing several motifs (Figure 6A). At the N terminal end from amino acids 13-24, there is a putative leucine nuclear export sequence (NES) [50]. There are two short patches of basic residues, similar to bipartite nuclear localization sequences (NLSs) found at positions 54–59 and 148–153 [124, 125]. At its center, Scm3 has an evolutionarily conserved core motif. This motif resembles a coiled-coil domain in that it has repeating heptad units with hydrophobic residues occupying the fourth position and polar residues in the first position [126, 127]. The C-terminal 58 amino acids are acid-rich (40% D + E).

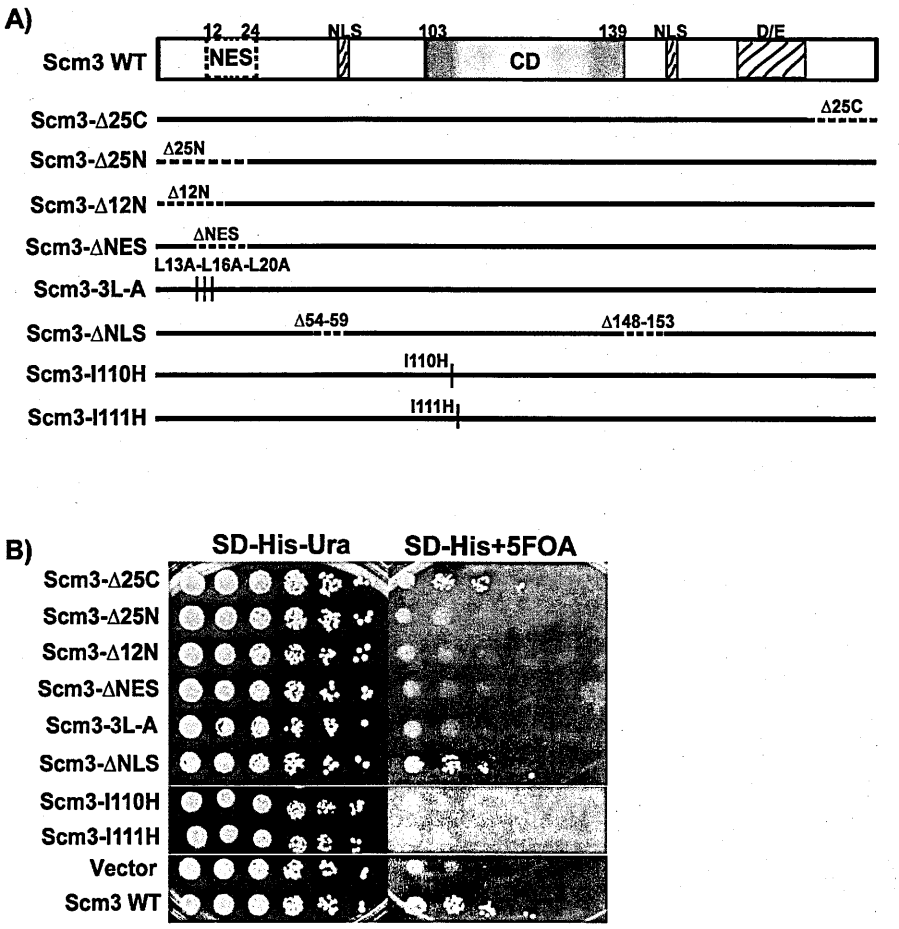

Figure. 6 Mutational analysis of Scm3
(A) Schematic diagrams of wild-type Scm3 and site-directed Scm3 mutants. The nuclear export signal (NES), conserved motif (CD), potential nuclear localization sequence (NLS) and C-terminal acidic (D/E) regions are boxed. (B) Plasmid shuffle complementation tests of mutants shown in (A). Growth on 5-fluroorotic acid (FOA) medium indicates the respective mutant allele provides Scm3 function.

To identify essential motifs we carried out site-directed mutagenesis for each of these motifs and tested the mutant proteins for function using a plasmid shuffle assay (Figure 6B). Deletion of either the C-terminal 25 amino acids (Scm3-Δ25C) or the bipartite NLS (Scm3-ΔNLS) did not result in a loss of growth. In contrast, mutations in evolutionarily conserved residues in the central motif or deletion of the N-terminal 25 amino acids (Scm3-Δ25N) were lethal. To further define the essential portion of the N-terminal region we deleted residues 2-12, 13-24 (which contains the NES motif), or mutated the leucines in the NES motif. All of these mutations were lethal, suggesting that

the NES as well as the amino acids upstream are essential, consistent with previous mutational analysis of Scm3 [50]. We conclude that Scm3 has two essential motifs, the N-terminal 25 amino acids and the conserved core motif.

2. The conserved motif of Scm3 is essential for interaction with Cse4 and its localizationto centromeres

Scm3 physically associates with Cse4 and Ndc10 [50-52]. We tested the proficiency of the lethal mutants for interactions with Cse4 and Ndc10 *in vivo*. For this study we have used a Gal-*SCM3* conditional allele ($pGal_{1\text{-}10}$-3HA-*SCM3*) so that we can shut off the wild-type chromosomal copy of Scm3 by switching to glucose medium for 2hr. This switch eliminates Scm3 as measured by western blotting [52]. Mutant versions of Scm3 are Flag tagged on a plasmid under the control of the endogenous promoter. Results shown in Figure 7 reveal that point mutations (I110H, I111H) in the conserved motif of Scm3 disrupt the interaction with Cse4 while deletion of the N terminus of Scm3 (Scm3-Δ25N) does not disrupt this interaction (Figure 7A). However, all the lethal mutants interact with Ndc10 (Figure 7B). These results demonstrate that the conserved motif is important for interaction with Cse4.

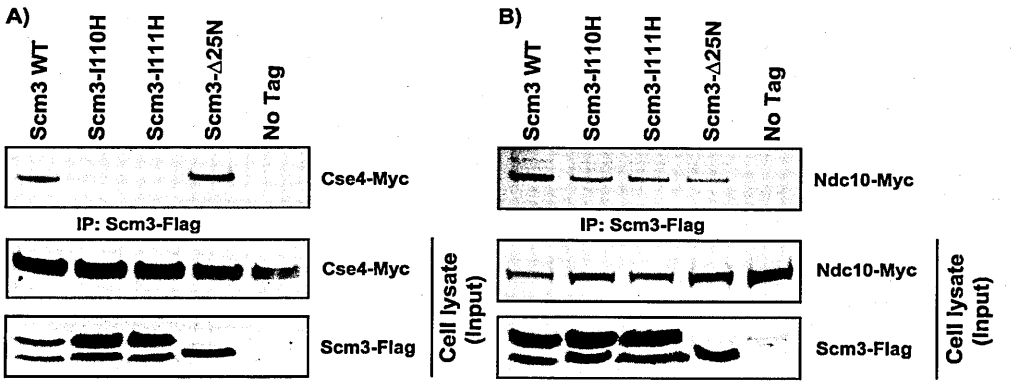

Figure 7. Co-immunoprecipitation of Scm3 mutants with Cse4 and Ndc10
Immunoprecipitations of Scm3-FLAG mutants were performed in a background containing Cse4-myc or Ndc10-myc "No Tag" indicates that Scm3 does not have FLAG tag. Western blotting was carried out with anti-myc antibody. Full-length Scm3-Flag often runs as a doublet for reasons that are currently unclear. (A) The evolutionarily conserved motif is required for Cse4 interaction. Point mutants in this motif no longer interact with Cse4. When the 25 N terminal amino acids of Scm3 are deleted, this protein

still pulls down Cse4. (B) Both point mutants in the conserved motif and deletion of 25 amino acids from N-terminus still co-immunoprecipitate with Ndc10.

By using a similar strategy as above, we tested whether Cse4 is present at the centromere in these lethal mutants by ChIP/qPCR (Figure 8). Interestingly Cse4 is present at CEN1 with the Scm3-Δ25N protein, but in the case of Scm3-I110H, Cse4 is not localized to the centromere (Figure 8B). Although Scm3-Δ25N can interact with Ndc10 and Cse4, and can apparently localize Cse4, this mutation is still lethal. While the conserved motif appears to be essential for localization of Cse4 at centromeres, the essential function of the N-terminus is not clear at present.

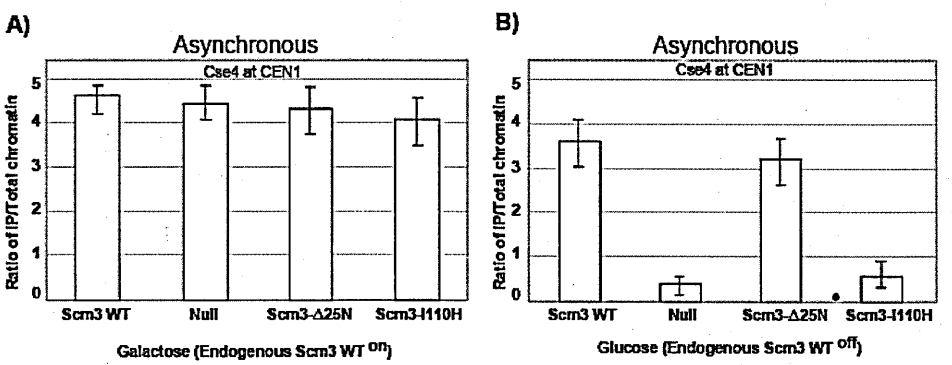

Figure 8. The evolutionarily conserved core motif of Scm3 is required to load Cse4 at the centromere

Strains were constructed in which the endogenous copy of Scm3 was under control of the gal promoter, a plasmid contained another source of Scm3, and Cse4 was tagged with 12xMyc epitopes. In galactose containing medium, Scm3 is expressed (A,) but in glucose (B) the only source of Scm3 is the plasmid. The ChIP/qPCR from the galactose cultures serves as a control. ChIP/qPCR shows that Cse4 is not present at CEN1 in the Scm3-I110H mutant background in glucose in either asynchronous culture (B). Error bars represent ± the average deviation of biological replicates. A control ChIP omitting antibody was performed for each sample; all values were below 0. 01 (Ratio of no antibody/total chromatin).

3. The two essential motifs of Scm3 cannot be differentiated by point of execution in the cell cycle

Cse4 appears to load at centromeres during S-phase [37, 128]. Without Cse4 the kinetochore will be defective, leading to a spindle checkpoint arrest [52, 129]. In previous work we showed that when Scm3 was depleted in the G1 phase of the cell cycle, the spindle check point was not activated. In contrast, if Scm3 was depleted in S phase or G2/M the spindle checkpoint is activated [52]. Since Scm3 cannot be depleted in G2/M without activating the checkpoint, Scm3 function appears to be required even after centromeric chromatin is formed. We performed the same type of point-of-execution experiments with the Scm3 lethal mutants, in order to determine if one motif was more critical for checkpoint signaling.

We conducted arrest-deplete-release experiments. Cells were grown in galactose medium and synchronized in the G1, S, and G2/M phase of the cell cycle with alpha factor, hydroxyurea and nocodazole, respectively. At this point, wild type Scm3 either continued to be expressed (galactose) or was depleted by transfer of cells to glucose-containing medium (glucose). Then cells were released into the cell cycle. Cultures were monitored by flow cytometry. When we deplete wild-type Scm3 and express the mutant proteins at G1 phase, there is a decrease in cells with 4N DNA content compared to the total absence of Scm3 (Figure 9A). In the Scm3 null background we could visualize a population of cells containing 4N DNA content compared to the two lethal mutants. We have also visualized DNA by DAPI staining to verify the presence of multiple DNA masses in a single cell (Figure 9). Taken together, these results suggest the spindle checkpoint is activated more efficiently in the *scm3* lethal mutants as compared to the null background. When wild-type Scm3 was depleted in early S or G2/M phase, there were no significant differences between the null case and the two lethal mutants in terms of DNA content (Figure 9C-D). In all cases cells arrest with 2N DNA content, and are large budded with a single DAPI mass, suggesting the spindle checkpoint is efficiently

activated.

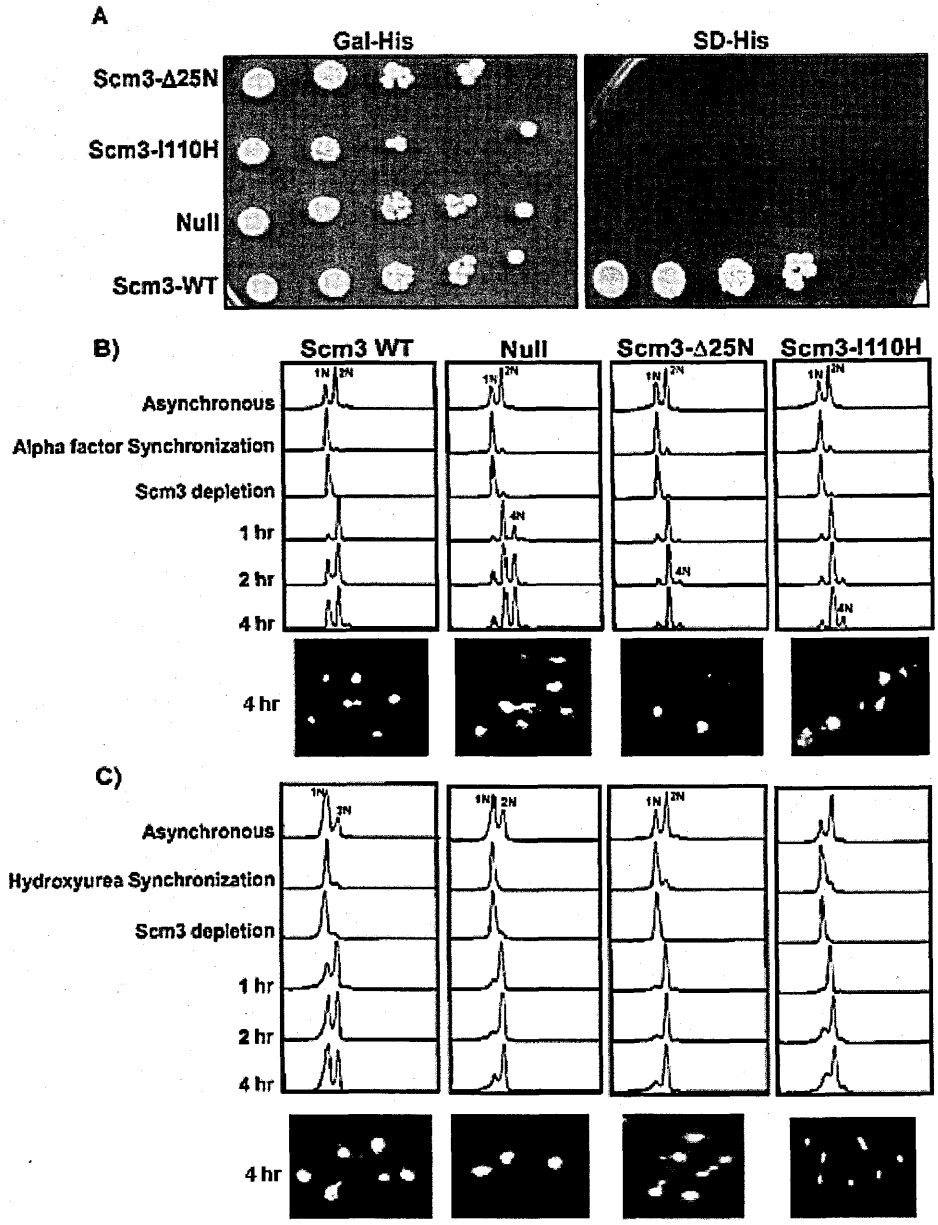
A
Gal-His
SD-His
Scm3-Δ25N
Scm3-I110H
Null
Scm3-WT
B)
Scm3 WT
Null
Scm3-Δ25N
Scm3-I110H
1N
2N
4N
Asynchronous
Alpha factor Synchronization
Scm3 depletion
1 hr
2 hr
4 hr
4 hr
C)
Asynchronous
Hydroxyurea Synchronization
Scm3 depletion
1 hr
2 hr
4 hr
4 hr

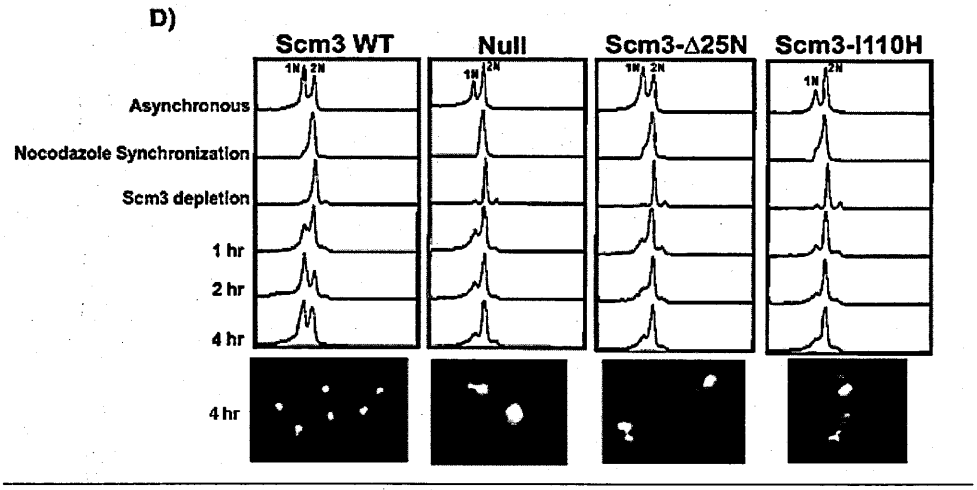

Figure 9. Effect of Scm3 lethal mutations on DNA content at different stages of the cell cycle
A) Dilution assay for *scm3* mutants demonstrating the lethality of the *scm3* mutants in the strain in which the chromosomal copy of Scm3 can be shut off by switch to glucose medium (SD-his). Strains containing Cse4-myc and Scm3 controlled by the GAL_{1-10} promoter and a mutant copy under the control of the endogenous promoter were grown in galactose-containing medium and arrested in (B) G1 phase with alpha factor, (C) mid S phase with hydroxyurea and (D) G2/M phase with nocodazole, switched to glucose medium to deplete gal-Scm3, and then released into glucose medium (glucose). DNA content following release was monitored using flow cytometry (1hr, 2hr and 4hr). DAPI stained cells showing one intact or fragmented nucleus for each lane of FACs profile (4hr).

Next we tested whether Cse4 and Ndc10 were present at centromeres in G2/M by ChIP/qPCR when Scm3 was depleted in a G1 arrest. Cse4 was not detected at the centromere in the Scm3-I110H background but was present at the centromere in the Scm3-Δ25N background (Figure 10A-B). However, Ndc10 was present at centromeres in both the Scm3-I110H and Scm3-Δ25N backgrounds (Figure 10C-D), consistent with the result that both of these mutants can interact with Ndc10 (Figure 8B). Ndc10 is necessary for activation of the spindle checkpoint [130]. The efficient localization of Ndc10 in the mutants as compared to the null is the most likely explanation for the difference in checkpoint activation. Taken together, these results suggest that Scm3 has two distinct functions: 1) Cse4 deposition, which requires the evolutionarily conserved motif and 2) recruitment of Ndc10 in order to activate the spindle assembly checkpoint. The point of execution for each of the two essential motifs cannot be differentiated with respect to

Ndc10 recruitment/checkpoint function.

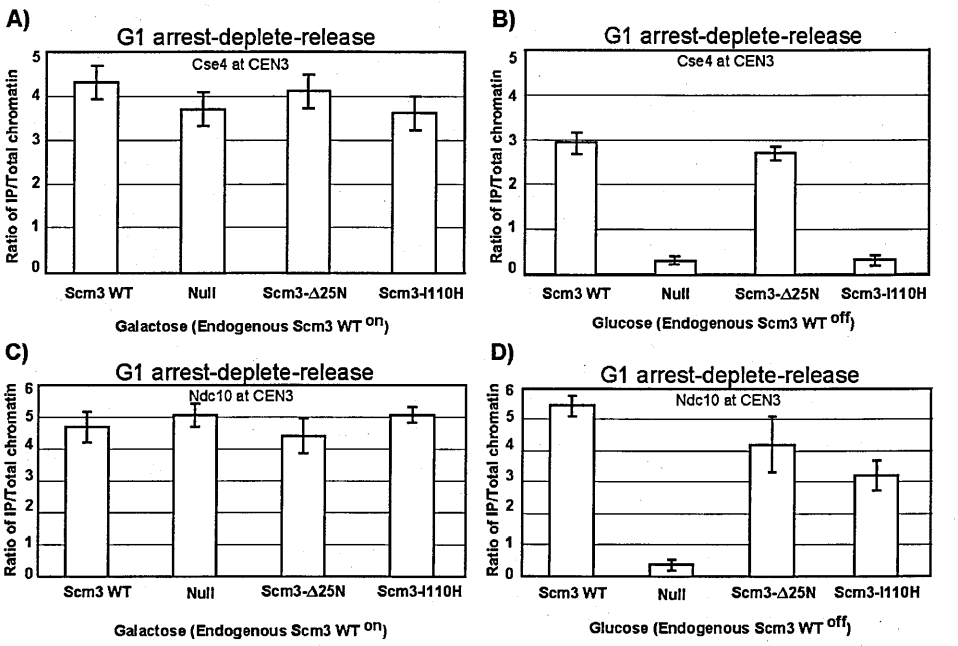

Figure10. The evolutionarily conserved core motif of Scm3 is required to load Cse4 but not Ndc10 at the centromere

ChIP/qPCR analysis for Cse4 & Ndc10 in G1 arrested and released (4 hr) cultures from Figure 9. In galactose containing medium, Scm3 is expressed (A & C) but in glucose (B & D) the only source of Scm3 is the plasmid. The ChIP/qPCR from the galactose cultures serves as a control. ChIP/qPCR shows that Cse4 is not present at CEN1 in the Scm3-I110H mutant background in glucose at CEN3 in G1 arrested and released (4 hr) cultures (B) but Ndc10 present (D). Error bars represent ± the average deviation of biological replicates. A control ChIP omitting antibody was performed for each sample; all values were below 0. 01 (Ratio of no antibody/total chromatin).

4. Both Scm3 lethal mutants can separate H2A/H2B dimers from Cse4 octamer.

It was previously reported that when Scm3 was added to Cse4-containing octamers, H2A-H2B dimers were evicted, and a Scm3-Cse4-H4 complex was formed [51]. We reconstituted the Cse4 octamers and purified them (Figure 11), then analyzed how recombinant Scm3 lethal mutant proteins behaved with respect to octamer splitting. Interestingly, when each lethal mutant was incubated with Cse4 octamers, the octamers were split into two distinct populations, one that contained Scm3/Cse4/H4 and one that contained Scm3/H2A/H2B as measured by gel filtration chromatography (Figure 12C-D). We did not find any difference between Scm3 lethal mutants with respect to H2A/H2B eviction as both mutants were able to split the octamers. We further tested whether

Scm3 is present in a complex with Cse4/H4 or H2A/H2B by pull downs from the fractions containing the split species. As previously shown [51], Scm3 interacts with Cse4/H4, but not H2A/H2B (Figure 12F).

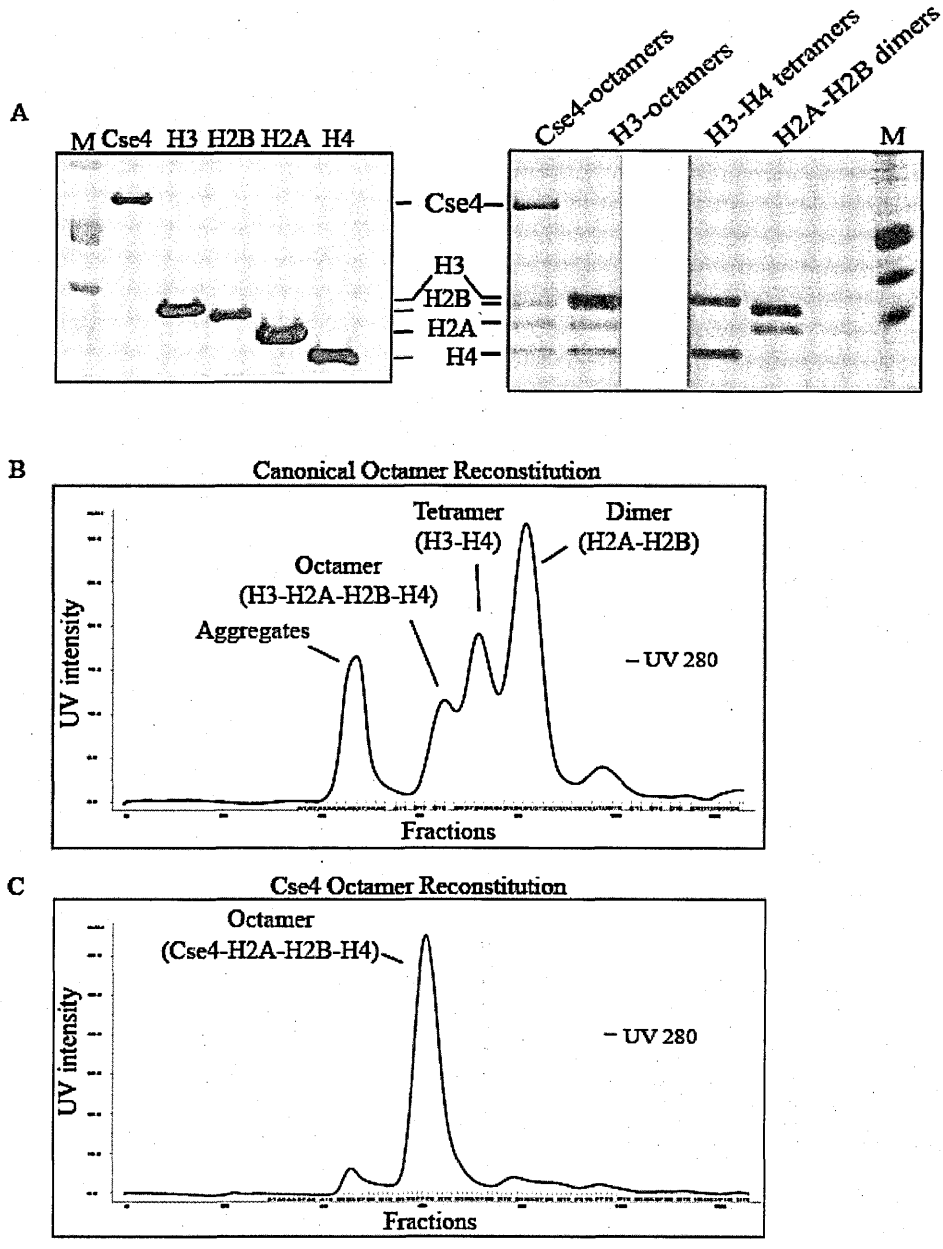

Figure 11. Reconstitution of Cse4 and canonical octamers
A) Individual histones were purified from *E. coli* inclusion bodies and Cse4 and canonical octamers were reconstituted using salt dilution [131]. B) Canonical octamers were assembled by salt dialysis and purified by FPLC. When gel filtration chromatography fractions are collected for canonical octamers, four distinct populations are present: octamers, tetramers, dimers, and aggregates. C) When Cse4 octamers are reconstituted, only the octamer population is detected in the gel filtration fractions. The protein composition of all above peaks was verified on a Coomasie-stained poly-acrylamide gel (data not shown).

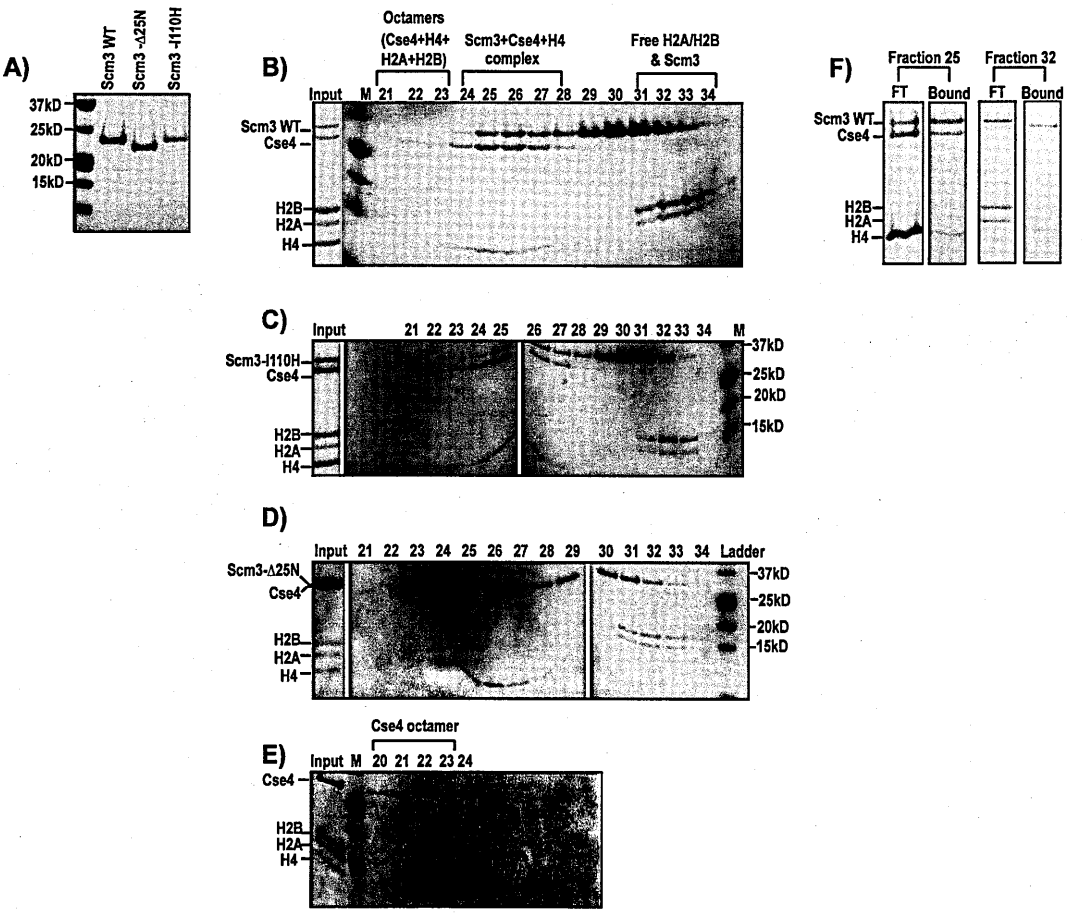

Figure 12. Both lethal mutants can separate H2A/H2B from preassembled Cse4 octamers

(A) Recombinant Scm3 and lethal mutants were purified from *E. coli.* (B) Scm3 was mixed with Cse4 octamers at a 1:1 ratio in 2 M NaCl, incubated for 1 hour at 30°C, and subjected to gel filtration chromatography. Fractions were subjected to SDS-PAGE followed by staining with Coomassie blue. (C) Scm3-I110H was mixed with Cse4 octamers as in (B). (D) Scm3-Δ25N was mixed with Cse4 octamers as in (B). (E) As a control, Cse4 octamers were incubated for 1 hour at 30°C in the absence of Scm3 and subjected to gel filtration chromatography. Both Scm3 lethal mutants were able to split the Cse4 octamers as efficiently as Scm3 since no remaining Cse4 octamers are observed in fraction number 22 in (B), (C), and (D). (F) As previously shown [51], Scm3 associates with Cse4/H4 but not H2A/H2B when fractions number 25 and 32 are tested by a pull down assay with Talon beads. Flow through (FT) and bound proteins are indicated.

5. The conserved core motif is necessary for de novo Scm3/Cse4/H4 complex formation

It was previously shown that recombinant Scm3, Cse4, and histone H4 form a stoichiometric complex with a molecular weight consistent with a hexamer [51]. However, results in chapter 4 call the composition of the complex into question. We tested whether the lethal Scm3 mutants could make a *de novo* Scm3/Cse4/H4 complex when mixed with recombinant Cse4 and H4. To address this question, wild-type or mutant Scm3 was mixed with Cse4 and H4 in 2M NaCl. Scm3-WT and Scm3-ΔN25 were able to form a Scm3/Cse4/H4 complex with Cse4 and H4; Scm3-I110H could not (Figure 13A). This result is consistent with the inability of the Scm3-I110H protein to co-immunoprecipitate with Cse4. Previously a Scm3 mutant protein consisting of amino acids 93-143 was shown to be sufficient for Scm3/Cse4/H4 complex formation [51]. Together these results suggest the conserved motif is essential to interact with Cse4.

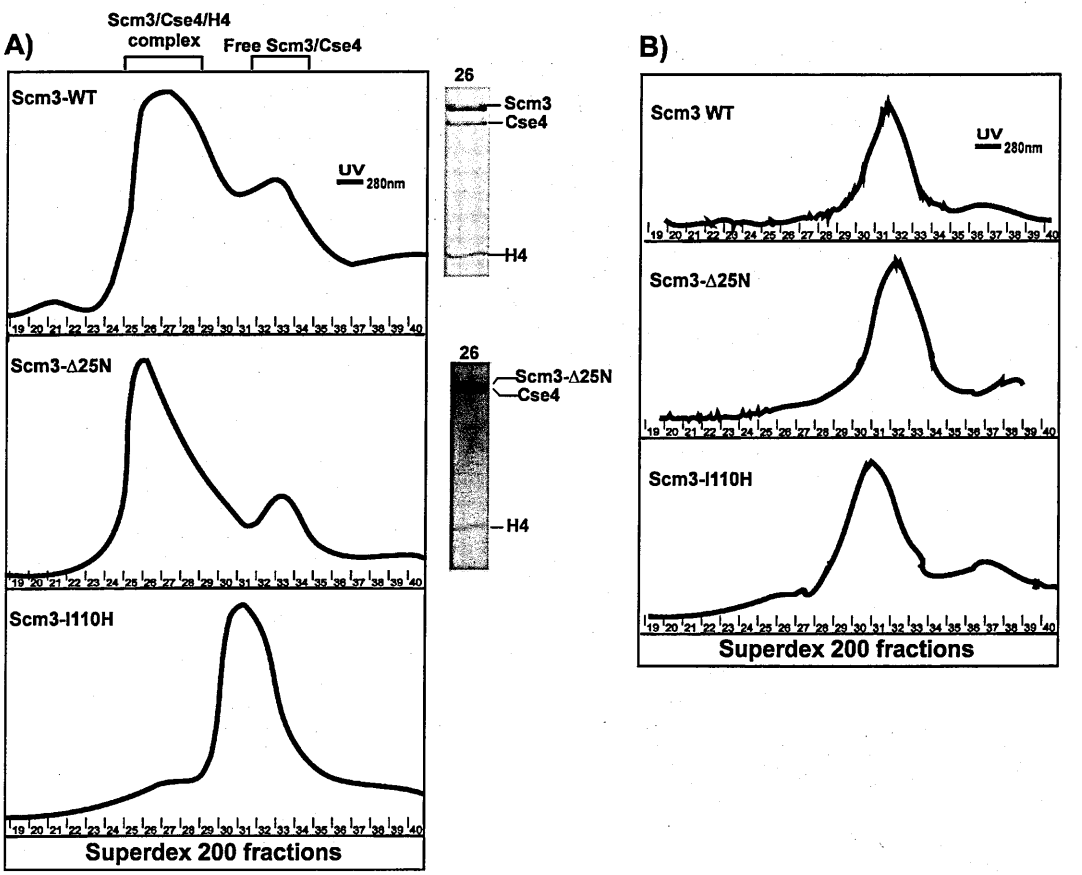

Figure 13. The conserved domain of Scm3 is required for Scm3/Cse4/H4 complex formation

The Scm3/mutants-Cse4-H4 complex was reconstituted from individually purified histones and Scm3 proteins (see Experimental Procedures). Reconstituted samples were fractionated (A) on a 2. 4 ml Superdex 200 PC 3. 2/30 gel filtration column (Amersham Biosciences) on a SMART system (Pharmacia Biotech). Samples (50 µl load) were run in refolding buffer (2M NaCl, 10mM Tris-HCl, pH 7. 5, 1mM EDTA, 2 mM β-mercaptoethanol) at a flow rate of 25 µl per minute, and 30 µl fractions were collected. Peak fractions were analyzed by SDS-PAGE and Coomassie blue staining (shown to the right of each elution profile). Scm3 and Scm3-Δ25N can form a Scm3/Cse4/H4 complex (fractions 26), but Scm3-I110H could not. In the reaction with Scm3-I110H we observed protein aggregates and unassociated Cse4 and Scm3 proteins (fractions 31-34), and H4 (fractions not shown). Cse4 and Scm3 have the same molecular weight. (B) Superdex 200 PC 3. 2/30 gel filtration profiles of free Scm3 wild-type, Scm3-Δ25N and Scm3-I110H.

6. Scm3 assembles nucleosomes *in vitro*.

Scm3 is necessary for the localization of Cse4 to centromeres *in vivo*. We tested whether Scm3 could facilitate the assembly of nucleosomes *in vitro*. To measure the chromatin assembly activity of Scm3 *in vitro*, we used a standard plasmid supercoiling assay. In standard plasmid supercoiling assay the, reconstitution of assembled particles onto a closed circular plasmid DNA is performed in the presence of topoisomerase I, which relaxes the compensatory torsional stress on DNA during nucleosome assembly. Subsequent removal of proteins yields a closed circular DNA, in which additional turns, each originally induced by the wrapping of DNA around one histone core particle, are now irreversibly trapped [132]. When these plasmids are electrophoretically separated, each additional full turn of nucleosome-wrapped DNA contributes to compaction relative to relaxed open circles, yielding a ladder of topoisomers. This assay is indicative of the number of nucleosomes assembled on the plasmid. We tested two plasmids (Figure 14A), one containing 10 copies of a 5S nucleosome positioning sequence (pG5E4-5S, a gift from the Workman lab) and one containing ten tandem copies of a yeast centromere 1 (CEN1) repeat unit. Following the assembly reaction, DNA was deproteinized, and plasmid topoisomers were resolved by agarose gel electrophoresis. Incubation of purified 6xHIS-Scm3 and Cse4 octamers with either pG5E4-5S or pCEN1-10X resulted in the induction of several supercoils compared with controls (Figure 14B), demonstrating that Scm3 can assemble Cse4 containing chromatin on both plasmids. With both plasmids we observed an increase of supercoils in a dose dependent manner to a certain level, followed by a decrease which may be related to the precipitation of Scm3 at higher concentrations. Nap1, a well-studied histone chaperone [14], was also able to induce supercoils with Cse4 octamers on both plasmids (Figure 14C). These experiments demonstrate that Scm3 can induce supercoils with Cse4 chromatin irrespective of DNA sequence. Scm3 alone does not mediate the supercoiling reaction (Figure 14D)

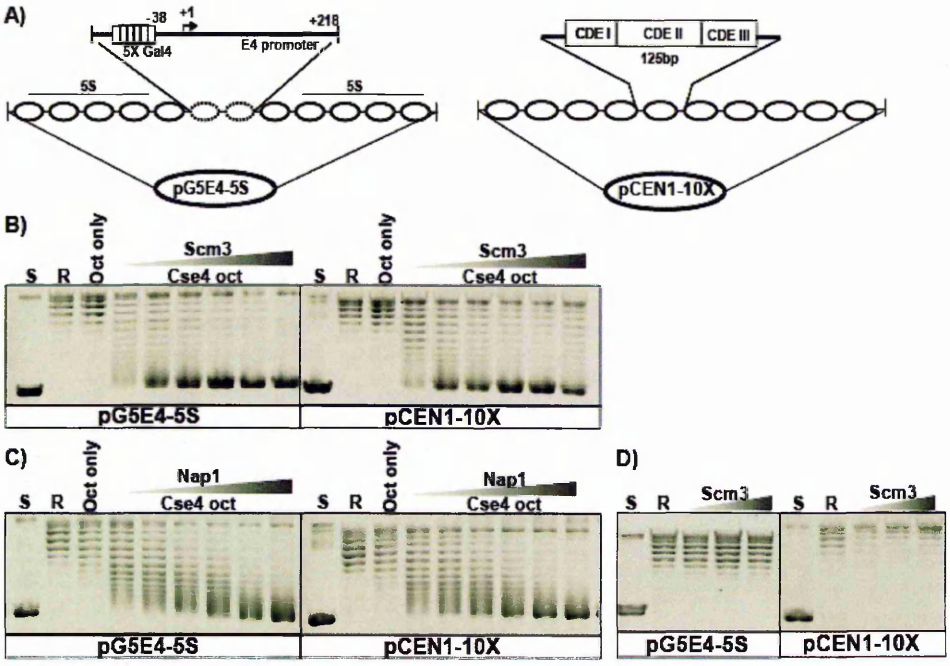

Figure 14. Scm3 can assemble Cse4 containing nucleosomes *in vitro*
Nucleosome assembly activity of Scm3 was studied with a plasmid supercoiling assay. Supercoiled plasmids were purified from *E. coli* (S) and relaxed by addition of topoisomerase I (R). Octamers alone ("Oct only") was included as a control for each assembly experiment. (A) Schematic diagram of plasmid construct pG5E4-5S and pCEN1-10X plasmids. (B) Chromatin assembly was performed by incubating the relaxed plasmids with purified 6xHIS-Scm3 and Cse4 octamers. DNA and Cse4 octamer amounts are held constant at a ratio of 1:1 and Scm3 is added at a ratio of 0. 6, 0. 8, 1. 0, 1. 2, 1. 4, and 1. 6. (C) Nap1 was incubated with Cse4 octamers. DNA and Cse4 octamer amounts are held constant at a ratio of 1:1 and Nap1 is added at a ratio of 1. 0, 1. 2, 1. 4, 1. 6, 1. 8, and 2. 0. (D) A control assembly reaction with only 6xHIS-Scm3 at a ratio to DNA of 0. 6 and 0. 8 does not yield any supercoils on either of the plasmids. Higher amounts also had no effect.

7. The conserved core of Scm3 is necessary for chromatin assembly

Since the conserved motif, but not the N-terminal motif of Scm3, is necessary for localization of Cse4 *in vivo*, we wanted to address whether these motifs are required for chromatin assembly *in vitro*. To address this we used purified recombinant Scm3 lethal mutant proteins (Scm3-Δ25N and Scm3-I110H) in chromatin assembly assays. Scm3-Δ25N was able to induce supercoils on both the pG5E4-5S and pCEN1-10X plasmid (Figure 15A), but Scm3-I110H could not (Figure 15B). Therefore the conserved motif is essential for nucleosome assembly.

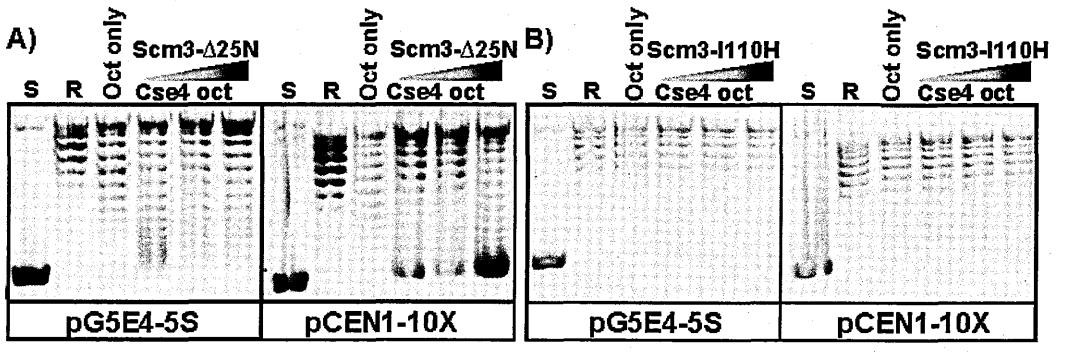

Figure 15. The conserved core of Scm3 is necessary for chromatin assembly
Chromatin assembly reactions were performed by incubating the relaxed pG5E4-5S or pCEN1-10X plasmid with Cse4 octamers and either (E) Scm3-Δ25N or (F) Scm3-I110H.

8. Scm3 is a Cse4-specific nucleosome assembly factor and requires the Cse4 CATD for nucleosome assembly activity

In order to test the specificity of Scm3 for Cse4, assembly reactions were carried out with H3 octamers. Strikingly there was no addition of topoisomers when we use canonical octamers on either the CEN plasmid or the 5S plasmid (Figure 16A). These H3 octamers could be assembled into chromatin using the chaperone Nap1 (Figure 16B).

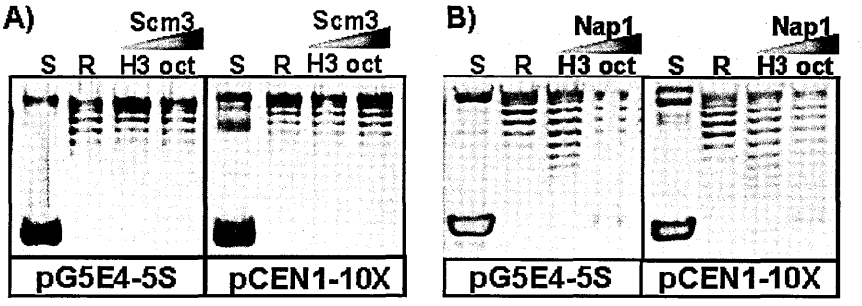

Figure 16. Scm3 is a Cse4-specific nucleosome assembly factor
(A) Scm3 mediated chromatin assembly reaction was performed by incubating the relaxed plasmids and yeast canonical octamers at a ratio of 1:1 with increasing amounts of Scm3 (ratio of 1. 0, 1. 2). Higher amounts also had no effect. (B) Chromatin assembly performed on relaxed plasmids with Nap1 and yeast canonical octamers as in part A (ratio of 1. 0, 1. 2).

We next aimed to identify the motif/sequence in Cse4 that is required for Scm3 nucleosome assembly activity. Cse4 has two domains, 1) a divergent N-terminal essential domain (END) and 2) a highly conserved histone fold domain (HFD) [133]. The centromere targeting domain (CATD), consisting of loop 1 and helix 2 of the histone fold domain, is required for centromeric loading of centromeric histone variants [47]. The CATD is a key regulator of Cse4 protein stability [134]. HJURP, the human ortholog of Scm3, binds to CENP-A through its CATD domain and this interaction occur via the TLTY box of HJURP [46]. Scm3 lacks a TLTY motif, which is conserved only in vertebrates [46]. To test whether Scm3 nucleosome assembly activity requires the CATD domain of Cse4, we made octamers containing a H3/Cse4 chimeric protein in which H3 contains the Cse4 CATD domain [48]. Although H3 octamers are not assembled into nucleosomes by Scm3, octamers containing this chimeric H3/Cse4 protein were assembled into nucleosomes (Figure 17), suggesting the CATD domain is sufficient for Scm3 nucleosome assembly activity.

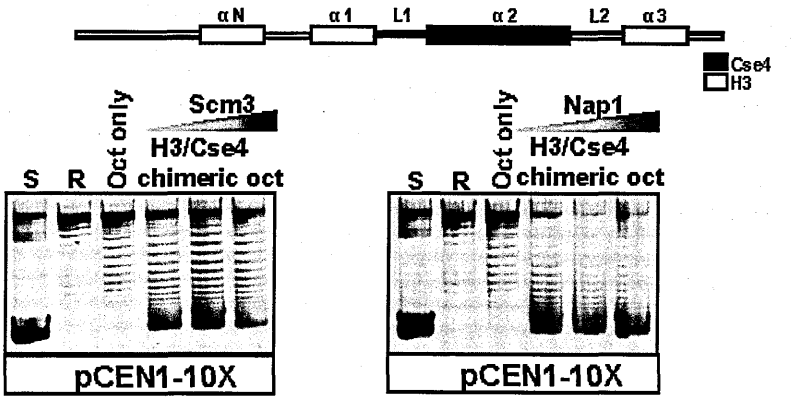

Figure17. Scm3 nucleosome assembly activity requires the Cse4-CATD domain
Diagram of the H3/Cse4 chimeric protein is shown. Chromatin assembly reactions were performed on the relaxed pCEN1-10X plasmid with increasing amounts of reconstituted octamers containing H3/Cse4 chimeric protein and Scm3 or Nap1.

9. H2A/H2B dimers are critical for Scm3 to induce supercoiling

The composition of centromeric nucleosomes has been hotly debated [97, 135, 136]. At present there are three models for the composition of the budding yeast centromeric nucleosome. One model suggests that Cse4 replaces H3 in an octameric nucleosome that contains Cse4, H2A, H2B, and H4 [97]. Octameric nucleosomes containing human CENP-A can be reconstituted *in vitro* [64, 137]. A second model proposes that centromeric nucleosomes contain a single molecule each of CenH3, H2A, H2B, and H4, which forms a tetrameric structure called a "hemisome" [136]. This hemisomal complex was purified from interphase *Drosophila* S2 cells by crosslinking and immunoprecipitation (IP) of CID. Hemisomes appear half as tall as canonical nucleosomes when analyzed by atomic force microscopy and are predicted to contain <120 bp of DNA [136]. A third model is a "hexameric nucleosome", composed of two copies each of Scm3, Cse4 and H4 [51]. Given these models, we decided to test whether addition of the Scm3/Cse4/H4 complex (Figure 13) would induce supercoiling in our assembly assay. We did not observe supercoiling on either type of plasmid (Figure 18A). Recently Vishnapuu and Greene reported that they reconstituted nucleosomes using the Scm3/Cse4/H4 complex and linear λ DNA [138], but we were not able to replicate this outcome on a circular plasmid. Interestingly, addition of H2A/H2B dimers results in some supercoiling (Figure 18B) on both plasmids, suggesting H2A/H2B are necessary for the assembly reaction.

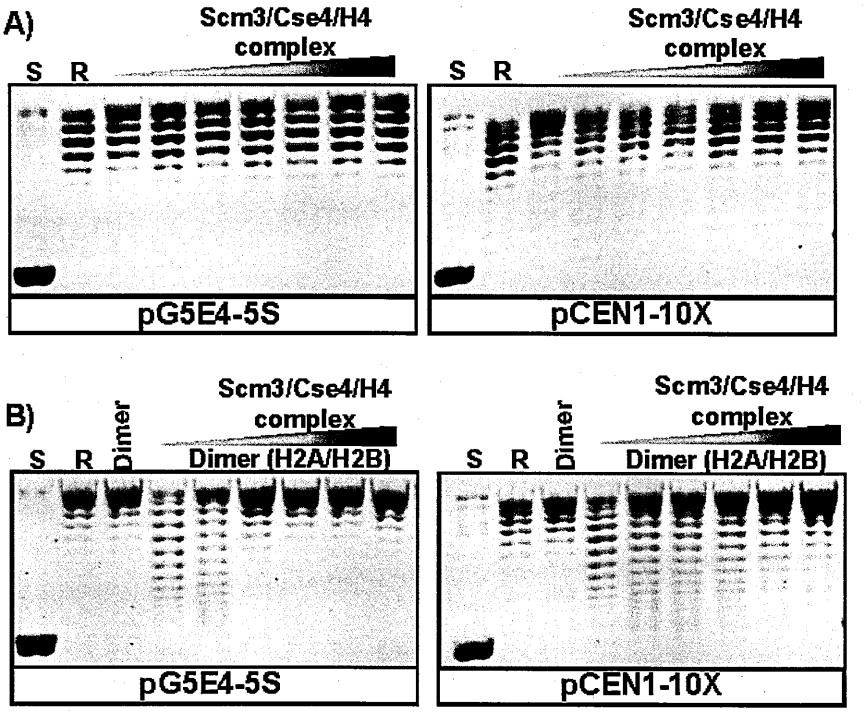

Figure 18. H2A/H2B is critical for Scm3 to induce supercoiling
Chromatin assembly reactions were performed under the conditions in Figure 4B by incubating the relaxed pG5E4-5S and pCEN1-10X plasmid with (D) increasing amounts of reconstituted Scm3/Cse4/H4 complex alone (6xHIS-Scm3/Cse4/H4), or (E) Scm3/Cse4/H4 complex with an equivalent molar ratio of H2A/H2B dimers. In the lane labeled "dimer," H2A/H2B dimers were added at a ratio of 0. 8 to the DNA.

10. Overexpression of Crm1 specifically rescues scm3Δ12N.

The conserved motif of Scm3 is specifically required to interact with Cse4 and point mutation in this domain is lethal because of absence of interaction with Cse4. However, the function of the N terminus is still unclear. It has been shown that the N-terminus of Scm3 contains a leucine rich functional NES [50]. Crm1 is an exporter of leucine rich NES containing proteins from the nucleus to cytoplasm [139]. When we care fully analyzed our previous Cse4-Myc and H2A-Flag MudPIT (Table.3) data, we observed the presence of few karyopherin peptide counts, particularly Crm1, which were absent in H2A-Flag IP. We carried out a co-IP to test whether Crm1 and Scm3 interact *in vivo* but we did not observe an interaction (data not shown). However, we can not rule out the possibility that Scm3 interacts with Crm1 but that the interaction is disturbed by the two epitope tags we used. Alternatively such an interaction might be transient or spe-

cific to a particular point in the cell cycle. To further examine the possibility that the N-terminus of Scm3 and Crm1 interact functionally, we took a genetic approach, and asked whether overexpression of Crm1might rescue any of the N-terminal mutants.

	Cse4-Myc IP	Cse4-Myc IP	H2A-FLAG IP
Kap123	5	11	0
Crm1	4	2	0
Sxm1	2	5	0
Kap95	1	3	0

Table 3. Peptide counts in Cse4-Myc and H2A-Flag MudPIT data
Two columns of Cse4-Myc represent 2L and 4L culture respectively.

Figure 19. Over expression of Crm1p specifically rescues the Scm3Δ12N
Plasmid shuffle assay with overexpression of Crm1p in a strain which has N-terminal *scm3* mutants (Figure 6) (Δ12N, 3L-A, ΔNES and Δ25N) in pRS423 (*HIS3* selection) and haploid Scm3 knockout strain maintained by pRS316 expressing Scm3 from its endogenous promoter on a CEN vector (*URA3* selection).

We tested this by using a plasmid shuffle assay in combination with overexpression of Crm1 in strains expressing a, N-terminal *scm3* mutant (Δ12N, 3L-A, ΔNES and Δ25N) on pRS423 (*HIS3* selection), and pRS316 expressing Scm3 from its endogenous promoter on a CEN vector (*URA3* selection). In these stains, the chromosomal copy of Scm3 was knocked out. We found that overexpressing Crm1 specifically rescues the Scm3-Δ12N (Figure 19). Even though Crm1 is weak suppressor of Scm3-Δ12N, this could be due to a positional effect of the NES. For example, if the first 12 amino acids were replaced by a different sequence rather than deleted, the suppression might improve.

11. Scm3 may facilitate positive supercoiling

It has been previously been reported that centromeric nucleosomes induce positive supercoiling. The authors of this report further argue that positive supercoiling is possible only if the centromeric nucleosomes are hemisomes or hexasomes. These ideas are consistent with their earlier work in Drosophila where they identified that the centromeric nucleosomes are hemisomes by analyzing the height of the crosslinked centromeric nucleosomes from interphase cells [135]. We were curious to know whether Scm3 induces positive or negative supercoils. In order to test the direction of supercoiling induced by Scm3, we used the same standard plasmid supercoiling assay and electrophoresed the deproteinized plasmids in the presence of the intercalating drug chloroqine, which reduces the twist of DNA [132, 135]. Since the linking number (Lk) is fixed in a covalently closed plasmid, the reduction in twist (Tw) must be compensated for by an increase in writhe (Wr), ($\Delta Lk = \Delta Tw + \Delta Wr$) [132]. On a normal agarose gel (without chloroquine) we can calculate the number of nuclesomes assembled on the circular plasmid by separating topoisomers, but we can not tell the direction of induced writhe, because both positive and negative supercoils cause compaction relative to relaxed circles [132, 135]. In a chloroquine gel, plasmids containing negative supercoils run slower because of the addition of positive writhe by chloroquine compared to relaxed plasmid.

Chloroquine intercalation causes topoisomers induced by Nap1 with Cse4 octamers to move slower than initially relaxed (R) circular plasmid (Figure 20B); therefore, these are negatively supercoliled. Strikingly, the topoisomers induced by Scm3 do not show clear negative or possitive supercoiling pattern compared to Nap1 assembled Cse4 nucleosomes. Thus, supercoils that form with Scm3 are different from Nap1 and may be more positive. If our assembly reactions contain a mixture of right & left handed nucleosomes, this could account for the observed results. In the future, the effect of Scm3 on DNA wrapping will be tested *in vivo*.

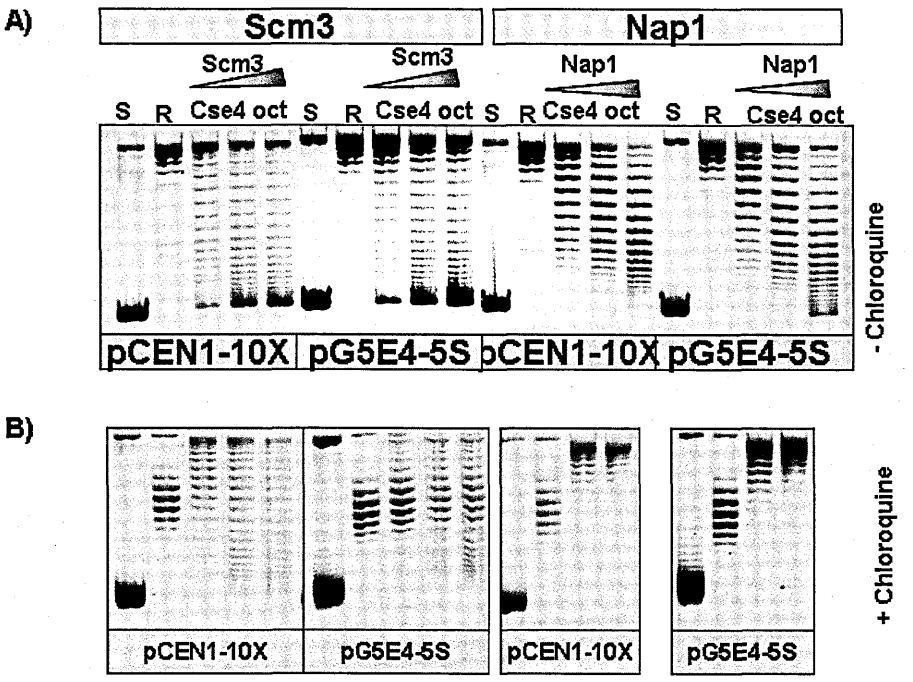

Figure 20. Scm3 may facilitates positive supercoils
Chromatin assembly reaction was performed by incubating the relaxed pCEN1-10X and pG5E4-5S plasmid with indicated protein complexes. Topoisomers are separated on agarose gel without chloroquine (A) or with chloroquine (B).

IV. Discussion

1. Functions of Scm3 in budding yeast

While Scm3 is an essential inner kinetochore protein, its precise molecular function has remained poorly understood. Herein we have shown that Scm3 appears to be a bona fide Cse4-specific chaperone. We further show that the chaperone activity depends on the evolutionarily conserved motif of Scm3 and the centromere targeting domain (CATD) of Cse4, but not centromeric DNA sequence. The conserved motif of Scm3 is required for interaction with and deposition of Cse4, but not Ndc10, at centromeres, arguing for two separable functions for Scm3. The deposition of Ndc10, and therefore the ability to activate the spindle assembly checkpoint, depends on Scm3, but not its chaperone function. Furthermore, this result suggests Ndc10 recruitment and spindle checkpoint activation does not depend on Cse4 deposition at the centromere.

Recently it has been shown that Psh1 is an E3 ubiquitin ligase that targets Cse4 [134, 140] and Scm3 appears to protect Cse4 from Psh1 [140]. Consistent with this proposal, Psh1 requires the CATD domain of Cse4 in order to target Cse4 [134]. Thus, it seems likely that Scm3 has an active function in Cse4 protein maintenance and nucleosome assembly that depends on the CATD domain. HJURP, a putative human ortholog of Scm3, also possesses assembly activity for CENP-A/H4 complexes with DNA *in vitro* [46]. HJURP interacts with CENP-A through its TLTY box, a highly conserved motif across vertebrates [46]. However, Scm3 lacks a TLTY motif. Instead Cse4 interaction and assembly activity all depend on the evolutionarily conserved core motif of Scm3.

The assembly of nucleosomes by Scm3 can occur on either centromeric DNA sequences, or a canonical nucleosome positioning sequence. Thus, the reactions we have conducted *in vitro* lack sequence specificity. This result is consistent with a recent report in which it was shown that Scm3 is required to load Cse4 at a non-centromeric sequence, the stable partitioning locus (STB) within the 2μ plasmid [134]. We speculate that se-

quence specificity *in vivo* is achieved by the CBF3 protein complex, which is a sequence specific binding complex found in point centromere containing organisms. In future studies it will be interesting to determine whether the addition of CBF3 or other components will increase the specificity for the centromere sequence. However, our observations suggest that Scm3 alone cannot provide sufficient DNA sequence specificity to restrict Cse4 nucleosomes to centromeres.

2. H2A-H2B dimers are essential for Scm3 to act as an assembly factor

One of the proposed structures for centromeric nucleosomes is a hexasome, which does not contain H2A/H2B [51, 138]. We have used a supercoiling assay to test whether the Scm3/Cse4/H4 complex would induce topoisomers. While the Scm3/Cse4/H4 complex fails to induce supercoiling, addition of H2A/H2B dimers along with Scm3/Cse4/H4 complex did result in supercoiling, suggesting H2A and H2B are critical for nucleosome formation. The requirement for H2A *in vitro* is consistent with previous data suggesting H2A is present in Cse4 nucleosomes [97] and is required for proper centromere function [141]. Thus, our results are most consistent with models for the centromeric nucleosome that contain H2A and H2B.

Chapter 4.

Composition and Structural analysis of centromeric nucleosomes in budding yeast

I. Abstract

The centromere is a specialized chromosomal structure that regulates faithful chromosome segregation during cell division, as it dictates the site of assembly of the kinetochore. In eukaryotes all the centromeres are universally marked by presence of a histone H3 variant. In budding yeast, the histone H3 variant Cse4 is present in a single centromeric nucleosome. Cse4 containing centromeric nucleosomes are assembled by the Cse4-specific nucleosome assembly factor Scm3. Presently, experimental evidence in the literature supports several different models for the structure and composition of these centromeric nucleosomes. 1) the hemisome model (Cse4-H4-H2A-H2B) [135], 2) the octasome $(Cse4\text{-}H4\text{-}H2A\text{-}H2B)_2$ [97, 137, 142, 143] and 3) the hexasome $(Scm3\text{-}Cse4\text{-}H4)_2$ [51]. 4) the tetrasome model $(H3\text{-}H4)_2$ [122] and 5) the reversome [144]. We find that Micrococcal nuclease digestion of Scm3 assembled Cse4 nucleosomes results in a shorter length of DNA protected compared to Nap1 assembled Cse4 nucleosomes, suggesting structural differences. Fluorescence correlation spectroscopy and brightness measurements in conjugation with confocal imaging experiments in live cells reveal that centromeres at G1 phase have one copy of Cse4 per centromeric nucleosome whereas two copies are detected at anaphase. The apparent structural change occurs at the metaphase to anaphase transition. Our experimental evidence supports the existence of both the hemisome and the octasome in budding yeast.

II. Introduction

The centromere in all eukaryotic organisms including humans plays a critical role in chromosome segregation in mitosis and meiosis. Centromeres are the site at which the kinetochore is built. The kinetochore mediates the attachment of chromosome to spindle microtubules. The centromere is defined by specific DNA sequences as well as by a spe-

cialized chromatin structure. Although centromere proteins are well conserved among all organisms [31, 41, 112, 145-147], the DNA sequence at the centromere is not conserved [148, 149]. Centromeres range in size from the ~125bp found in budding yeast to kilobase pairs in *S. pombe* to several megabasepairs in human centromeres [150]. Based on the size, centromeres are classified as two types: "point" centromeres and "regional" centromeres. Regional centromeres are typically found in higher eukaryotes and consist of hundreds of kilobases of repetitive DNA [151]. The human centromere is made up of alpha satellite DNA repeats [152]. Point centromeres found in the budding yeast *Saccharomyces cerevisiae* are short and simple, and consist of common sequence elements (CDE I, CDE II and CDE III) that span just ~125 bp [68]. CDE I and CDE III are binding sites for proteins that recruit other components of the centromere–kinetochore apparatus [83, 115]. CDEIII is the binding site for the CBF3 multiprotein complex [83]. This complex helps specify the loading site of single Cse4-containing nucleosome on each chromosome [52, 66]. Although the DNA sequences are highly variable between species, all eukaryotic centromeres are universally marked by the presence of a centromere specific histone variant (CenH3). This variant is called CENP-A in humans, CID in flies and Cse4 in budding yeast. This variant is essential for kinetochore formation and proper chromosome segregation [63, 142]. Cse4 can functionally complement for CENP-A [36], suggesting that the function of CenH3 is evolutionarily conserved.

Although it is clear that a histone variant replaces H3 at centromeres and these nucleosomes are very important for proper chromosome segregation, their composition and structure is poorly understood. Since these nucleosomes specify the centromere, they are likely to have unique characteristics to distinguish them from other nucleosomes. At present several models have been proposed to explain the composition and structure of these nucleosomes.

The octasome model: The most conventional model is an octameric configuration, having two copies of H4, H2B, H2A, and Cse4 [38, 97, 143, 153-156]. In these nucleosomes, DNA wraps around the histone octamer with a conventional left-handed wrap, as in a canonical nucleosome [137]. This model is proposed based on 1) strong sequence identity between the HFD of the CENP-A homologus that of H3, 2) CENP-A/Cse4 containing octameric nucleosomes can be reconstituted from purified components, [64, 97, 143, 157], 3) the presence of stoichiometric amounts of CENP-A, H4, H2A, and H2B in isolated chromatin from cultured cells [38, 154], 4) CENP-A has a higher affinity for itself than H3 so it is more likely to interact with itself than with H3 (homotypic interaction) [143], and 5) the CATD domain of CENP-A confers unique and distinguishing structural properties to heterotetramers $(Cse4\text{-}H4)_2$ and octameric CENP-A containing nucleosomes [137].

Hemisome model: the hemisome model is a unique and interesting model proposed by the Henikoff group in 2007 based initially on experimental evidence from Drosophila S2 cells. This model proposes that a single copy of each histone is present in the nucleosome. In support of this model, CID containing nucleosomes isolated from chromatin are half the height of canonical nucleosomes when analyzed by atomic force microscopy [136]. Recently, this model gained further support when the Dalal group found CENP-A containing nucleosomes from mammalian cells are also half the height of canonical nucleosomes [158]. In addition, the Henikoff group has shown that centromeric nucleosomes in budding yeast plasmids have DNA wrapped in a right-handed configuration, unlike the left-handed configuration in canonical nucleosomes. They argue that a hemisomal structure can supporting this wrapping [135].

Hexasome model: In 2007, Carl Wu and colleagues have proposed a hexasome model based on experimental evidence in budding yeast. They showed that the non histone protein Scm3, along with Cse4 and H4, assembles into a complex, whose size is compara-

ble to a hexameric complex containing two copies of Scm3, Cse4, and H4 [51]. In addition, H2A-H2B dimers are replaced by Scm3 from preassembled octamers *in vitro* and H2A-H2B was significantly diminished at centromeric DNA when measured by, *in vivo* chromatin immunoprecipitation [51]. Based on these results they have proposed that Scm3 is a part of centromeric nucleosomes. This model also lends support to the idea that a hexameric nucleosome may favor the positive supercoil configuration [135].

The reversome model: Lavelle et al proposed the reversome as a possible alternative to explain the positive supercoiling in centromeric nucleosomes shown by the Henikoff group. These reversomes are high-energy states [159]. Although this would be a possible explanation for the positive supercoiling, the occurrence of these nucleosomes in reconstituted chromatin (either H3 or Cse4) is limited and factors involved in stabilizing these structures are still unknown.

Using *in vitro* and *in vivo* experiments we present evidence for a structural oscillation of centromeric nucleosomes in budding yeast. Cse4-containing nucleosomes can be assembled by Nap1 and Scm3. However, Scm3 assembled Cse4 containing nucleosomes have less DNA. Using fluorescently labeled histone H4, we show that in both split and reconstituted Scm3-Cse4-H4 complexes there is only one copy of H4. This result is not easy to reconcile with a hexameric complex, as previously reported [51]. In order to gain a better understanding of the content and structure of Cse4-containing centromeric nucleosomes, we have developed a unique method to quantify the number of Cse4-GFP molecules per centromeric nucleosomes *in vivo* using FCS and calibrated confocal imaging. Interestingly, when we quantified the number of Cse4-GFP molecules per centromere cluster we find ~16 Cse4-GFP/centromere cluster at G1 and ~32 at anaphase. Since budding yeast have 16 chromosomes and each centromere contains one nucleosome [97, 119], our result suggest that one copy of Cse4 is present per nucleosome at G1 and two copies of Cse4 are present per nucleosome at anaphase. Measuring the dis-

tance between the SPBs reveals that the apparent structural change occurs at the metaphase to anaphase transition. Furthermore, when we irreversibly photobleach Cse4-GFP at metaphase, centromeric clusters were recovered during mid-anaphase, suggesting at this stage there can be incorporation of new Cse4. Fluorescence resonance energy transfer (FRET) measurements in cells expressing Cse4-GFP and Cse4-mCherry reveal that there is no FRET between Cse4s at G1, but after metaphase we observed an increase of FRET efficiency, consistent with two copies of Cse4 per centromeric nucleosome at anaphase. Taken together, our experimental evidence supports a cell cycle coupled oscillation between the hemisome and the octasome.

II. Results

1. Composition of Scm3 mediated Cse4 containing nucleosomes *in vitro*

Given the ability to assemble Cse4 nucleosomes with Scm3 *in vitro*, we wanted to characterize the composition of these nucleosomes. To address the composition we reconstituted chromatin (although we have used both types of plasmid for this purpose, here we are showing only the pCEN1-10X plasmid) then digested with MNase, and samples were subjected to gel filtration chromatography to isolate distinct protein and DNA populations (Figure 21A). We found that when we examined the DNA from the Nap1 and Scm3 reconstitutions with Cse4 octamers, there were fractions which contained DNA that was ~120-150 bp (Figure 21A and B). This is compared to the control reaction lacking histones (Figure 21C), which yielded only small fragments of DNA (<100 bp). When the fractions from the Nap1 reconstitution were subjected to SDS-PAGE followed by silver staining, all four histones were detected in the mononucleosome fractions (Figure 21A). When fractions from the Scm3 reconstitutions were subjected to analysis by western blotting, we find that the fractions with DNA ~120-150 bp contained all histones (Cse4/H4/H2A/H2B) in additionto Scm3 (Figure 21F). This suggests that Scm3, in contrast to Nap1, remains associated with the Cse4 mononucleosomes. We note that the mononucleosomes formed with Scm3 display a different elution profile than the mono-

nucleosomes formed with Nap1 (Figure 21D), suggesting the two species may be different. The size of the Scm3-assembled mononucleosomes is consistent with either a more compacted octamer species than the Nap1-assembled mononucleosomes, or a hemisome.

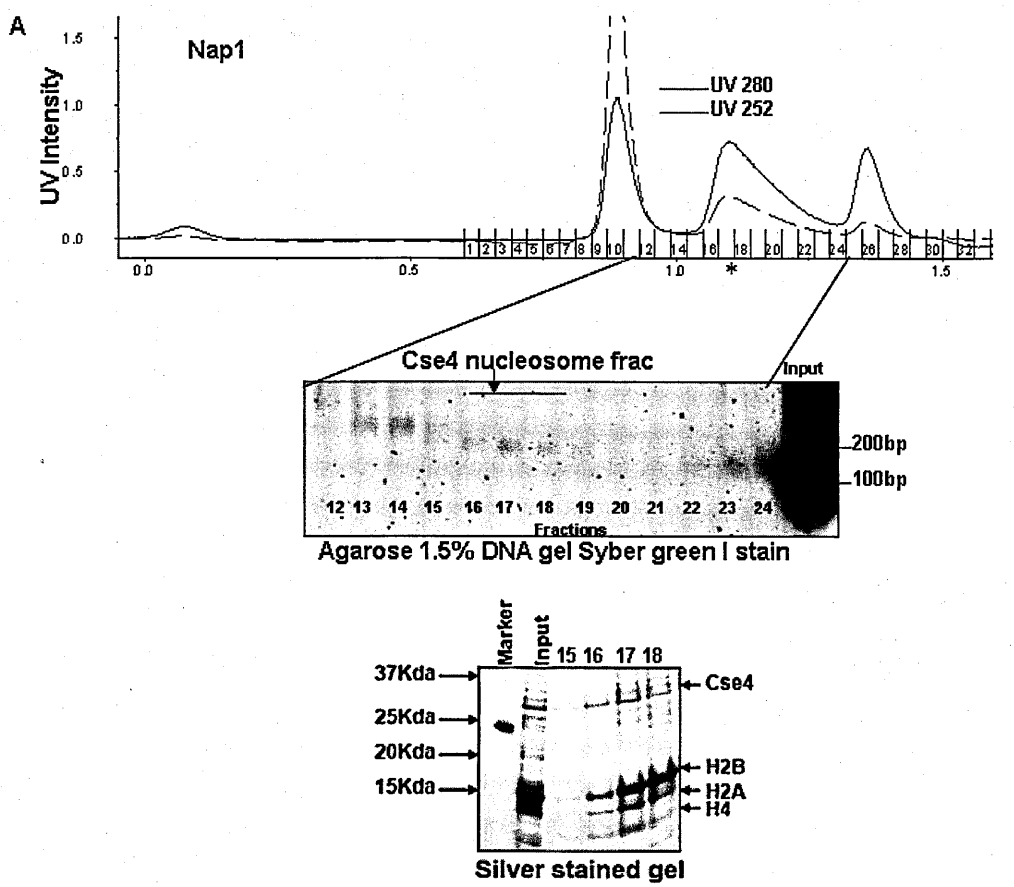

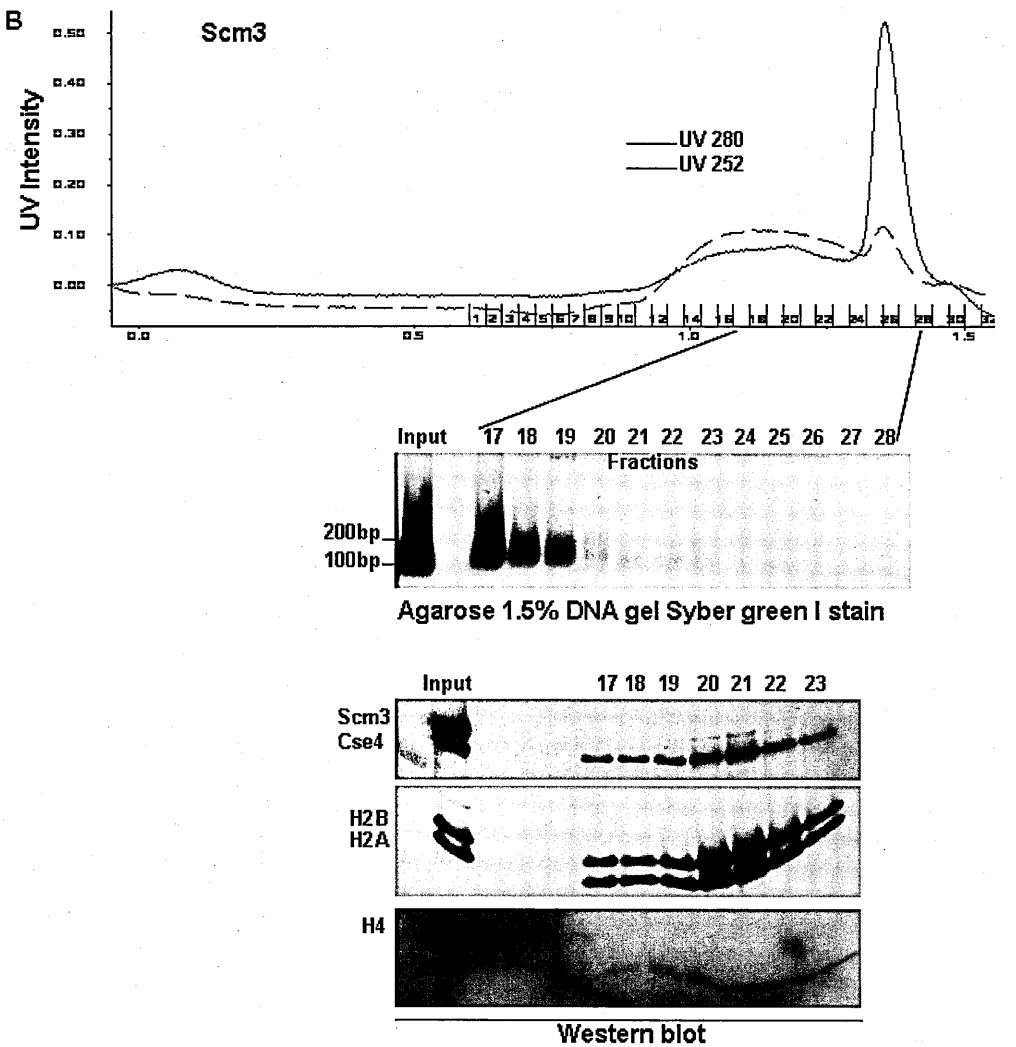
B
Scm3
UV Intensity
UV 280
UV 252
Input
17 18 19 20 21 22 23 24 25 26 27 28
Fractions
200bp
100bp
Agarose 1.5% DNA gel Syber green I stain
Input
17 18 19 20 21 22 23
Scm3
Cse4
H2B
H2A
H4
Western blot

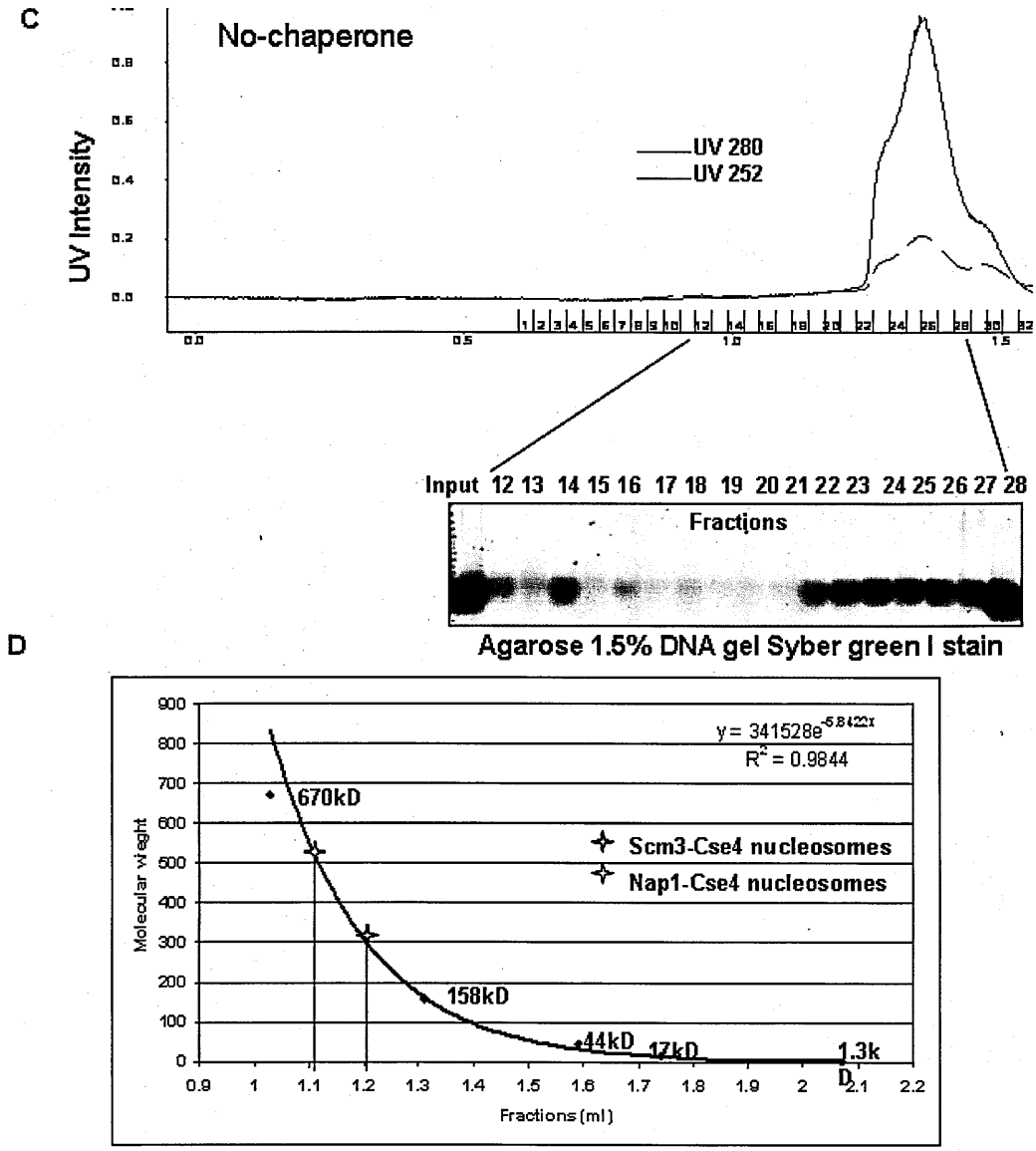

Figure 21. Composition of Scm3 mediated nucleosomes
Supercoiling assay was performed with Nap1 (A) and Scm3 (B) or without either of them (C), on pCEN1-10x using Cse4 octamers. Reconstituted chromatin was MNase treated for 5 minutes (A) and 8 minutes (B & C) and the mixture was fractionated on a superdex-200 column by using a Smart system. Upper panel in each set is the UV chromatograph, DNA content in the superdex 200 fractions were analyzed on 1. 5% agarose gel electrophoresis and stained with Syber green I. Protein content was analyzed by SDS-PAGE / western blotting. D) A molecular size standard was run on the same column used for fractionation, and an apparent MW standard curve was created. Error is estimated to be +/- 10 kD. The MW of an assembled nucleosome is calculated to be ~530 kD for Nap1 assembled (fraction 17) and ~320 kD for Scm3 assembled (fraction 20). If we calculate the size for an octamer & DNA it is ~229 kD, showing that those species are not migrating true to size, and shape may also influence their behavior on this column.

2. Cse4 lethal point mutants are defective in Cse4-Cse4 dimerization

Our lab in collaboration with Ali Shilatifard had identified six Cse4 lethal point mutants by single residue alanine-scaning mutagenesis (Figure 22A). Five of the six essential residues are located in close proximity to the Loop II-Helix III transition (Figure 22B) and four out of five of the identified Cse4 lethal point mutants at the loop II-helix III transition (H207A, R210A, T212A, D217A) have analogous lethal mutations in the H3-H3 dimer interface [160]. We were interested in testing if these mutations interfere with the structure and folding of Helix III, disrupting the dyad axis and subsequently the Cse4-Cse4 dimer interface at the four-helix bundle. Using purified recombinant Cse4 with the lethal point mutations and histones H2A, H2B, and H4, we assembled octamers *in vitro*. With the exception of L220A, we find that all of the point mutants exhibit a significant decrease in octamer reconstitution efficiency when compared to octamers reconstituted with wildtype Cse4 (Figure 22C).

The results of our *in vitro* reconstitutions suggest that Cse4-Cse4 dimers are required for Cse4 octamer formation. We further tested Cse4 interaction *in vivo*. We tested this by coexpressing two differentially epitope-tagged Cse4 proteins, Cse4-12xMyc and a 2xFLAG epitope-tagged lethal Cse4 point mutant. We found that for five of the six point mutants identified in the alanine-scanning mutagenesis, we lost the ability to coimmunoprecipitate the WT Cse4-12xMyc protein with the mutant copy to a significant degree (Figure 22D). Taken together, our results strongly suggest that Cse4-Cse4 dimers are required for Cse4 function. These results are most consistent with a model for the centromeric nucleosome that includes two copies of Cse4.

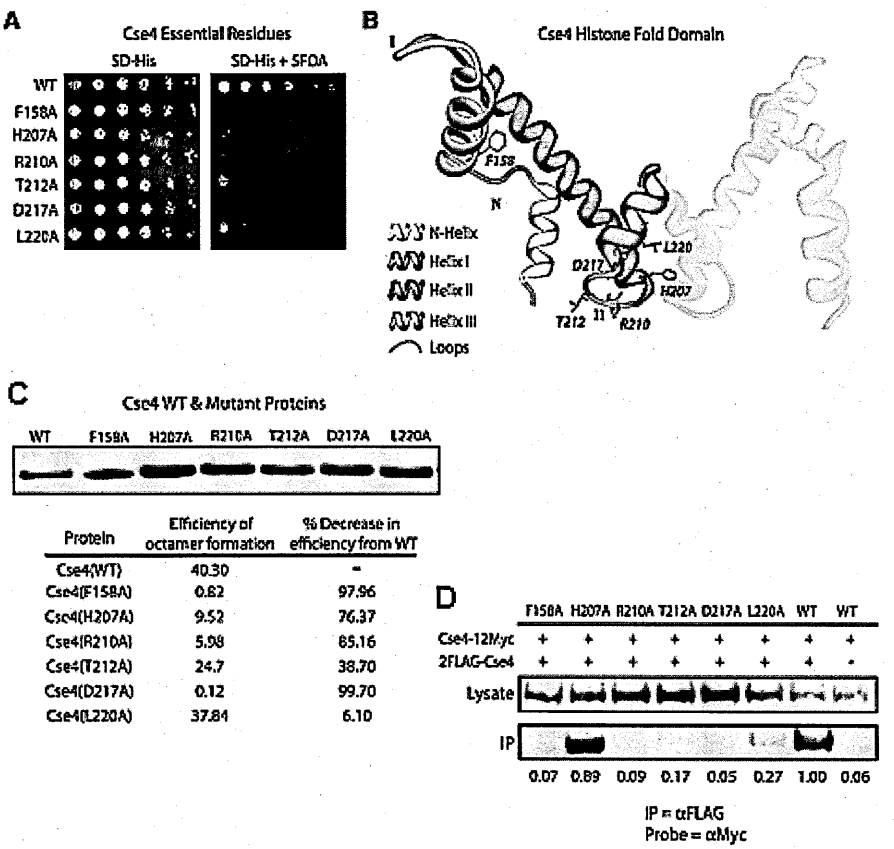

Figure 22. Cse4 lethal mutants are defective in Cse4-Cse4 dimerization

Alanine scanning mutagenesis of Cse4 in combination with a plasmid shuffle identified 6 lethal mutations. A. Growth on 5-FOA identified six single alanine substitutions that do not support growth in the *cse4Δ* background. B. Using the modeled Cse4 crystal structure as a guide (Bloom et al. 2006), the location of each of the 6 lethal point mutants was mapped. One molecule of Cse4 histone fold domain from the predicted Cse4 octamer crystal structure is shown in color and the essential residues are indicated. The second molecule of Cse4 is shown in grey. Five of six of the lethal point mutations lie in close proximity in either Loop II or Helix III. C. Each of the Cse4 mutants identified in alanine scanning mutagenesis (A) was purified from E. coli inclusion bodies. We then used these recombinant Cse4 point mutants to reconstitute octamers *in vitro*. Octamers were subjected to gel filtration chromatography. The efficiency of octamer formation was calculated by dividing the amount (mg) of octamer recovered by the amount of input histones (Cse4, H2A, H2B and H4). D) CoIP was performed from whole cell extract (WCE) isolated from a strain that expresses both Cse4-12xMyc and a 2xFLAG-Cse4 point mutants identified in the alanine-scanning mutagenesis (MM111-116), WT 2xFLAG-Cse4 (MM118), and Cse4 without a FLAG tag (MM117). FLAG-conjugated beads were used to pull down 2xFLAG-Cse4 from WCE, and the pull-down was probed by western blotting with the aMyc antibody. The values below each lane of the blot represent quantification of the IP band over the lysate band, with the WT sample set to 1.

2. Scm3-Cse4-H4 complex has only one copy of H4

Since Scm3 assembled Cse4 nucleosomes appear to be smaller than the Nap1 assembled Cse4 nucleosomes, we were interested in examining the copy number/stoichiometry of histones in the complex to examine whether these are really octasomes or hemisomes. To address this we have used fluorescently labeled histones. Firstly we examined the stoichiometry of H4 histone in purified octamer and the Scm3-Cse4-H4 complex. H4 was mutated to engineer a single cysteine at site T71 [161] and this protein was bacterially expressed and purified. Purified protein was used to conjugate Alexa-Fluor 488 C5 maleimide (Invitrogen) to the free cysteine (T71C). The fraction of labeled Cse4 was determined by Mass spectroscopy and the labeling efficiency was found to be ~92 %. This labeled protein was used to make Cse4 containing octamers. Then, Cse4 octamers were incubated with 6xHIS-Scm3 for 30 minutes at room temperature and the mixture was subjected to gel filtration chromatography to purify Scm3-Cse4-H4 complex. Peak fractions for octamers and Scm3-Cse4–H4 complex were taken for H4 copy number analysis (Figure 23A). Copy number was determined by measuring the Alexa-Fluor 488 brightness using FCS. The brightness of Alexa-Fluor-488 conjugated on H4 in these complexes was compared to the non-conjugated Alexa-Fluor 488. When we analyzed the octameric complex, the brightness values were nearly doubled compared to the free Alexa-Fluor-488. Surprisingly the Scm3-Cse4-H4 complex brightness values were same as the free Alexa-Fluor-488 (Figure 23B), suggesting only one copy of the H4 in the Scm3-Cse4-H4 complex.

To ensure that differences in brightness of Alexa-Fluor-488 in octamers and Scm3-Cse4-H4 complex is due to a real difference in H4 copy number and not due to quenching, fluorescent lifetime measurement of all Alexa-Fluor 488 labeled samples were made and compared to non-conjugated Alexa-Fluor 488 (Figure 23C). Differences in fluorescence lifetime were used to normalize the molecular brightness comparisions. There is a small amount of quenching in all Alexa-Fluor 488 labeled complexes but there

is no fluorescence lifetime difference between the octameric and Scm3-Cse4-H4 complex. This fluorescence lifetime measurement validates the brightness result, and strongly suggests that in the Scm3-Cse4-H4 complex there is only one copy of H4.

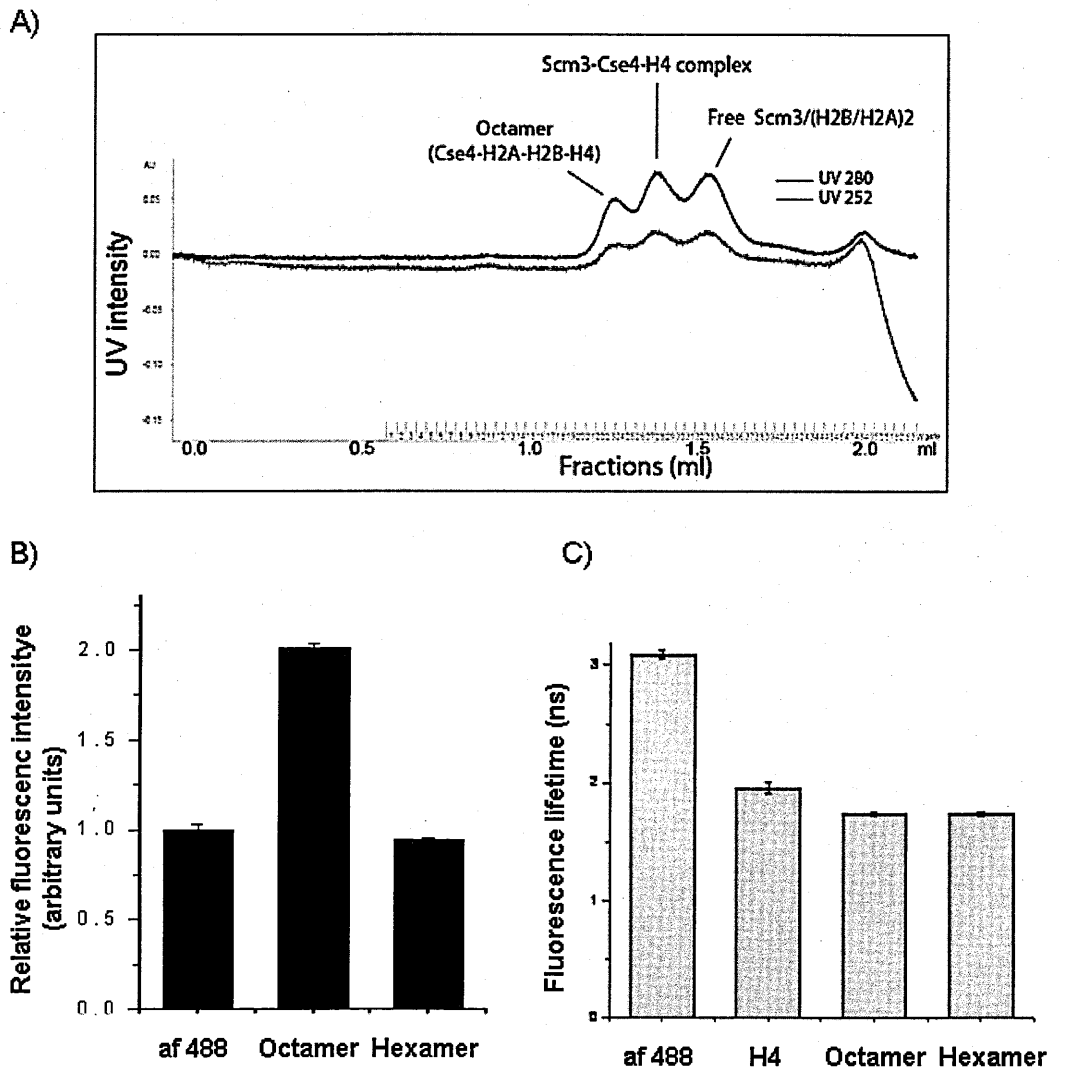

Figure 23. Scm3-Cse4-H4 complex contains only one copy of H4 histone
Alexa-Fluor 488 labeled on H4T71C and Cse4 containing octamers were incubated with Scm3 for 30 min at room temperature, then the sample was fractionated (A) to purify the Scm3-Cse4-H4 complex, on a 2. 4 ml Superdex 200 PC 3. 2/30 gel filtration column (Amersham Biosciences) on a SMART system (Pharmacia Biotech). B) Brightness measurements for un-conjugated Alexa-fluor 488, octamers and Scm3-Cse4-H4 complex. Alexa-fluor 488 brightness was normalized to the value of 1 and the brightness of octamers and Scm3-Cse4-H4 were compared. For brightness measurements peak fractions from (A) for octamers and Scm3-Cse4-H4 complex were taken. The brightness value for octamers doubled as expected and for Scm3-Cse4-H4 remains the same as that of un-conjugated Alexa-Fluor 488, suggesting only one copy of H4 is present. C) Fluorescent lifetime measurements for un-conjugated Alexa-Fluor 488, octamers and Scm3-Cse4-H4 complex.

2. Fluorescence Correlation Spectroscopy (FCS) calibrated intensity measurement of number of Cse4-GFP molecules in the centromere.

To gain a better understanding of the content and structure of Cse4 containing centromeric nucleosomes we quantified the number of Cse4-GFP molecules per centromere cluster *in vivo*. In budding yeast centromeres are clustered in interphase and throughout the mitotic cell cycle [162, 163]. Cse4-GFP is visible as a single focus in the nucleus of living yeast cells (Figure 24) throughout the cell cycle. In collaboration with Brian Slaughter and Jay Unruh, research advisers at Stowers Institute, we have developed a new method to quantify the number of immobile Cse4-GFP molecules in the yeast centromere by taking the advantage of the unique ability of FCS to determine the average number of molecules in the focal volume for a mobile and diffuse protein (1X-EGFP). Once this was determined, calibrated imaging was performed to compare the spot intensity of centromeric Cse4-GFP to the intensity obtained for this diffuse protein using identical imaging parameters. There is a considerable amount of Cse4-GFP present in the nucleus which might impact the intensity of the centromeric focus. To separate the fluorescence intensity of centromeric Cse4-GFP from non-centromeric, nuclear Cse4-GFP, we fit the intensity residing at the centromere to a 3 dimensional Gaussian distribution with non-zero background outside the peak. (see material and methods section).

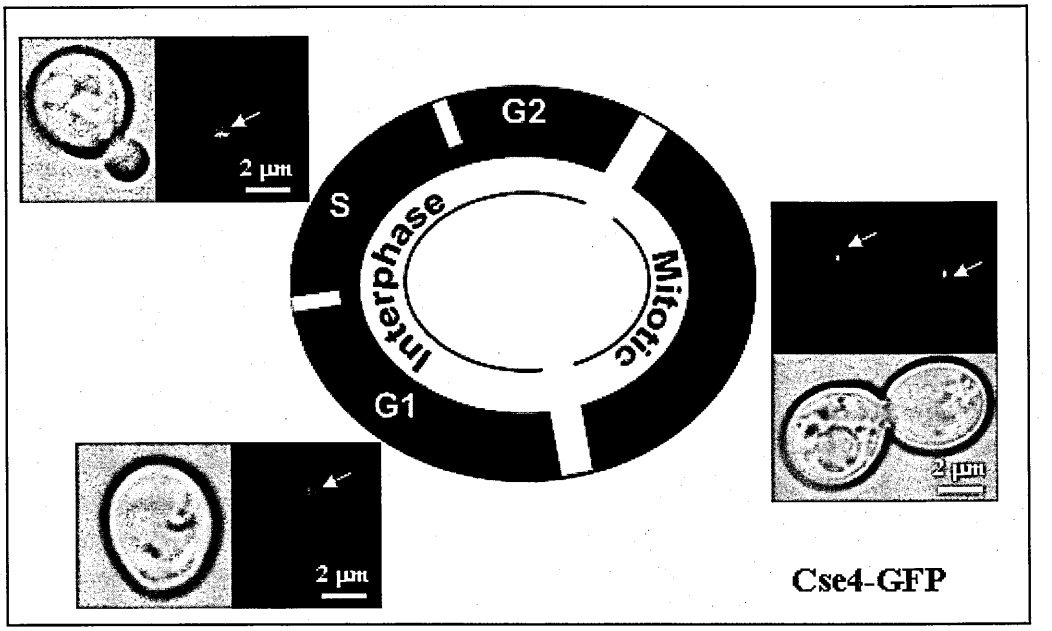

Figure 24. Live imaging of Cse4-GFP using APD-confocal microscopy
In live cells Cse4-GFP appears as a single focus in the nucleus (white arrows), likely corresponding to clustered centromeres. Interphase (G1 and S phase) and mitotic phase Cse4-GFP centromeric clusters are shown.

We quantified the number of Cse4-GFP molecules per centromere cluster for cycling cells (n=400). Strikingly there were two clustered distribution peaks (Figure 25A), one at ~16 Cse4-GFP molecules per centromere cluster and another at ~32. Since budding yeast have 16 chromosomes and a single centromeric nucleosome, this indicates one population of cells with 2 copies of Cse4/centromeric nucleosome and a second population with one copy of Cse4/centromeric nucleosome. This was very surprising to us as we expected either ~16 or ~32 based on the models, proposed for the composition and the structure of the centromeric nucleosomes [51, 97, 136]. Next, we were interested in determining the number of Cse4s/nucleosome at different stages of the cell cycle. To accomplish this we arrested the cells in G1 with alpha factor and counted the number of Cse4-GFP molecules per centromere cluster. In this case the distribution clustered at ~16 Cse4-GFP per centromere cluster (Figure 25B) suggesting only one copy of Cse4 per centromeric nucleosome. This is consistent with the hemisome structure previously proposed [135]. We reasoned the second peak in figure 25A at ~32 might be at the later

stages of cell cycle. Since the distance between SPBs increases slowly from 1-2 μm during G2/M and then rapidly to 4-10 μm during anaphase B [164], we decided to count the Cse4-GFP clusters as a function of spindle pole distance. We used a Spc42-mCherry as a marker for spindle pole body (SPB) to demarcate the cell cycle stage. The distance between the SPBs is measured in 3D (Image J). When we plot the number of Cse4-GFP per cluster as a function of SPB distance we could see two major clusters (Figure 26). Based on the SPB distance we classified them in to two groups: 1) < 3micrometer and 2) >3 micrometer. At a SPB distance of >3 μm, the fluorescence measurements suggests that there are two Cse4-GFP molecules per centromere. In the <3 μm group, we noticed that the brightness for the centromeric clusters ranged from 15 to 28 Cse4-GFP molecules per cluster. In the case of the >3 μm group, the majority of them ranged from 30-37 Cse4-GFP molecules per cluster. Interestingly we also found a few centromeric clusters in the brightness range from 15 to 30 at higher SPB distances (4-8 μm). One possible reason for this variability could be centromeric nucleosomes structural changes at telophase when the centromeric clusters move back from the end position. Our results suggest the transition from one to two copies of Cse4/nucleosome occurs in <3um group. This transition result was very surprising to us, as it has been shown by others that Cse4 containing centromeric nucleosomes are formed at S phase and are stable throrough the cell cycle [37]. We decided to examine and confirm this transition using other approaches namely FRAP (fluorescence recovery after photobleaching) and FRET (fluorescence resonance energy transfer).

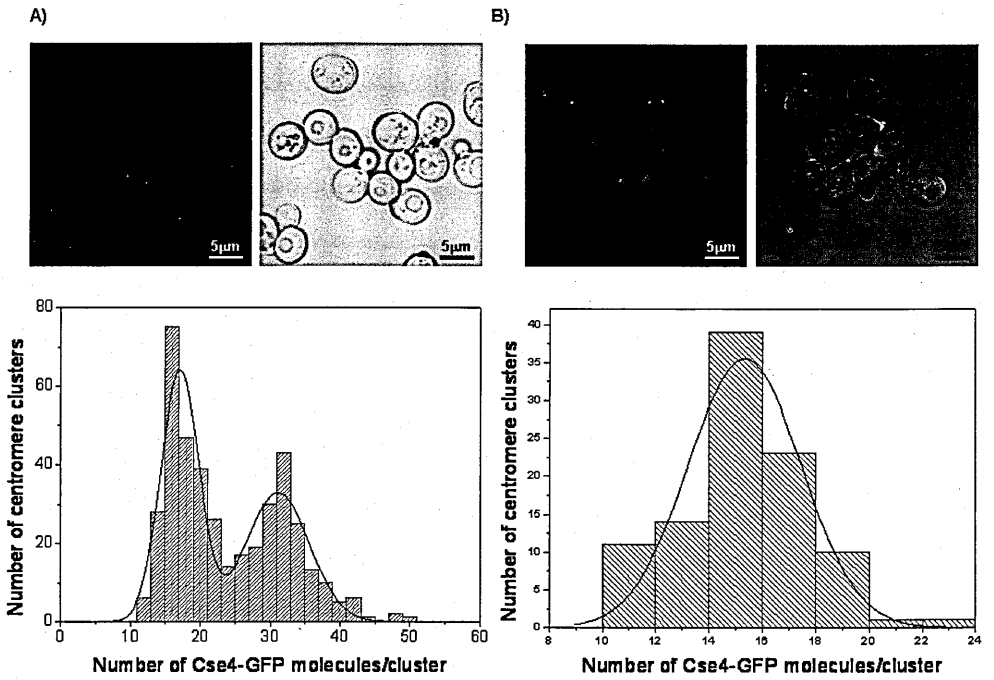

Figure 25. Stoichiometryof Cse4 at centromere measured *in vivo*, by FCS and calibrated imaging

A) Cse4-GFP in cycling cells (n=400) was taken for counting Cse4/centromere cluster. B) Alpha factor arrested cells (n=100). Below panels are the histograms for counted Cse4/clusters for respective figure panels.

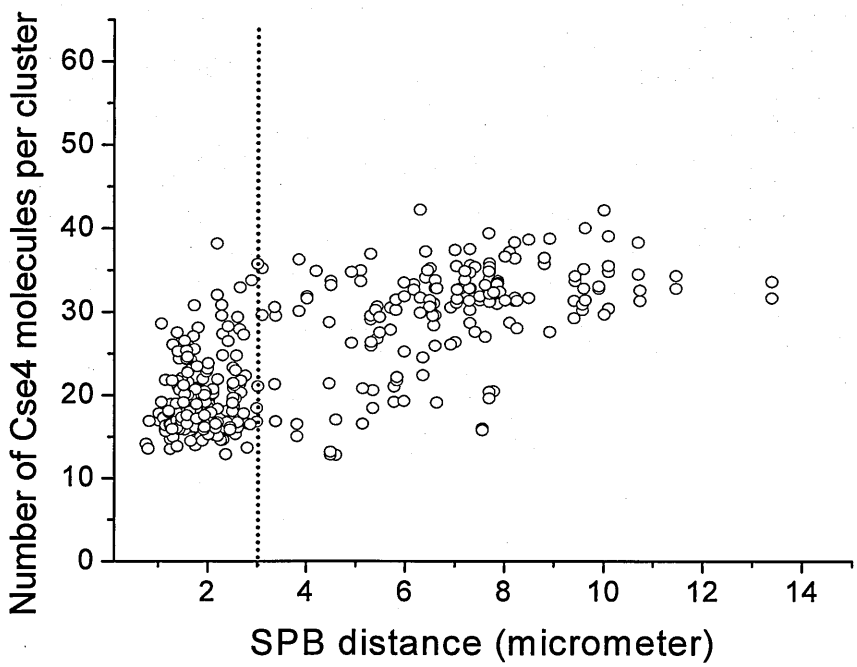

Figure 26. Two Cse4-GFP molecules per centromere when SPB distance >3μm

Histogram (Figure 25A) values were plotted as a function of SPB distance. Spc42-mCherry used as a marker for SPB and the distance measured in 3D (Image J).

3. Centromeric Cse4-GFP recovers after photobleaching

Next we used the Fluorescence Recovery after Photobleaching (FRAP) to examine whether Cse4-GFP recovers in the same cell cycle after photobleaching. Here we have selected live cells where two centromeric clusters are just separated. We photobleached the whole cell with 6 iterations, and then we followed the live image z-stack series at 10 minute intervals. After 40 minutes we are able to see the recovery of Cse4 in the nucleus. At this point cells are in later stages of anaphase (4μm SPBs distance). We quantified the recovered Cse4-GFP and brightness of each centromere cluster varied (Figure 27). The average recovery was ~32% (5 bleaching movies). This result was very surprising because in similar assays it was shown that the centromere focus does not recover significantly from photobleaching till the next S-phase [37]. Our results instead suggest recovery can occur at anaphase.

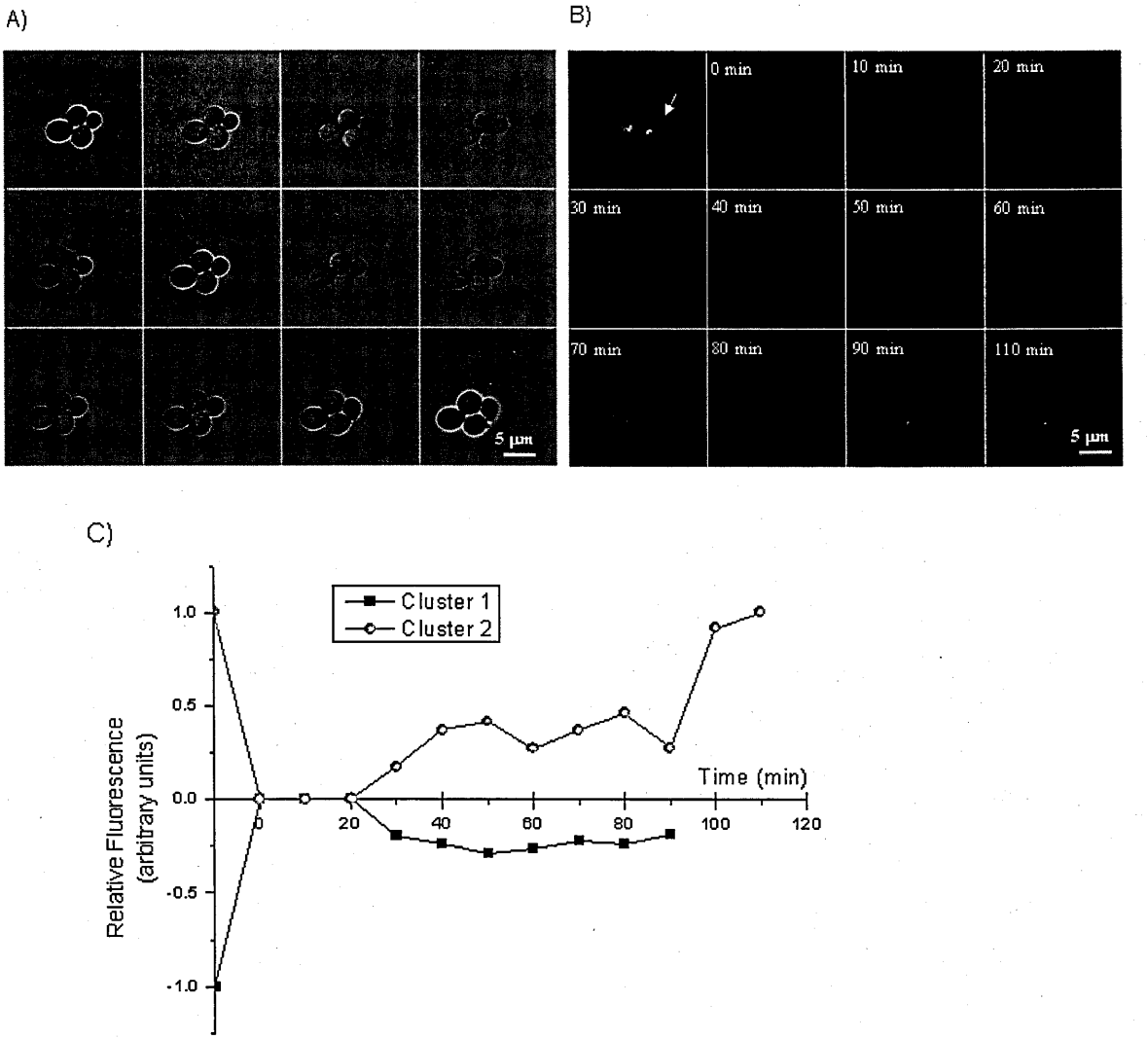

Figure 27. Photobleaching of Cse4 containing centromeric nucleosomes in budding yeast I

A) DIC image & B Cse4-GFP, Whole cells were photobleached (0 min) when two centromere clusters were separated. Fluorescence recovery was followed at 10 min intervals for 110 minute. C) A single example of fluorescence recovery was quantified when two centromeres clusters were separated. Average recovery was 32%. In (C) the cluster 1 (squares) & cluster 2 (circles) represents the two clustered centromeric foci in the lower cell (white arrow) in B). In case of cluster 2 the fluorescence was measured untill the next S phase, where we see drastic increase in brightness (110 min).

In order to verify the result we bleached the centromere focus in cells arrested in hydroxyurea. Centromeres are replicated in early S phase, and in hydroxyurea arrest most centromeres should be duplicated. We arrested the cells for 2 hr in hydroxyurea, released them, and bleached them and a live time series images were taken. Following hydroxyurea treatment, cells took nearly 40 minutes to resume the cell cycle. After 80

minutes recovery of the centromeric focus can be seen. At this time point cells are at later stage of anaphase (4.2μm SPB's distance). We also observed the recovery percentage at 47% nearly (Figure 28), 15% higher than in the previous experiment (Figure 27).

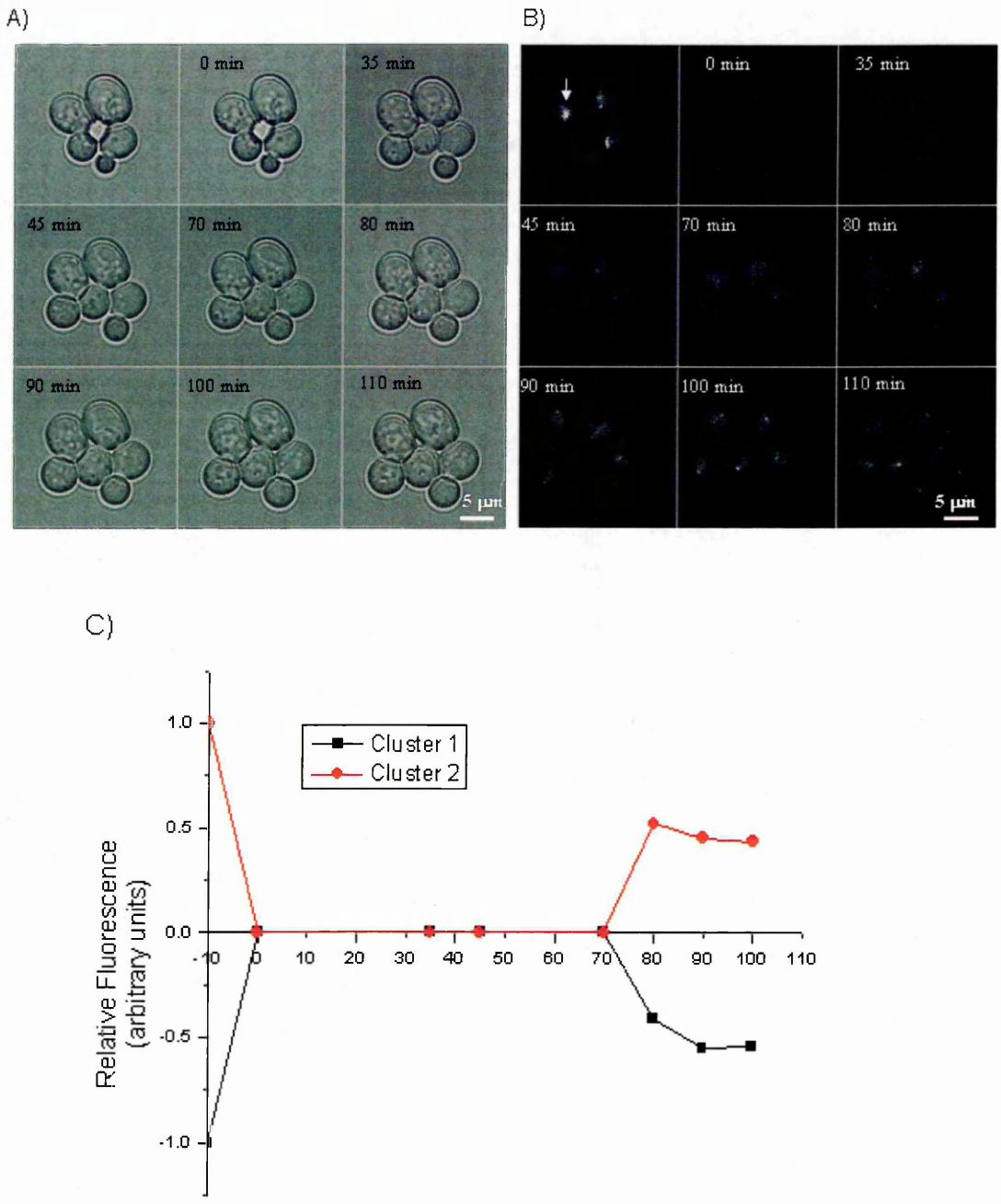

Figure 28. Photobleaching of Cse4 containing centromeric nucleosomes in budding yeast II

A) DIC & B Cse4-GFP image, Whole cells were photobleached (0 min) after a 2hr arrest in 0.2M hydroxyurea. Fluorescence recovery was followed at 35, 45, 70, 80, 90, 100 and 110 min intervals. C) A single example of fluorescence recovery was quantified before bleaching and after the two centromeres clusters were separated. Average recovery was 47%. In (C) the cluster 1 (squares) & cluster 2 (circles) represents the two clustered centromeric foci (white arrow) in B).

Collectively, our data suggest centromeric nucleosomes may exist as hemisomes from G1 to metaphase, and octasomes from the beginning of anaphase. If the nucleosome is an octasome then it contains exactly double the number of Cse4 molecules compared to the hemisomes. So we were interested specifically to examine brightness differences between G1 and late anaphase cells. To do this we have taken a z-stack image of an asynchronous cell culture, generated maximum intensity projection of the entire z stacks, and then developed a heat map (Figure 29). In figure 29 there is a clear increase in brightness between the centromeric spots of anaphase (spot 6) verses G1 cells (spot 1). S phase centromere cluster were also brighter than the metaphase or G1/telophase clusters because S phase centromeric clusters have 32 Cse4 per cluster.

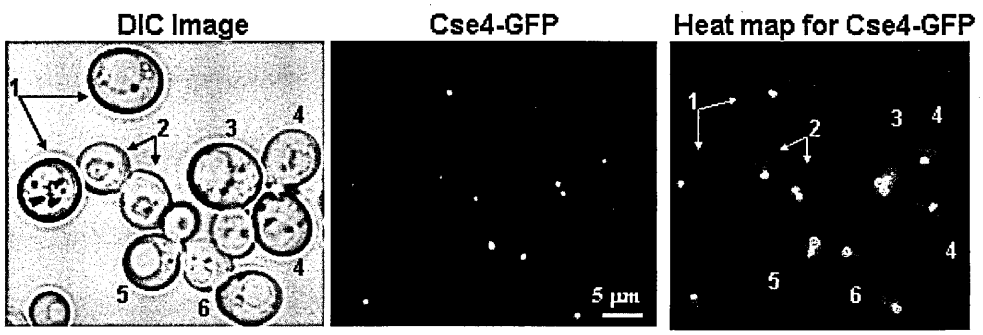

Figure 29. Anaphase Centromeric clusters are brighter than the G1 cells
Heat map for centromeric Cse4-GFP btightness in different stages of cells. Numbers in the images indictes: 1) G1, 2) Telophase/G1, 3) Metaphase, 4) Early S phase, 5) S phase and 6) Late anaphase. Centromere brightness in decending order: S phase and late anaphase> metaphase>G1 or telophase centromeres.

4. Preliminary results on FRET between Cse4-GFP and Cse4-mCHERRY

Since our brightness measurements and photobleaching results suggested that there is an oscillation between one copy of Cse4 at G1 and two copies of Cse4 per nucleosome at anaphase, we wanted to further examine Cse4 interactions by FRET analysis. In order to do this we made a diploid strain which has one copy of Cse4 tagged with GFP and other with mCHERRY. The fluorescence intensity of the Cse4-GFP was measured at the centromere from the most intense focus of a z-stack. Immediately following the initial z-stack, the Cse4-mCHERRY in the entire cell was irreversibly photobleached using

561 nm excitation. The intensity of Cse4-GFP in the centromere was re-measured after acceptor photobleaching. In the case where the donor (Cse4-GFP) is undergoing FRET, irreversible photobleaching of the acceptor probe will result in increased fluorescence of the donor (Cse4-GFP) (see material and methods section for more details).

We measured the FRET efficiency in cycling cells (n=60), and noticed cells that are at anaphase (based on the centromeric foci position) have FRET compared to G1 (round unbudded cells) and S phase cells, which do not show FRET (Figure 30). Since in brightness analysis we had seen the transition from 16 to 32 Cse4-GFP molecules per cluster occuring at the metaphase to anaphase transition, we were interested to know at what stage FRET was occurring. In budding yeast it is reported that centromeres are clustered near the spindle poles throughout the cell cycle [162], so we measured the distance between the centromere clusters and SPB over a cell cycle, and we found a difference of ~0.2 +/- 0.025μm. For example if the distance between the SPB is 2 μm, then centromere cluster distance would be ~1. 8μm. We have taken this centromere cluster distance to define the cell cycle stage. When we plot the FRET efficiency as a function of centromere cluster distance, we observe FRET when clusters are at a distance of <1μm. From 1 -10 μm we did not see any drastic change (Figure 30). This result also suggests that as centromere clusters separate, the centromeric nucleosome has two copies of Cse4-GFP, but prior to this, no FRET is observed, suggesting one copy. This result needs to be validated by collecting more data.

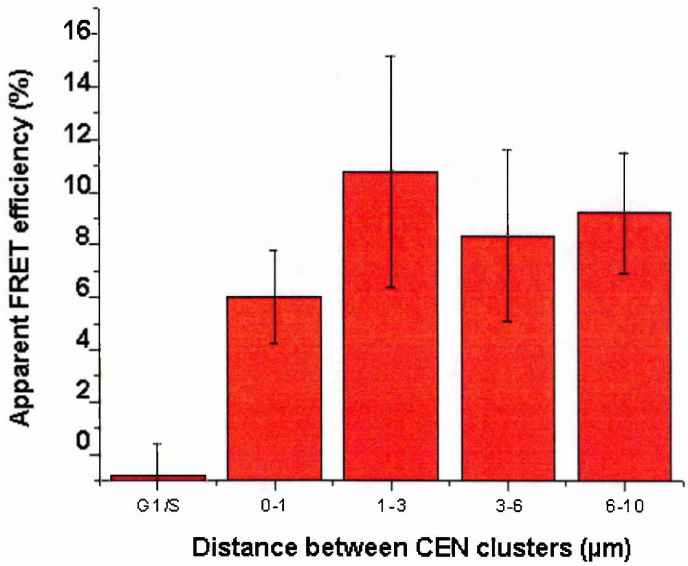

Figure 30. Preliminary FRET experiment shows interactions between Cse4-GFP and Cse4-mCherry once centromere clusters separate
Apparent FRET efficiency measured in cycling cells (n=60) and plotted as a function of distance between centromere clusters to define the cell cycle stage. FRET is not observed for G1 to metaphase. Following centromere cluster separation, FRET is observed.

5. Deletion of Cse4 E3 Psh1 does not affect structural oscillation of centromeric nucleosomes in an obvious way

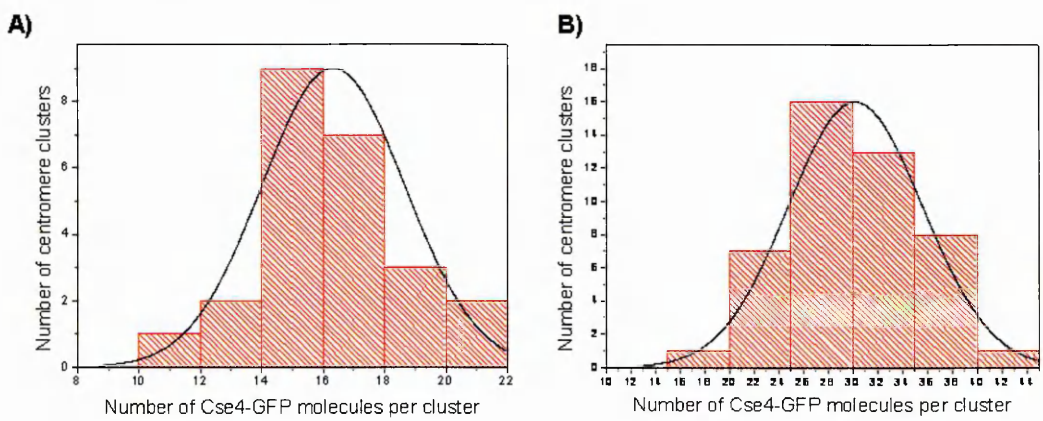

Figure 31. Deletion of Psh1 does not grossly affect the structural oscillation of centromeric nucleosome
Cse4-GFP brightness measurement in Psh1 deletion background, A) G1 cells (n=25) (round unbudded cells) and anaphase cells (n=45) (budded cells with two separated nuclei).

Recently we and Biggins and coworkers have identified Psh1 as an E3 ubiquitin ligase that targets Cse4 for degradation [134, 140]. Psh1 is localized at centromeres throughout the cell cycle and physically and specifically interacts with Cse4 [140]. Psh1 targets Cse4 through binding to the CATD domain of Cse4 and mediates the interaction between Cse4 and Spt16, a component of FACT complex [134]. We wanted to examine whether destruction of Cse4 by Psh1 might affect the structural oscillation of Cse4 nucleosomes. To test this, we deleted Psh1 and counted the centromere brightness in G1 and anaphase cells. We do not observe any major changes in the brightness measurements (Figure 31) compared to wild-type controls (Figure 25). However, more experiments will be required to determine whether Psh1 subtly influences the oscillation.

IV. Discussion

To understand the structure and composition of centromeric nucleosomes in budding yeast, we have undertaken several biochemical and microscopic experiments. Herein we have demonstrated that, depending on the nucleosome assembly factor, budding yeast CenH3 (Cse4) can form different types of nucleosomes *in vitro*. Our *in vivo* chromatin immunoprecipitation and *in vitro* Cse4 containing octamer reconstitution with Cse4 lethal point mutants strongly suggests Cse4-Cse4 dimerization occurs and is important for function. The requirement for dimerization is an indication of the presence of octameric nucleosomes. Additionally, topoisomers separated on chloroquine gels (Figure 20) suggest that Cse4 nucleosomes are capable of wrapping DNA in a conventional left handed manner, with induction of negative supercoils. CENP-A also forms octameric nucleosomes with negative supercoiling [137]. Collectively all these data strongly support the existence of octasomes.

When we analysed the Scm3-Cse4-H4 complex for stoichiometry we observed that they contain only one copy of H4. Recently, the structure of Scm3-Cse4-H4 has been solved and Scm3 forms a trimeric complex with Cse4-H4 [165]. Although this complex has been called a hexamer [51], our results suggest it may be a trimer. Furthermore elu-

tion profiles of Scm3 assembled nucleosomes suggested that these nucleosomes are smaller in size compared to Nap1 assembled nucleosomes, suggesting Scm3 assembled nucleosomes are different from Nap1 assembled nucleosomes. Taken together this series of results is most consistent with another proposed model for centromeric chromatin, one in which a single molecule of each CENP-A (Cse4), H2A, H2B, and H4 forms a structure called a hemisome [136].

To further study the centromeric nucleosomes *in vivo*, we quantified the Cse4-GFP brightness in asynchronous cultures and found one Cse4/nucleosome at G1 and two copies of Cse4/nucleosome at anaphase. Although unexpected, this result is consistent with our *in vitro* experiments and strongly implies the presence of two different types of Cse4 containing nucleosomes. Additionally, photobleaching experiments indicated that Cse4 is incorporated into centromeric nucleosomes during anaphase, similar to CID in Drosophila. FRET analysis also showed that Cse4-Cse4 interaction occurs only at anaphase. Taken together, our *in vitro* and *in vivo* data support the presence of a hemisome at G1 and an octasome at anaphase.

We were able to pinpoint when structural change occurs by measuring SPB distance. At a distance of >3 μm, most of the cluster ranges from 30-37 Cse4/cluster, which is closer to a value of two copies of Cse4/nucleosome. When clusters were within 3 μm we noticed a wider range, from 15-28 Cse4/cluster, suggesting the hemisome is in the process of switching to an octasome. This data is further supported by the FRET analysis where we analyzed the efficiency of FRET based on the distance between the centromeric clusters. We were able to see a low level of FRET at the distance of < 1 μm. Even though we need to validate this result by taking more data, it seems likely that the centromeric nucleosome undergoes a structural change at the metaphase to anaphase transition. The sum of all of our experiments strongly suggests that the centromeric nucleosomes are hemisomes at G1 and octasomes at anaphase.

There has been a heated debate over the structure of centromeric nucleosomes.

Several models have reasonable experimental support. Our studies help to reconcile part of the debate. We have experimental evidence to support the to support the idea that there are two types of centromeric nucleosomes in the same organism: 1) octasomes and 2) hemisomes. Strong support for the existence of octasomes came from the importance of the Cse4 dimerization surface that mediates octamer formation. In these experiments, Cse4 dimerization was measured in asynchronous cultures, where a significant amount of anaphase cells are present. It is possible that the Cse4-Cse4 interactions measured were due to the anaphase cells in the population. The hemisome model was proposed based on the experimental evidence in Drosophila S2 cells [136] and in HeLa cells [158] showing centromeric nucleosomes were half as tall as canonical nucleosomes. Furthermore, cross linking studies were also consistent with hemisomes. The centromeric nucleosomes used for these studies were purified from interphase cells. Our data suggests that from G1 to metaphase, cells have hemisomic centromeric nucleosomes. This model was further supported by the demonstration of positive supercoils, from centromeric nucleosomes in mini chromosomes from budding yeast [135]. In these experiments, cells were synchronized with alpha factor at 25°C and 2 hr after release collected for supercoiling measurements. Because anaphase quite short, it is likely that the majority of the cells used for this experiment would have been non-anaphase cells. Another explanation for the positive supercoiling could be transcriptional artifacts or nonspecific binding of Ndc10 to the centromeric DNA. However, we prefer the interpretation that the positive supercoiling is due to a hemisomal configuration.

The hexasomal model also bears evaluation in light of our data. Copy number analysis of H4 in the Scm3-Cse4-H4, complex reveals a single copy of H4 in this complex. This result is difficult to reconcile with the hexamer. Furthermore, H2A/H2B were required *in vitro* for nucleosome formation. Moreover, the Scm3-Cse4-H4 structure has been solved, and it has been shown that Scm3 forms a trimeric complex with Cse4-H4 [165]. It is possible that this complex runs at the molecular size of a hexamer on gel fil-

tration columns due to unusual shapes. To explain the lack of H2A/H2B at centromeres by ChIP, we suggest that accessibility of these histones to antibodies is limited at the centromere due to the kinetochore.

V. Importance of the present findings

Over the last decade, our knowledge of how centromere identity is propagated from one generationto the next has increased enormously. Many factors have been identified and a number of them have been shown to affect the incorporation or maintenance of Cse4/CENP-A at centromeres. However, the exact role of these factors remains unknown. Here we have deciphered the role of Scm3 in targeting and assembling Cse4 nucleosomes at centromeres. Scm3 orthologs have been identified in other organisms including a human ortholog called HJURP. Sequence analysis indeed suggests the presence of a common domain in these proteins [49]. We demonstrate that Scm3 assembles Cse4 nucleosomes in a CATD (centromere targeting domain) dependent manner in budding yeast, suggesting that the CATD of CENP-A and HJURP are similarly involved in nucleosome assembly in humans.

Our second major discovery is that the number of Cse4 molecules per centromere oscillates with the cell cycle. Our data suggest that a right handed hemisome may be the functional centromeric nucleosome for the majority of the cell cycle, and this unusual structure may help to distinguish the centromere [135, 136]. Why does the structure appear to switch to an octameric nucleosome in anaphase? One possible explanation is microtubule force. Consider the following findings from other groups: 1) the right handed wrapping of Cse4 nucleosomes resists condensation [136], 2) the octasome structure facilitates the uniform packaging of H3 nucleosomes in pericentric heterochromatin, 3) the CATD of CENP-A causes compaction of the CENP-A octamer relative to H3 octamers [47, 48], and 4) spindle elongation before initiation of anaphase is smooth but when anaphase A is initiated (2.5-3.0 μm spindle length) there is a jump in spindle length of 1.8μm (average) in less than 26 s [166]. Together these findings lead us to speculate that there may be more microtubule force applied at centromeres during early anaphase in order to facilitate the rapid jump in spindle elongation.

This is the same time at which we observe a transition of hemisome to octasome. Based on findings in the literature and our results we speculate that the hemisome structure may be disrupted by the microtubule force during early anaphase, converting to a more stable octasome structure which is able to withstand the microtubule force during early anaphase.

VI. Followup

We have used our data and the current information in the literature to create a working model to explain the assembly and structural changes of centromeric nucleosomes (Figure 32). To futher test this model we propose several additional experiments. We would like to test the cell cycle specificity of the Cse4-Cse4 interaction using the co-IP method from Figure 22 and staged cells. We would also like to test the DNA topology of centromeric nucleosomes in minichromosomes over the cell cycle, expecting positive supercoils at G1 and negative supercoils at anaphase. To test this we could use the same method employed by the Henikoff group. One discovery previously reported by our lab is that overexpression of Cse4 can rescue the Scm3 deletion [97]. We would like to test what type of centromeric nucleosomes is formed in absence of Scm3.

Since the structural transition from hemisome to octasome occurs at the metaphase to anaphase transition, we speculate that tension/force exerted on the centromeric nucleosome by microtubules in association with sister chromatid cohesion could influence the transition. To test this we will measure the Cse4-GFP brightness in the cells where chromatids have no tension/force by using a Gal-CDC6 with additional use of Nocodazole. By these additional experiments we can test and further refine our working model for the cell cycle coupled state of centromeric nucleosomes. In the future it will be exciting to see if basic features of centromeric nucleosome deposition and structural oscillations are evolutionarily conserved.

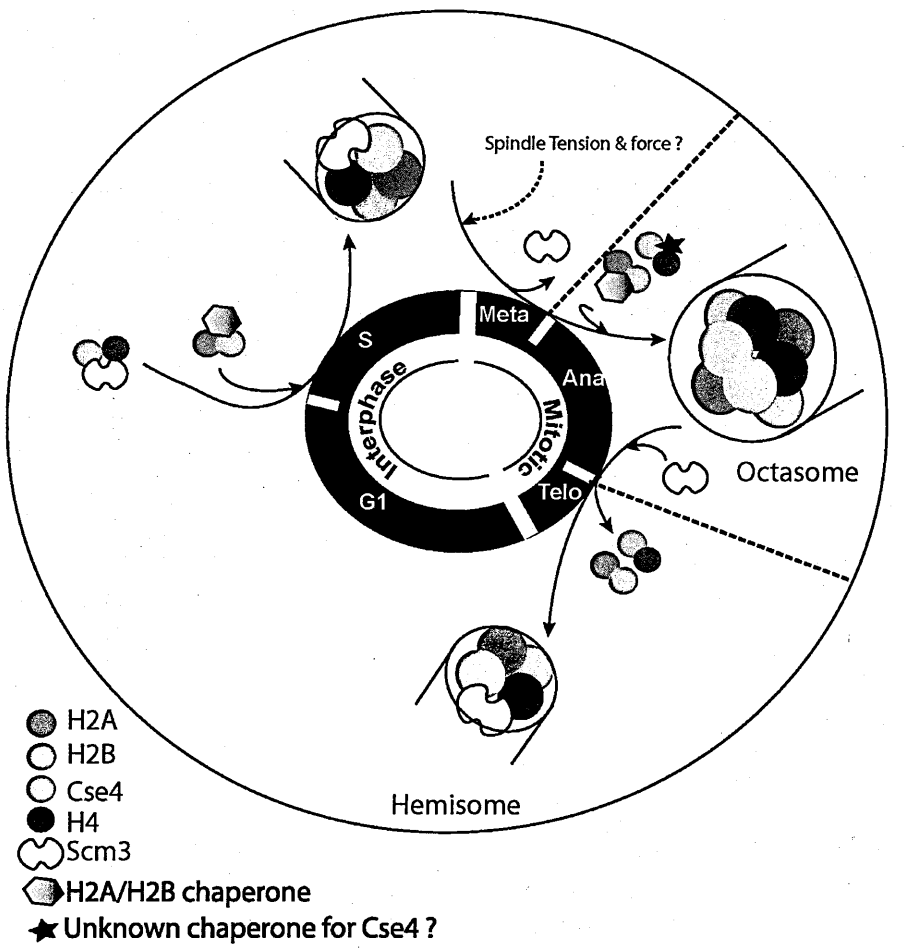

Figure 32. Model for the centromeric nucleosome formation and structural oscillation

Scm3 targets Cse4-H4 to the centromere in a trimer form and then H2A/H2B joins to form a hemisome at early S phase. Spindle tension & force on the centromeric nucleosome causes destabilization and Scm3 leaves the centromere. As soon as Scm3 leaves the centromeric nucleosome, becomes an octasome with two copies of Cse4, H4, H2A, and H2B. When the spindle force subsides in telophase, which is also coincides with incoming Scm3, the octasome is split and a hemisome forms.

VI. References

1. Kornberg, R.D., *Chromatin Structure: A Repeating Unit of Histones and DNA.* Science, 1974. **184**(4139): p. 868-871.
2. Wu, R.S. and W.M. Bonner, *Separation of basal histone synthesis from S-phase histone synthesis in dividing cells.* Cell, 1981. **27**(2, Part 1): p. 321-330.
3. Alberts, B.J., Alexander. Lewis, Julian. Raff, Martin. Roberts, Keith. and Walter Peter. , *Molecular Biology of the Cell, 4th edition.* New York: Garland Science; 2002., 2002.
4. Luger, K., et al., *Crystal structure of the nucleosome core particle at 2.8[thinsp]A resolution.* Nature, 1997. **389**(6648): p. 251-260.
5. Tyler, J.K., *Chromatin assembly.* European Journal of Biochemistry, 2002. **269**(9): p. 2268-2274.
6. Adams, C.R. and R.T. Kamakaka, *Chromatin assembly: biochemical identities and genetic redundancy.* Current Opinion in Genetics & Development, 1999. **9**(2): p. 185-190.
7. Verreault, A., *De novo nucleosome assembly: new pieces in an old puzzle.* Genes & Development, 2000. **14**(12): p. 1430-1438.
8. Krude, T., *Chromatin assembly during DNA replication in somatic cells.* European Journal of Biochemistry, 1999. **263**(1): p. 1-5.
9. Ahmad, K. and S. Henikoff, *The Histone Variant H3.3 Marks Active Chromatin by Replication-Independent Nucleosome Assembly.* Molecular Cell, 2002. **9**(6): p. 1191-1200.
10. Ray-Gallet, D., et al., *HIRA Is Critical for a Nucleosome Assembly Pathway Independent of DNA Synthesis.* Molecular Cell, 2002. **9**(5): p. 1091-1100.
11. Tagami, H., et al., *Histone H3.1 and H3.3 Complexes Mediate Nucleosome Assembly Pathways Dependent or Independent of DNA Synthesis.* Cell, 2004. **116**(1): p. 51-61.
12. Laskey, R.A., et al., *Nucleosomes are assembled by an acidic protein which binds histones and transfers them to DNA.* Nature, 1978. **275**(5679): p. 416-420.
13. De Koning, L., et al., *Histone chaperones: an escort network regulating histone traffic.* Nat Struct Mol Biol, 2007. **14**(11): p. 997-1007.
14. Andrews, A.J., et al., *The Histone Chaperone Nap1 Promotes Nucleosome Assembly by Eliminating Nonnucleosomal Histone DNA Interactions.* Molecular Cell, 2010. **37**(6): p. 834-842.
15. Park, Y.-J. and K. Luger, *Histone chaperones in nucleosome eviction and histone exchange.* Current Opinion in Structural Biology, 2008. **18**(3): p. 282-289.
16. Shibahara, K.-i. and B. Stillman, *Replication-Dependent Marking of DNA by PCNA Facilitates CAF-1-Coupled Inheritance of Chromatin.* Cell, 1999. **96**(4): p. 575-585.
17. Gaillard, P.-H.L., et al., *Chromatin Assembly Coupled to DNA Repair: A New Role for Chromatin Assembly Factor I.* Cell, 1996. **86**(6): p. 887-896.
18. Green, E.M., et al., *Replication-Independent Histone Deposition by the HIR Complex and Asf1.* Current Biology, 2005. **15**(22): p. 2044-2049.
19. Loppin, B., et al., *The histone H3.3 chaperone HIRA is essential for chromatin assembly in the male pronucleus.* Nature, 2005. **437**(7063): p. 1386-1390.
20. Luger, K. and J.C. Hansen, *Nucleosome and chromatin fiber dynamics.* Current Opinion in Structural Biology, 2005. **15**(2): p. 188-196.
21. Workman, J.L., *Nucleosome displacement in transcription.* Genes & Development, 2006. **20**(15): p. 2009-2017.
22. Zlatanova, J., C. Seebart, and M. Tomschik, *Nap1: taking a closer look at a juggler*

protein of extraordinary skills. The FASEB Journal, 2007. **21**(7): p. 1294-1310.
23. Reinberg, D. and R.J. Sims, *de FACTo Nucleosome Dynamics.* Journal of Biological Chemistry, 2006. **281**(33): p. 23297-23301.
24. Kireeva, M.L., et al., *Nucleosome Remodeling Induced by RNA Polymerase II: Loss of the H2A/H2B Dimer during Transcription.* Molecular Cell, 2002. **9**(3): p. 541-552.
25. Belotserkovskaya, R. and D. Reinberg, *Facts about FACT and transcript elongation through chromatin.* Current Opinion in Genetics & Development, 2004. **14**(2): p. 139-146.
26. Moggs, J.G., et al., *A CAF-1-PCNA-Mediated Chromatin Assembly Pathway Triggered by Sensing DNA Damage.* Mol. Cell. Biol., 2000. **20**(4): p. 1206-1218.
27. Kamakaka, R.T. and S. Biggins, *Histone variants: deviants?* Genes & Development, 2005. **19**(3): p. 295-316.
28. Buttinelli, M., et al., *The role of histone H1 in chromatin condensation and transcriptional repression.* Genetica, 1999. **106**(1): p. 117-124.
29. Meneghini, M.D., M. Wu, and H.D. Madhani, *Conserved Histone Variant H2A.Z Protects Euchromatin from the Ectopic Spread of Silent Heterochromatin.* Cell, 2003. **112**(5): p. 725-736.
30. Chadwick, B.P. and H.F. Willard, *Histone H2A variants and the inactive X chromosome: identification of a second macroH2A variant.* Human Molecular Genetics, 2001. **10**(10): p. 1101-1113.
31. Stoler, S., et al., *A mutation in CSE4, an essential gene encoding a novel chromatin-associated protein in yeast, causes chromosome nondisjunction and cell cycle arrest at mitosis.* Genes & Development, 1995. **9**(5): p. 573-586.
32. Black, B.E. and E.A. Bassett, *The histone variant CENP-A and centromere specification.* Current Opinion in Cell Biology, 2008. **20**(1): p. 91-100.
33. Torras-Llort, M., O. Moreno-Moreno, and F. Azorin, *Focus on the centre: the role of chromatin on the regulation of centromere identity and function.* EMBO J, 2009. **28**(16): p. 2337-2348.
34. Morey, L., et al., *The Histone Fold Domain of Cse4 Is Sufficient for CEN Targeting and Propagation of Active Centromeres in Budding Yeast.* Eukaryotic Cell, 2004. **3**(6): p. 1533-1543.
35. Gascoigne, K.E. and I.M. Cheeseman, *Kinetochore assembly: If you build it, they will come.* Current Opinion in Cell Biology, 2011. **23**(1): p. 102-108.
36. Wieland, G., et al., *Functional Complementation of Human Centromere Protein A (CENP-A) by Cse4p from Saccharomyces cerevisiae.* Mol. Cell. Biol., 2004. **24**(15): p. 6620-6630.
37. Pearson, C.G., et al., *Stable Kinetochore-Microtubule Attachment Constrains Centromere Positioning in Metaphase.* Current Biology, 2004. **14**(21): p. 1962-1967.
38. Shelby, R.D., O. Vafa, and K.F. Sullivan, *Assembly of CENP-A into Centromeric Chromatin Requires a Cooperative Array of Nucleosomal DNA Contact Sites.* The Journal of Cell Biology, 1997. **136**(3): p. 501-513.
39. Jansen, L.E.T., et al., *Propagation of centromeric chromatin requires exit from mitosis.* The Journal of Cell Biology, 2007. **176**(6): p. 795-805.
40. Schuh, M., C.F. Lehner, and S. Heidmann, *Incorporation of Drosophila CID/CENP-A and CENP-C into Centromeres during Early Embryonic Anaphase.* Current Biology, 2007. **17**(3): p. 237-243.
41. Takahashi, K., E.S. Chen, and M. Yanagida, *Requirement of Mis6 Centromere Connector for Localizing a CENP-A-Like Protein in Fission Yeast.* Science, 2000. **288**(5474): p. 2215-2219.
42. Takahashi, K., et al., *Two distinct pathways responsible for the loading of CENP-A to centromeres in the fission yeast cell cycle.* Philosophical Transactions of the

Royal Society B: Biological Sciences, 2005. **360**(1455): p. 595-607.
43. Lermontova, I., et al., *Loading of Arabidopsis Centromeric Histone CENH3 Occurs Mainly during G2 and Requires the Presence of the Histone Fold Domain.* The Plant Cell Online, 2006. **18**(10): p. 2443-2451.
44. Foltz, D.R., et al., *Centromere-Specific Assembly of CENP-A Nucleosomes Is Mediated by HJURP.* Cell, 2009. **137**(3): p. 472-484.
45. Dunleavy, E.M., et al., *HJURP Is a Cell-Cycle-Dependent Maintenance and Deposition Factor of CENP-A at Centromeres.* Cell, 2009. **137**(3): p. 485-497.
46. Shuaib, M., et al., *HJURP binds CENP-A via a highly conserved N-terminal domain and mediates its deposition at centromeres.* Proceedings of the National Academy of Sciences, 2010. **107**(4): p. 1349-1354.
47. Black, B.E., et al., *Structural determinants for generating centromeric chromatin.* Nature, 2004. **430**(6999): p. 578-582.
48. Black, B.E., et al., *Centromere Identity Maintained by Nucleosomes Assembled with Histone H3 Containing the CENP-A Targeting Domain.* Molecular Cell, 2007. **25**(2): p. 309-322.
49. Sanchez-Pulido, L., et al., *Common Ancestry of the CENP-A Chaperones Scm3 and HJURP.* Cell, 2009. **137**(7): p. 1173-1174.
50. Stoler, S., et al., *Scm3, an essential Saccharomyces cerevisiae centromere protein required for G2/M progression and Cse4 localization.* Proceedings of the National Academy of Sciences, 2007. **104**(25): p. 10571-10576.
51. Mizuguchi, G., et al., *Nonhistone Scm3 and Histones CenH3-H4 Assemble the Core of Centromere-Specific Nucleosomes.* Cell, 2007. **129**(6): p. 1153-1164.
52. Camahort, R., et al., *Scm3 Is Essential to Recruit the Histone H3 Variant Cse4 to Centromeres and to Maintain a Functional Kinetochore.* Molecular Cell, 2007. **26**(6): p. 853-865.
53. Hartwell, L.H., Dutcher, S. K., Wood, 1. and G. S., B., *The fidelity of mitotic chromosome reproduction in S. cerevisiae.* Rec. Adv. Yeast Mol. BioI, 1982. **1**: p. 28-38.
54. Rieder, C.L., et al., *Anaphase onset in vertebrate somatic cells is controlled by a checkpoint that monitors sister kinetochore attachment to the spindle.* The Journal of Cell Biology, 1994. **127**(5): p. 1301-1310.
55. Hoyt, M.A., L. Totis, and B.T. Roberts, *S. cerevisiae genes required for cell cycle arrest in response to loss of microtubule function.* Cell, 1991. **66**(3): p. 507-517.
56. Li, R. and A.W. Murray, *Feedback control of mitosis in budding yeast.* Cell, 1991. **66**(3): p. 519-531.
57. Guenette, S., M. Magendantz, and F. Solomon, *Suppression of a conditional mutation in alpha-tubulin by overexpression of two checkpoint genes.* J Cell Sci, 1995. **108**(3): p. 1195-1204.
58. Wells, W.A. and A.W. Murray, *Aberrantly segregating centromeres activate the spindle assembly checkpoint in budding yeast.* The Journal of Cell Biology, 1996. **133**(1): p. 75-84.
59. Neff, M.W. and D.J. Burke, *A delay in the Saccharomyces cerevisiae cell cycle that is induced by a dicentric chromosome and dependent upon mitotic checkpoints.* Mol. Cell. Biol., 1992. **12**(9): p. 3857-3864.
60. Weiss, E. and M. Winey, *The Saccharomyces cerevisiae spindle pole body duplication gene MPS1 is part of a mitotic checkpoint.* The Journal of Cell Biology, 1996. **132**(1): p. 111-123.
61. Hardwick, K.G., et al., *Activation of the Budding Yeast Spindle Assembly Checkpoint Without Mitotic Spindle Disruption.* Science, 1996. **273**(5277): p. 953-956.
62. Pangilinan, F. and F. Spencer, *Abnormal kinetochore structure activates the spindle assembly checkpoint in budding yeast.* Mol. Biol. Cell, 1996. **7**(8): p. 1195-1208.

63. Henikoff, S. and Y. Dalal, *Centromeric chromatin: what makes it unique?* Current Opinion in Genetics & Development, 2005. **15**(2): p. 177-184.
64. Yoda, K., et al., *Human centromere protein A (CENP-A) can replace histone H3 in nucleosome reconstitution in vitro.* Proceedings of the National Academy of Sciences of the United States of America, 2000. **97**(13): p. 7266-7271.
65. Blower, M.D., B.A. Sullivan, and G.H. Karpen, *Conserved Organization of Centromeric Chromatin in Flies and Humans.* Developmental Cell, 2002. **2**(3): p. 319-330.
66. Meluh, P.B., et al., *Cse4p Is a Component of the Core Centromere of Saccharomyces cerevisiae.* Cell, 1998. **94**(5): p. 607-613.
67. Lamb, N.E. and T.J. Hassold, *Nondisjunction — A View from Ringside.* New England Journal of Medicine, 2004. **351**(19): p. 1931-1934.
68. Fitzgerald-Hayes, M., L. Clarke, and J. Carbon, *Nucleotide sequence comparisons and functional analysis of yeast centromere DNAs.* Cell, 1982. **29**(1): p. 235-244.
69. Carbon, J., *Yeast centromeres: Structure and function.* Cell, 1984. **37**(2): p. 351-353.
70. McGrew, J., B. Diehl, and M. Fitzgerald-Hayes, *Single base-pair mutations in centromere element III cause aberrant chromosome segregation in Saccharomyces cerevisiae.* Mol. Cell. Biol., 1986. **6**(2): p. 530-538.
71. Cumberledge, S. and J. Carbon, *Mutational Analysis of Meiotic and Mitotic Centromere Function in Saccharomyces cerevisiae.* Genetics, 1987. **117**(2): p. 203-212.
72. Steiner, N.C., K.M. Hahnenberger, and L. Clarke, *Centromeres of the fission yeast Schizosaccharomyces pombe are highly variable genetic loci.* Mol. Cell. Biol., 1993. **13**(8): p. 4578-4587.
73. Wood, V., et al., *The genome sequence of Schizosaccharomyces pombe.* Nature, 2002. **415**(6874): p. 871-880.
74. Sun, X., et al., *Sequence Analysis of a Functional Drosophila Centromere.* Genome Research, 2003. **13**(2): p. 182-194.
75. Murphy, T.D. and G.H. Karpen, *Localization of centromere function in a drosophila minichromosome.* Cell, 1995. **82**(4): p. 599-609.
76. Manuelidis, L. and J.C. Wu, *Homology between human and simian repeated DNA.* Nature, 1978. **276**(5683): p. 92-94.
77. Jin, W., et al., *Maize Centromeres: Organization and Functional Adaptation in the Genetic Background of Oat.* Plant Cell, 2004. **16**(3): p. 571-581.
78. Kato, A., J.C. Lamb, and J.A. Birchler, *Chromosome painting using repetitive DNA sequences as probes for somatic chromosome identification in maize.* Proceedings of the National Academy of Sciences of the United States of America, 2004. **101**(37): p. 13554-13559.
79. Ananiev, E.V., R.L. Phillips, and H.W. Rines, *Chromosome-specific molecular organization of maize (Zea mays L.) centromeric regions.* Proceedings of the National Academy of Sciences of the United States of America, 1998. **95**(22): p. 13073-13078.
80. Cheeseman, I.M., D.G. Drubin, and G. Barnes, *Simple centromere, complex kinetochore.* The Journal of Cell Biology, 2002. **157**(2): p. 199-203.
81. McAinsh, A.D., J.D. Tytell, and P.K. Sorger, *Structure, Function, and regulation of budding yeast kinetochores.* Annual Review of Cell and Developmental Biology, 2003. **19**(1): p. 519-539.
82. Westermann, S., et al., *Architecture of the budding yeast kinetochore reveals a conserved molecular core.* The Journal of Cell Biology, 2003. **163**(2): p. 215-222.
83. Lechner, J. and J. Carbon, *A 240 kd multisubunit protein complex, CBF3, is a major component of the budding yeast centromere.* Cell, 1991. **64**(4): p. 717-725.
84. Niedenthal, R.K., et al., *Cpf1 protein induced bending of yeast centromere DNA*

element I. Nucleic Acids Research, 1993. **21**(20): p. 4726-4733.
85. Tanaka, Y., et al., *Crystal structure of the CENP-B protein-DNA complex: the DNA-binding domains of CENP-B induce kinks in the CENP-B box DNA.* EMBO J, 2001. **20**(23): p. 6612-6618.
86. Meluh, P. and D. Koshland, *Evidence that the MIF2 gene of Saccharomyces cerevisiae encodes a centromere protein with homology to the mammalian centromere protein CENP-C.* Mol. Biol. Cell, 1995. **6**(7): p. 793-807.
87. De Wulf, P., A.D. McAinsh, and P.K. Sorger, *Hierarchical assembly of the budding yeast kinetochore from multiple subcomplexes.* Genes & Development, 2003. **17**(23): p. 2902-2921.
88. Euskirchen, G.M., *Nnf1p, Dsn1p, Mtw1p, and Nsl1p: a New Group of Proteins Important for Chromosome Segregation in Saccharomyces cerevisiae.* Eukaryotic Cell, 2002. **1**(2): p. 229-240.
89. Janke, C., et al., *The budding yeast proteins Spc24p and Spc25p interact with Ndc80p and Nuf2p at the kinetochore and are important for kinetochore clustering and checkpoint control.* EMBO J, 2001. **20**(4): p. 777-791.
90. Wigge, P.A. and J.V. Kilmartin, *The Ndc80p Complex from Saccharomyces cerevisiae Contains Conserved Centromere Components and Has a Function in Chromosome Segregation.* The Journal of Cell Biology, 2001. **152**(2): p. 349-360.
91. Heald, R., *Motor Function in the Mitotic Spindle Minireview.* Cell, 2000. **102**(4): p. 399-402.
92. Goffeau, A., et al., *Life with 6000 Genes.* Science, 1996. **274**(5287): p. 546-567.
93. Lee, W., et al., *A high-resolution atlas of nucleosome occupancy in yeast.* Nat Genet, 2007. **39**(10): p. 1235-1244.
94. Human Genome Sequencing, C., *Finishing the euchromatic sequence of the human genome.* Nature, 2004. **431**(7011): p. 931-945.
95. Sambrook, J., and Russell, D.W, *Molecular cloning: A laboratory manual, 3rd edition. Cold Spring Harbour, New York: Cold Spring Harbour Laboratory Press, 2001.*
96. Luger, K., et al., *Characterization of nucleosome core particles containing histone proteins made in bacteria.* Journal of Molecular Biology, 1997. **272**(3): p. 301-311.
97. Camahort, R., et al., *Cse4 Is Part of an Octameric Nucleosome in Budding Yeast.* Molecular Cell, 2009. **35**(6): p. 794-805.
98. Ito, T., et al., *ACF, an ISWI-Containing and ATP-Utilizing Chromatin Assembly and Remodeling Factor.* Cell, 1997. **90**(1): p. 145-155.
99. Yang, J.G. and G.J. Narlikar, *FRET-based methods to study ATP-dependent changes in chromatin structure.* Methods, 2007. **41**(3): p. 291-295.
100. Park, Y.-J. and K. Luger, *The structure of nucleosome assembly protein 1.* Proceedings of the National Academy of Sciences of the United States of America, 2006. **103**(5): p. 1248-1253.
101. Washburn, M.P., D. Wolters, and J.R. Yates, *Large-scale analysis of the yeast proteome by multidimensional protein identification technology.* Nat Biotech, 2001. **19**(3): p. 242-247.
102. Mohan, M., et al., *Linking H3K79 trimethylationto Wnt signaling through a novel Dot1-containing complex (DotCom).* Genes & Development, 2010. **24**(6): p. 574-589.
103. Longtine, M.S., et al., *Additional modules for versatile and economical PCR-based gene deletion and modification in Saccharomyces cerevisiae.* Yeast, 1998. **14**(10): p. 953-961.
104. Huang, G.-L., H.-C. Zhang, and P.-G. Wang, *Hydrolysis characteristics of a β-1,3-d-glucan elicitor from yeast.* Biotechnology and Applied Biochemistry, 2005. **42**(3): p. 219-222.
105. Weber, S.A., et al., *The Kinetochore Is an Enhancer of Pericentric Cohesin*

Binding. PLoS Biol, 2004. **2**(9): p. e260.
106. Skinner, J.P., Y. Chen, and J.D. Müller, *Fluorescence Fluctuation Spectroscopy in the Presence of Immobile Fluorophores.* Biophysical Journal, 2008. **94**(6): p. 2349-2360.
107. Slaughter, B.D., et al., *SAM Domain-Based Protein Oligomerization Observed by Live-Cell Fluorescence Fluctuation Spectroscopy.* PLoS ONE, 2008. **3**(4): p. e1931.
108. Thompson, N., *Topics in Fluorescence Spectroscopy Techniques* ed J R Lakowicz (New York: Plenum) 1991. **1**: p. 337-378.
109. Hess, S.T. and W.W. Webb, *Focal Volume Optics and Experimental Artifacts in Confocal Fluorescence Correlation Spectroscopy.* Biophysical Journal, 2002. **83**(4): p. 2300-2317.
110. Gu, Y., et al., *Quantitative fluorescence resonance energy transfer (FRET) measurement with acceptor photobleaching and spectral unmixing.* Journal of Microscopy, 2004. **215**(2): p. 162-173.
111. Meraldi, P., et al., *Phylogenetic and structural analysis of centromeric DNA and kinetochore proteins.* Genome Biology, 2006. **7**(3): p. R23.
112. Brown, M.T., L. Goetsch, and L.H. Hartwell, *MIF2 is required for mitotic spindle integrity during anaphase spindle elongation in Saccharomyces cerevisiae.* The Journal of Cell Biology, 1993. **123**(2): p. 387-403.
113. Rodrigo-Brenni, M.C., et al., *Sgt1p and Skp1p Modulate the Assembly and Turnover of CBF3 Complexes Required for Proper Kinetochore Function.* Mol. Biol. Cell, 2004. **15**(7): p. 3366-3378.
114. Goh, P.Y. and J.V. Kilmartin, *NDC10: a gene involved in chromosome segregation in Saccharomyces cerevisiae.* The Journal of Cell Biology, 1993. **121**(3): p. 503-512.
115. Ng, R. and J. Carbon, *Mutational and in vitro protein-binding studies on centromere DNA from Saccharomyces cerevisiae.* Mol. Cell. Biol., 1987. **7**(12): p. 4522-4534.
116. Espelin, C.W., et al., *Binding of the Essential Saccharomyces cerevisiae Kinetochore Protein Ndc10p to CDEII.* Mol. Biol. Cell, 2003. **14**(11): p. 4557-4568.
117. Doheny, K.F., et al., *Identification of essential components of the S. cerevisiae kinetochore.* Cell, 1993. **73**(4): p. 761-774.
118. Henikoff, S., K. Ahmad, and H.S. Malik, *The Centromere Paradox: Stable Inheritance with Rapidly Evolving DNA.* Science, 2001. **293**(5532): p. 1098-1102.
119. Furuyama, S. and S. Biggins, *Centromere identity is specified by a single centromeric nucleosome in budding yeast.* Proceedings of the National Academy of Sciences, 2007. **104**(37): p. 14706-14711.
120. Keith, K.C., et al., *Analysis of Primary Structural Determinants That Distinguish the Centromere-Specific Function of Histone Variant Cse4p from Histone H3.* Mol. Cell. Biol., 1999. **19**(9): p. 6130-6139.
121. Luk, E., et al., *Chz1, a Nuclear Chaperone for Histone H2AZ.* Molecular Cell, 2007. **25**(3): p. 357-368.
122. Williams, J.S., et al., *Fission Yeast Scm3 Mediates Stable Assembly of Cnp1/CENP-A into Centromeric Chromatin.* Molecular Cell, 2009. **33**(3): p. 287-298.
123. Huang, C.-C., et al., *Cse4 (CenH3) Association with the Saccharomyces cerevisiae Plasmid Partitioning Locus in Its Native and Chromosomally Integrated States: Implications in Centromere Evolution.* Mol. Cell. Biol., 2011. **31**(5): p. 1030-1040.
124. Jans, D.A., C.-Y. Xiao, and M.H.C. Lam, *Nuclear targeting signal recognition: a key control point in nuclear transport?* BioEssays, 2000. **22**(6): p. 532-544.
125. Bogerd, H., et al., *Protein sequence requirements for function of the human T-cell*

leukemia virus type 1 Rex nuclear export signal delineated by a novel in vivo randomization-selection assay. Mol. Cell. Biol., 1996. **16**(8): p. 4207-4214.
126. Parry, D.A.D., R.D.B. Fraser, and J.M. Squire, *Fifty years of coiled-coils and [alpha]-helical bundles: A close relationship between sequence and structure.* Journal of Structural Biology, 2008. **163**(3): p. 258-269.
127. Lupas, A., M. Van Dyke, and J. Stock, *Predicting coiled coils from protein sequences.* Science, 1991. **252**(5009): p. 1162-1164.
128. Bloom, K., S. Sharma, and N.V. Dokholyan, *The path of DNA in the kinetochore.* Current Biology, 2006. **16**(8): p. R276-R278.
129. Espelin, C.W., K.B. Kaplan, and P.K. Sorger, *Probing the Architecture of a Simple Kinetochore Using DNAâ€"Protein Crosslinking.* The Journal of Cell Biology, 1997. **139**(6): p. 1383-1396.
130. Fraschini, et al., *Role of the kinetochore protein Ndc10 in mitotic checkpoint activation in<SMALL> Saccharomyces cerevisiae</SMALL&gt.* Molecular Genetics and Genomics, 2001. **266**(1): p. 115-125.
131. Li, B., et al., *Preferential occupancy of histone variant H2AZ at inactive promoters influences local histone modifications and chromatin remodeling.* Proceedings of the National Academy of Sciences of the United States of America, 2005. **102**(51): p. 18385-18390.
132. Prunell, A., *A Topological Approach to Nucleosome Structure and Dynamics: The Linking Number Paradox and Other Issues.* Biophysical Journal, 1998. **74**(5): p. 2531-2544.
133. Chen, Y., et al., *The N Terminus of the Centromere H3-Like Protein Cse4p Performs an Essential Function Distinct from That of the Histone Fold Domain.* Mol. Cell. Biol., 2000. **20**(18): p. 7037-7048.
134. Ranjitkar, P., et al., *An E3 Ubiquitin Ligase Prevents Ectopic Localization of the Centromeric Histone H3 Variant via the Centromere Targeting Domain.* Molecular Cell, 2010. **40**(3): p. 455-464.
135. Furuyama, T. and S. Henikoff, *Centromeric Nucleosomes Induce Positive DNA Supercoils.* Cell, 2009. **138**(1): p. 104-113.
136. Dalal, Y., et al., *Tetrameric Structure of Centromeric Nucleosomes in Interphase Drosophila Cells.* PLoS Biol, 2007. **5**(8): p. e218.
137. Sekulic, N., et al., *The structure of (CENP-A-H4)2 reveals physical features that mark centromeres.* Nature, 2010. **467**(7313): p. 347-351.
138. Visnapuu, M.-L. and E.C. Greene, *Single-molecule imaging of DNA curtains reveals intrinsic energy landscapes for nucleosome deposition.* Nat Struct Mol Biol, 2009. **16**(10): p. 1056-1062.
139. Fornerod, M., et al., *CRM1 Is an Export Receptor for Leucine-Rich Nuclear Export Signals.* Cell, 1997. **90**(6): p. 1051-1060.
140. Hewawasam, G., et al., *Psh1 Is an E3 Ubiquitin Ligase that Targets the Centromeric Histone Variant Cse4.* Molecular Cell, 2010. **40**(3): p. 444-454.
141. Pinto, I. and F. Winston, *Histone H2A is required for normal centromere function in Saccharomyces cerevisiae.* EMBO J, 2000. **19**(7): p. 1598-1612.
142. Meluh, P.B. and D. Koshland, *Budding yeast centromere composition and assembly as revealed by in vivo cross-linking.* Genes & Development, 1997. **11**(24): p. 3401-3412.
143. Kingston, I.J., J.S.Y. Yung, and M.R. Singleton, *Biophysical Characterization of the Centromere-specific Nucleosome from Budding Yeast.* Journal of Biological Chemistry, 2011. **286**(5): p. 4021-4026.
144. Lavelle, C., et al., *Right-Handed Nucleosome: Myth or Reality?* Cell, 2009. **139**(7): p. 1216-1217.
145. Baum, M. and L. Clarke, *Fission Yeast Homologs of Human CENP-B Have Redundant Functions Affecting Cell Growth and Chromosome Segregation.* Mol.

Cell. Biol., 2000. **20**(8): p. 2852-2864.
146. Buchwitz, B.J., et al., *Cell division: A histone-H3-like protein in C. elegans.* Nature, 1999. **401**(6753): p. 547-548.
147. Earnshaw, W., et al., *Molecular cloning of cDNA for CENP-B, the major human centromere autoantigen.* The Journal of Cell Biology, 1987. **104**(4): p. 817-829.
148. Malik, H.S. and S. Henikoff, *Conflict begets complexity: the evolution of centromeres.* Current Opinion in Genetics & Development, 2002. **12**(6): p. 711-718.
149. Willard, H.F., *Centromeres: the missing link in the development of human artificial chromosomes.* Current Opinion in Genetics & Development, 1998. **8**(2): p. 219-225.
150. Cleveland, D.W., Y. Mao, and K.F. Sullivan, *Centromeres and Kinetochores: From Epigenetics to Mitotic Checkpoint Signaling.* Cell, 2003. **112**(4): p. 407-421.
151. Waye, J.S. and H.F. Willard, *Structure, organization, and sequence of alpha satellite DNA from human chromosome 17: evidence for evolution by unequal crossing-over and an ancestral pentamer repeat shared with the human X chromosome.* Mol. Cell. Biol., 1986. **6**(9): p. 3156-3165.
152. Sullivan, K.F., *A solid foundation: functional specialization of centromeric chromatin.* Current Opinion in Genetics & Development, 2001. **11**(2): p. 182-188.
153. Conde e Silva, N., et al., *CENP-A-containing Nucleosomes: Easier Disassembly versus Exclusive Centromeric Localization.* Journal of Molecular Biology, 2007. **370**(3): p. 555-573.
154. Foltz, D.R., et al., *The human CENP-A centromeric nucleosome-associated complex.* Nat Cell Biol, 2006. **8**(5): p. 458-469.
155. Palmer, D.K. and R.L. Margolis, *Kinetochore components recognized by human autoantibodies are present on mononucleosomes.* Mol. Cell. Biol., 1985. **5**(1): p. 173-186.
156. Palmer, D., et al., *A 17-kD centromere protein (CENP-A) copurifies with nucleosome core particles and with histones.* The Journal of Cell Biology, 1987. **104**(4): p. 805-815.
157. Black, B.E., et al., *An epigenetic mark generated by the incorporation of CENP-A into centromeric nucleosomes.* Proceedings of the National Academy of Sciences, 2007. **104**(12): p. 5008-5013.
158. Dimitriadis, E.K., et al., *Tetrameric organization of vertebrate centromeric nucleosomes.* Proceedings of the National Academy of Sciences, 2010. **107**(47): p. 20317-20322.
159. Bancaud, A., et al., *Nucleosome Chiral Transition under Positive Torsional Stress in Single Chromatin Fibers.* Molecular Cell, 2007. **27**(1): p. 135-147.
160. Nakanishi, S., et al., *A comprehensive library of histone mutants identifies nucleosomal residues required for H3K4 methylation.* Nat Struct Mol Biol, 2008. **15**(8): p. 881-888.
161. Park, Y.-J., et al., *A New Fluorescence Resonance Energy Transfer Approach Demonstrates That the Histone Variant H2AZ Stabilizes the Histone Octamer within the Nucleosome.* Journal of Biological Chemistry, 2004. **279**(23): p. 24274-24282.
162. Jin, Q.W., J. Fuchs, and J. Loidl, *Centromere clustering is a major determinant of yeast interphase nuclear organization.* J Cell Sci, 2000. **113**(11): p. 1903-1912.
163. Jin, Q.-w., et al., *Yeast Nuclei Display Prominent Centromere Clustering That Is Reduced in Nondividing Cells and in Meiotic Prophase.* The Journal of Cell Biology, 1998. **141**(1): p. 21-29.
164. Yeh, E., et al., *Spindle dynamics and cell cycle regulation of dynein in the budding yeast, Saccharomyces cerevisiae.* The Journal of Cell Biology, 1995. **130**(3): p. 687-700.

165. Zhou, Z., et al., *Structural basis for recognition of centromere histone variant CenH3 by the chaperone Scm3.* Nature, 2011. **advance online publication.**
166. Straight, A.F., et al., *Mitosis in Living Budding Yeast: Anaphase A But No Metaphase Plate.* Science, 1997. **277**(5325): p. 574-578.

Appendix 1- Yeast Strains

Type of Experiment	Strain Name	Genotype
Plasmid shuffle	MS1	MATa *ura3-1 leu2,3-112 his3-1 trp1-1 ade2-1 can1-100 Δbar1 scm3Δ*::TRP1 pRS316-SCM3::URA3 pRS423-SCM3::HIS3
	MS2	MATa *ura3-1 leu2,3-112 his3-1 trp1-1 ade2-1 can1-100 Δbar1 scm3Δ*::TRP1 pRS316-SCM3::URA3 pRS423
	MS3	MATa *ura3-1 leu2,3-112 his3-1 trp1-1 ade2-1 can1-100 Δbar1 scm3Δ*::TRP1 pRS316-SCM3::URA3 pRS423-*scm3-ΔNES*::HIS3
	MS4	MATa *ura3-1 leu2,3-112 his3-1 trp1-1 ade2-1 can1-100 Δbar1 scm3Δ*::TRP1 pRS316-SCM3::URA pRS423-*scm3-3L-A*::HIS3
	MS5	MATa *ura3-1 leu2,3-112 his3-1 trp1-1 ade2-1 can1-100 Δbar1 scm3Δ*::TRP1 pRS316-SCM3::URA3 pRS423-*scm3-ΔNLS*::HIS3
	MS6	MATa *ura3-1 leu2,3-112 his3-1 trp1-1 ade2-1 can1-100 Δbar1 scm3Δ*::TRP1 pRS316-SCM3::URA3 pRS423-*scm3-Δ2-12*:: HIS3
	MS7	MATa *ura3-1 leu2,3-112 his3-1 trp1-1 ade2-1 can1-100 Δbar1 scm3Δ*::TRP1 pRS316-SCM3::URA3 pRS423-*scm3-Δ25C*::HIS3
	MS8	MATa *ura3-1 leu2,3-112 his3-1 trp1-1 ade2-1 can1-100 Δbar1 scm3Δ*::TRP1 pRS316-SCM3::URA3 pRS423-*scm3-Δ25N*::HIS3
	MS14	MATa *ura3-1 leu2,3-112 his3-1 trp1-1 ade2-1 can1-100 Δbar1 scm3Δ*::TRP1 pRS316-SCM3::URA3 pRS423-*scm3-I110H*::HIS3
	MS15	MATa *ura3-1 leu2,3-112 his3-1 trp1-1 ade2-1 can1-100 Δbar1 scm3Δ*::TRP1 pRS316-SCM3::URA pRS423-*scm3-I111H*::HIS3
Ndc10-Myc ChIPs and Point of execution experiment	MS19	MATa *ura3-1 leu2,3-112 his3-1 trp1-1 ade2-1 can1-100 Δbar1* NDC10-13myc::TRP1 GAL1-10-3HA-SCM3::KAN pRS423-SCM3::HIS3
	MS20	MATa *ura3-1 leu2,3-112 his3-1 trp1-1 ade2-1 can1-100 Δbar1* NDC10-13myc::TRP1 GAL1-10-3HA-SCM3::KAN pRS423
	MS21	MATa *ura3-1 leu2,3-112 his3-1 trp1-1 ade2-1 can1-100 Δbar1* NDC10-13myc::TRP1 GAL1-10-3HA-SCM3::KAN pRS423- *scm3-Δ25N*::HIS3
	MS22	MATa *ura3-1 leu2,3-112 his3-1 trp1-1 ade2-1 can1-100 Δbar1* NDC10-13myc::TRP1 GAL1-10-3HA-SCM3::KAN pRS423-*scm3-I110H*::HIS3
Cse4-Myc ChIPs and Point of execution experiment	MS28	MATa *ura3-1 leu2,3-112 his3-1 trp1-1 ade2-1 can1-100 Δbar1* CSE4::CSE4-12myc::URA3 GAL_{1-10}-3HA-SCM3::KAN pRS423
	MS29	MATa *ura3-1 leu2,3-112 his3-1 trp1-1 ade2-1 can1-100 Δbar1* CSE4::CSE4-12myc::URA3 GAL_{1-10}-3HA-SCM3::KAN pRS423-*scm3-Δ25N*::HIS3
	MS30	MATa *ura3-1 leu2,3-112 his3-1 trp1-1 ade2-1 can1-100 Δbar1* CSE4::CSE4-12myc::URA3 GAL_{1-10}-3HA-SCM3::KAN
	MS31	MATa *ura3-1 leu2,3-112 his3-1 trp1-1 ade2-1 can1-100 Δbar1* CSE4::CSE4-12myc::URA3 GAL_{1-10}-3HA-SCM3::KAN pRS423-*scm3-I110H*::HIS3
Ndc10-Myc IP	MM67	MATa *ura3-1 leu2,3-112 his3-1 trp1-1 ade2-1 can1-100 Δbar1* NDC10-13myc::KAN pPRS423-2NFLAG-SCM3::HIS3
	MM151	MATa *ura3-1 leu2,3-112 his3-1 trp1-1 ade2-1 can1-100 Δbar1* NDC10-13myc::KAN pRS423-2NFLAG-*scm3-I110H*::HIS3
	MM152	MATa *ura3-1 leu2,3-112 his3-1 trp1-1 ade2-1 can1-100 Δbar1* NDC10-13myc::KAN pRS423-2NFLAG-*scm3-I111H*::HIS3
	MM63	MATa *ura3-1 leu2,3-112 his3-1 trp1-1 ade2-1 can1-100 Δbar1* NDC10-13myc::KAN pRS423-2NFLAG-*scm3-Δ25N*::HIS3

Appendix 1- Yeast strains (Cont)

	MM157	MATa *ura3-1 leu2,3-112 his3-1 trp1-1 ade2-1 can1-100 Δbar1* NDC10-13myc::KAN pPRS423-SCM3::HIS3
Cse4-Myc IP	RC217	MATa *ura3-1 leu2,3-112 his3-1 trp1-1 ade2-1 can1-100 Δbar1* CSE4::CSE4-12myc::URA3 GAL_{1-10}-3HA-SCM3::KAN pRS423-2NFLAG-*scm3-I111H*::HIS3
	RC218	MATa *ura3-1 leu2,3-112 his3-1 trp1-1 ade2-1 can1-100 Δbar1* CSE4::CSE4-12myc::URA3 GAL_{1-10}-3HA-SCM3::KAN pRS423-2NFLAG-*scm3-I110H*::HIS3
	RC220	MATa *ura3-1 leu2,3-112 his3-1 trp1-1 ade2-1 can1-100 Δbar1* CSE4::CSE4-12myc::URA3 GAL_{1-10}-3HA-SCM3::KAN pRS423-2NFLAG-SCM3::HIS3
	RC221	MATa *ura3-1 leu2,3-112 his3-1 trp1-1 ade2-1 can1-100 Δbar1* CSE4::CSE4-12myc::URA3 GAL_{1-10}-3HA-SCM3::KAN pRS423-2NFLAG-*scm3-Δ25N*::HIS3
	MM156	MATa *ura3-1 leu2,3-112 his3-1 trp1-1 ade2-1 can1-100 Δbar1* CSE4::CSE4-12myc::URA3 GAL_{1-10}-3HA-SCM3::KAN pRS423-SCM3::HIS3
Microscopy	MS173	MATa *his3Δ1;leu2Δ0;met15Δ0;ura3Δ0* CSE4::CSE4-GFP::HIS3
	MS171	MATa *his3Δ1;leu2Δ0;met15Δ0;ura3Δ0* BZZ1::1X-GFP::HIS3
	MS194	MATa *his3Δ1;leu2Δ0;met15Δ0;ura3Δ0* CSE4::CSE4-GFP::HIS3 pRS315-SPC42-mCHERRY::LEU2

Appendix 2- Published papers and Meeting Abstracts

Publications

Shivaraju M, Camahort R, Mattingly M, Gerton JL. (2011). Scm3 is a centromeric nucleosome assembly factor. ***Journal of Biological Chemistry***.286 (14):12016-23.

Hewawasam, G. , **Shivaraju, M.** , Mattingly, M. , Venkatesh, S. , Brown, MS. , Florens, L. , Workman, JL. , and Gerton, JL. (2010). Psh1 is an E3 ubiquitin ligase that targets the centromeric histone variant Cse4. ***Molecular Cell.*** 40(3): 444-454

Camahort R, **Shivaraju M**, Mattingly M, Li B, Nakanishi S, Zhu D, Shilatifard A, Workman JL, Gerton JL. Cse4 is part of an octameric nucleosome in budding yeast. (2009) ***Molecular Cell.*** Sep 24; 35(6):794-805

Meeting Abstracts

Manjunatha Shivaraju, Brian Slaughter, Jay Unruh, Mark Mattingly and Jennifer L. Gerton. Structurally oscilating centromeric nucleosomes in budding yeast. Stowers Institute for Medical Research Young Investigator's Research Day, Kansas City, April, 2011 (poster).

Shivaraju M, Camahort R, Mattingly M, Gerton JL. Scm3 is a Cse4-specific nucleosome assembly factor. Stowers Institute for Medical Research Young Investigator's Research Day, Kansas City, April, 2010 (poster).

Shivaraju M, Camahort R, Mattingly M, Gerton JL. Scm3, an inner kinetochore protein, has two essential domains. Stowers Institute for Medical Research Young Investigator's Research Day, Kansas City, April, 2009 (poster).

Shivaraju M, Camahort R, Mattingly M, Gerton JL. Scm3, an inner kinetochore protein, has two essential domains. Chromatin: Structure & Function Conference, Costa Rica. 2009 (poster)

Shivaraju M, Camahort R, Mattingly M, Gerton JL. Structural and Functional Analysis of Scm3, a Novel Inner Kinetochore Protein. Stowers Institute for Medical Research Young Investigator's Research Day, Kansas City, April, 2008 (poster).

Appendix 3- Collaborator's Contributions

I would like to thank and acknowledge the collaborators listed below for their contributions to the following figures.

Figure 7 & Figure 22. M. Mattingly performed the co-immunoprecipitation.

All the microscopic work is done in collabarotion with Jay Unruh and Brian Slaughter, research advisers in Stowers Institute for Medical Research.